NAVAL POSTGRADUATE SCHOOL
Monterey, California

THESIS

VALIDATION/EVALUATION OF POLARIZATION
VERSION OF SEARAD MODEL

by

Panagiotis Karavas

June 1999

Thesis Advisor:	Alfred W. Cooper
Thesis Co-Advisor:	Ron J. Pieper

Approved for public release; distribution is unlimited.

REPORT DOCUMENTATION PAGE

Form Approved
OMB No. 0704-0188

Public reporting burden for this collection of information is estimated to average 1 hour per response, including the time for reviewing instruction, searching existing data sources, gathering and maintaining the data needed, and completing and reviewing the collection of information. Send comments regarding this burden estimate or any other aspect of this collection of information, including suggestions for reducing this burden, to Washington headquarters Services, Directorate for Information Operations and Reports, 1215 Jefferson Davis Highway, Suite 1204, Arlington, VA 22202-4302, and to the Office of Management and Budget, Paperwork Reduction Project (0704-0188) Washington DC 20503.

1. AGENCY USE ONLY (Leave blank)	2. REPORT DATE June 1999	3. REPORT TYPE AND DATES COVERED Master's Thesis

4. TITLE AND SUBTITLE VALIDATION/EVALUATION OF POLARIZATION VERSION OF SEARAD MODEL 6. AUTHOR(S) Panagiotis Karavas, LTJG	5. FUNDING NUMBERS

7. PERFORMING ORGANIZATION NAME(S) AND ADDRESS(ES) Naval Postgraduate School Monterey, CA 93943-5000	8. PERFORMING ORGANIZATION REPORT NUMBER

9. SPONSORING / MONITORING AGENCY NAME(S) AND ADDRESS(ES)	10. SPONSORING / MONITORING AGENCY REPORT NUMBER

11. SUPPLEMENTARY NOTES

The views expressed in this thesis are those of the author and do not reflect the official policy or position of the Department of Defense or the U.S. Government.

12a. DISTRIBUTION / AVAILABILITY STATEMENT Approved for public release; distribution unlimited.	12b. DISTRIBUTION CODE

13. ABSTRACT (maximum 200 words)

Until recently no standard atmospheric propagation codes included the effects of polarization. Recently a research grade upgrade to MODTRAN (Zeisse, Nrad) has allowed the polarized case. This upgrade, called SEARAD, calculates the infrared polarization of sea surface radiance. Data available in the EOPACE data base were used for a direct comparison of the code prediction to the measurements. The data consist of polarized and unpolarized images of the R/V POINT SUR in the Long Wave Infrared (LWIR), taken with the AGA 780 camera during an experiment conducted in San Diego Bay in April 1996. Meteorological, geographical, and external ship temperature data were recorded along with the images. The analysis of the EOPACE data was conducted by using IDL (Interactive Data Language) analysis programs and included 34 sets of images. The sea pixels were extracted from the images, and correlated with meteorological, and geographical data to provide input to the SEARAD code. The comparison of the experimental data with the SEARAD predictions yielded an average error of 1.57 $Wm^{-2}sr^{-1}$ in unpolarized sea radiance, which is within approximately 5 % of the experimental radiance, and an average 0.51 absolute difference between the predicted and experimental degree percentage of polarization.

14. SUBJECT TERMS Infrared Radiation, Radiance, Degree of Polarization, Atmospheric Propagation Codes.	15. NUMBER OF PAGES 149
	16. PRICE CODE

17. SECURITY CLASSIFICATION OF REPORT Unclassified	18. SECURITY CLASSIFICATION OF THIS PAGE Unclassified	19. SECURITY CLASSIFI- CATION OF ABSTRACT Unclassified	20. LIMITATION OF ABSTRACT UL

NSN 7540-01-280-5500

Standard Form 298 (Rev. 2-89)
Prescribed by ANSI Std. 239-18

VALIDATION/EVALUATION OF POLARIZATION VERSION OF SEARAD MODEL

Panagiotis Karavas
Lieutenant Junior Grade, Hellenic Navy
B.S., Hellenic Naval Academy, 1990

Submitted in partial fulfillment of the
requirements for the degrees of

MASTER OF SCIENCE IN APPLIED PHYSICS,
AND MASTER OF SCIENCE IN ELECTRICAL ENGINEERING

from the

NAVAL POSTGRADUATE SCHOOL
June 1999

ABSTRACT

Until recently no standard atmospheric propagation codes included the effects of polarization. Recently a research grade upgrade to MODTRAN (Zeisse, Nrad) has allowed the polarized case. This upgrade, called SEARAD, calculates the infrared polarization of sea surface radiance. Data available in the EOPACE data base were used for a direct comparison of the code prediction to the measurements. The data consist of polarized and unpolarized images of the R/V POINT SUR in the Long Wave Infrared (LWIR), taken with the AGA 780 camera during an experiment conducted in San Diego Bay in April 1996. Meteorological, geographical, and external ship temperature data were recorded along with the images. The analysis of the EOPACE data was conducted by using IDL (Interactive Data Language) analysis programs and included 34 sets of images. The sea pixels were extracted from the images, and correlated with meteorological, and geographical data to provide input to the SEARAD code. The comparison of the experimental data with the SEARAD predictions yielded an average error of $1.57 \, \mathrm{Wm^{-2}sr^{-1}}$ in unpolarized sea radiance, which is within approximately 5 % of the experimental radiance, and an average 0.51 absolute difference between the predicted and experimental degree percentage of polarization.

TABLE OF CONTENTS

ACKNOWLEDGEMENTS

I.   INTRODUCTION

Recent developments in modern sea warfare, such as the stealth technology and new ECM techniques, mandate the use of passive means for the detection of targets, along with the use of radar. Infrared (IR) systems meet the requirements of such a passive sensor, and therefore are becoming an increasingly important part of integrated combat systems.

The main restriction imposed on current IR sensors, such as Infrared Search and Track (IRST) systems or Forward Looking Infrared (FLIR) systems, is that they have to operate in a heavily cluttered sea background. In the frequencies used by radar a detection is achieved when the signal to noise ratio is greater than one. Unlike the microwave wavelengths used in radar, in the IR wavelengths the target detection is more frequently based on the signal to background ratio, instead of the signal to noise ratio, because in the IR region of the electromagnetic spectrum the background is very intense. FLIR systems particularly are contrast limited in performance rather than noise limited.

Many techniques have been developed to deal with the problem of background suppression in IR sensors. These techniques, which include spatial filtering and advanced signal processing, improve the detection probability, but do not provide a satisfactory solution. Polarization filtering is a relatively new approach to the problem of improving the target contrast against sea background.

A number of studies, [Ref. 1,2,3,4,5,6,7] in the past seven years by the Naval Postgraduate School, suggest that polarization effects in the observed IR radiation by the sea background could be exploited to improve target contrast.

Atmospheric propagation prediction codes, such as LOWTRAN and MODTRAN, play an important role in the development of IR sensors. Thus far none of these codes included polarization effects. Recently, a research grade upgrade to MODTRAN developed by C.R. Zeisse at SPAWAR SYSTEMS CENTER [Ref. 8], has allowed the polarized case. The new code is the polarization version of SEARAD. It is capable of predicting the values of the polarized components of the observed sea IR radiance and the degree of polarization of the apparent radiance.

This thesis uses experimental data available in the Electro-Optical Propagation Assessment in the Coastal Environment (EOPACE) data base, to perform a direct comparison to the SEARAD predictions. The specific data employed were taken by the Naval Postgraduate School during a multinational experiment in San Diego Bay on April 1996. The data include IR images of the Research Vessel (R/V) POINT SUR, recorded using an AGA 780 camera. For a given period of time, the ship's image against the sea background, was recorded with a polarizer filter in the horizontal direction, in the vertical direction, and removed. In that way, three sets of images were obtained: vertically polarized images, horizontally polarized images and unpolarized images. Meteorological and geographical data were recorded on board the R/V POINT SUR by the NPS Boundary Layer Meteorology Group and the NPS Center for Infrared Technology (NACIT).

2

The objective of this thesis is to correlate, and to analyze these data from the EOPACE database, and compare the results with those predicted by the polarized version of SEARAD, to validate the new code.

This thesis begins in Chapter II with a brief discussion of IR fundamentals. In Chapter III the polarization theory used by the SEARAD code is provided. Chapter IV describes the experimental data acquisition and analysis. Chapters V and VI present the results, the conclusions, and the recommendations, respectively.

II.   INFRARED FUNDAMENTALS

The analysis developed in this study deals with concepts related to infrared radiation. To better understand these concepts, this chapter presents the basics of infrared theory and terminology.

A.   THE NATURE OF INFRARED RADIATION

The prefix "infra" has a Latin origin, meaning below or beneath. So the word infrared refers to the region of the electromagnetic spectrum below the red end of the visible light. Infrared radiation was discovered in 1800 by the English astronomer Sir William Herschel. All objects radiate infrared radiation, unless they have a temperature of 0 Kelvins. IR radiation obeys Maxwell's equations in its propagation. Furthermore, the same laws of diffraction, reflection, and refraction that apply to visible light, radio waves, and microwaves, also apply to the infrared radiation.

The position of the infrared spectrum is between visible light and microwaves as shown in Figure 2.1. The wavelengths of infrared radiation (IR) vary from 0.7 μm to 1000 μm. The infrared spectrum is further subdivided into IR bands, based on criteria such as the atmospheric transmission, the method of detection and the form of radiation. These bands are:

- The near infrared (NIR) from 0.75 μm to 3.0 μm.

- The mid wave infrared (MWIR) or Middle infrared from 3.0 μm to 6.0 μm.

- The long wave infrared (LWIR) or Far infrared from 6.0 μm to 15.0 μm.

- The extreme infrared (XIR) from 15.0 μm to 1000 μm.
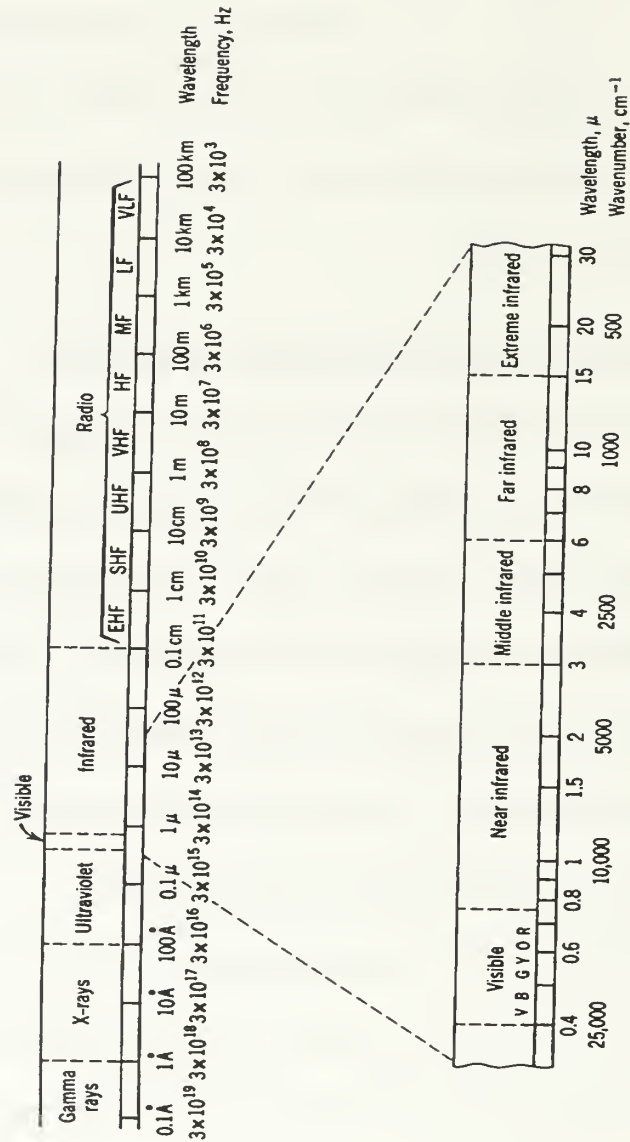
Figure 2.1 Electromagnetic and Infrared Spectrum [Ref. 9]

Reflected Solar radiation is the dominant component of infrared energy in the NIR band. On the other hand infrared radiation in the MWIR and LWIR bands, is predominantly due to object emission. The latter IR radiation is also called "thermal

6

radiation" because it is temperature dependent. Most practical applications of infrared do not include the XIR band.

B.   INFRARED TERMINOLOGY AND RADIOMETRIC UNITS

The infrared community, like many other branches of engineering and science, uses its own terminology and units to describe the phenomena associated with the IR radiation.

The basic units used are summarized in Table 2.1. Although the area units are frequently expressed in cm^2, in this thesis they will be expressed in m^2. The reason for this is that the polarized model of SEARAD uses meters squared as area units.

Area (A)	Square centimeters (cm^2) or Square meters (m^2)
Wavelength (λ)	Micrometers (μm)
Temperature (T)	Degrees Kelvin (K)
Plane angle	Radian (rad)
Solid angle (Ω)	Steradian (Sr)

Table 2.1 Basic Units Used in IR Theory

Infrared theory uses specific radiometric quantities to describe the IR phenomena. These quantities are the following:

7

- Radiant Flux Density – Exitance (M): It is the radiant flux leaving an area of a surface divided by that surface

- Irradiance (E): It is the radiant power incident on an area of a surface divided by that area

- Radiant Intensity (I): It is the radiant power leaving a point source per unit solid angle.

- Radiance (N): It is the radiant power leaving or arriving at a surface at a point in a given direction per solid angle and per unit area normal to that direction.

The units used for the radiometric quantities are laid out in Table 2.2. As mentioned above, square meters are chosen as the area units, for compatibility with SEARAD.

Often there is a need to refer to the radiometric quantities over a specific bandwidth and not over all wavelengths. When doing so the word "spectral" will precede the name of the radiometric quantity, and the corresponding units will be divided by the μm which is the unit of wavelength.

Radiometric Quantity	Units
M	Watts/m^2
E	Watts/m^2
I	Watts/Sr
N	Watts/m^{2}Sr

Table 2.2 Radiometric Units

C.   RADIATION LAWS

1.   Blackbody Radiation and Kirchhoff's Law

The maximum power which can be radiated by an object at a given temperature is called blackbody radiation. A blackbody is an ideal object, which is both a perfect emitter and perfect absorber of radiation. An object which emits or absorbs less radiation than the blackbody, but with the same spectral distribution, is called a graybody.

The emissivity ε of an object is defined as the ratio of the exitance M_e from the object to the exitance M_o from the blackbody at the same temperature:

$$\varepsilon = M_e / M_o \tag{2.1}$$

The absorptance α of an object can be defined as the ratio of the radiant flux per unit area being absorbed by the surface of the object to the radiant flux per unit area incident on the surface.

$$\alpha = E_a / E_i \tag{2.2}$$

Kirchhoff's Law states that, if a graybody is placed in an enclosure in thermal equilibrium, then the spectral emissivity is equal to the spectral absorptance:

$$\varepsilon(\lambda) = \alpha(\lambda) \tag{2.3}$$

Equation 2.3 implies that the spectral radiant flux per unit area being emitted by the object is equal to the spectral radiant flux per unit area being absorbed by the object in a state of thermal equilibrium. This equation can be applied more widely to bodies not in thermal equilibrium.

By the law of conservation of energy, the incident power P_i upon an object, is equal to the sum of the transmitted power P_τ, the reflected power P_ρ, and the absorbed power P_α:

$$P_i = P_\tau + P_\rho + P_\alpha \tag{2.4}$$

Dividing both sides of the Equation 2.4 by P_i, and by defining $\tau = P_\tau/P_i$ as the transmittance, and $\rho = P_\rho/P_i$ as the reflectance we get:

$$\tau + \rho + \alpha = 1 \tag{2.5}$$

For a blackbody there is no reflection or transmission i.e. $\tau = \rho = 0$, so $\alpha = \varepsilon = 1$. Also for opaque graybodies since there is no transmission, $\tau = 0$:

$$\alpha = \varepsilon = 1 - \rho \tag{2.6}$$

10

2.   Planck's Law

The blackbody radiates or absorbs, over a wide range of wavelengths. Max Planck first postulated that this radiation is due to vibrating atoms that emit or absorb radiation in discrete quanta of energy, which are given by the following equation:

$$E = h\nu \qquad (2.7)$$

where:

- E is the energy change in Joules
- h is the Planck's constant equal to 6.6256×10^{-34} Joules sec
- ν is the frequency in Hz

Planck's radiation law, can be deduced from Equation 2.7. It was initially developed as an empirical fit to experimental measurements, where h is the fitting parameter, and is given by the following equation:

$$M_\lambda(T) = \frac{2\pi c^2 h / \lambda^5}{\exp(\frac{hc}{\lambda kT}) - 1} \qquad (2.8)$$

where:

- $M_\lambda(T)$ is the spectral exitance at a temperature T, in W/cm^2-μm.
- T is the temperature of the source in K.

11

- λ is the wavelength in μm.

- h is the Planck's constant equal to 6.6256×10^{-34} Joules sec.

- k is the Boltzmann's constant equal to 1.38054×10^{-23} J/K.

- c is the speed of light in vacuum equal to 3×10^8 m/sec.

Planck's law, gives the spectral exitance for a blackbody. The corresponding spectral exitance for a graybody can be obtained by multiplying the blackbody spectral exitance by the greybody's emittance. Figure 2.2 gives the spectral exitance for a blackbody at certain temperatures. It is observed in this figure that the higher the temperature of the object is, the smaller the wavelength is, at which the peak of spectral exitance occurs. This is expressed by Wien's displacement law described next.

3.   **Wien's Displacement Law**

By differentiating Planck's Law with respect to wavelength and then by equating the result to zero we get the maximum of the spectral exitance for a specific temperature. Wien's displacement law is the solution of the differentiation, and it is expressed as follows:

$$\lambda_{max} T = 2897.8 \ \mu mK \tag{2.9}$$

where:

- λ_{max} is the wavelength in μm, for which maximum exitance occurs.

- T is the temperature of the source in K.
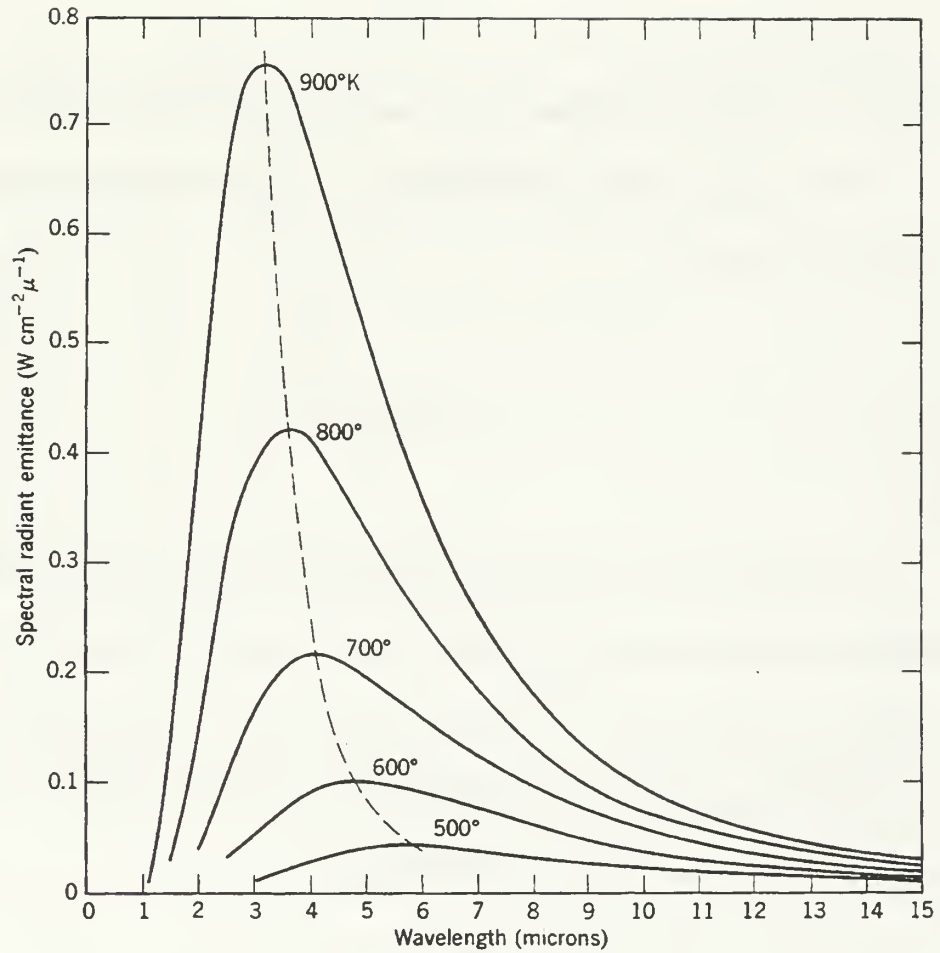
Figure 2.2 Graphical Representation of Planck's Law [Ref. 9]

4. Stefan – Boltzmann Law

To obtain a closed form expression for the total exitance from a blackbody, Planck's law can be integrated over all wavelengths. The result is known as the Stefan-Boltzmann law and it is given by the following equation:

$$M(T) = \frac{2\pi^5 k^4}{12c^2 h^3} T^4 = \sigma T^4 \qquad (2.10)$$

where σ is the Stefan-Boltzmann constant and is equal to 5.6697×10^{-12} W/cm^{2}K^4.

For a graybody, which has an emissivity which is constant over all wavelengths, the exitance becomes:

$$M(T) = \varepsilon \sigma T^4 \qquad (2.11)$$

A practical way of calculating the spectral exitance without having to solve the Planck's law integral directly is through the use of the universal blackbody curve depicted in Figure 2.3. This curve is a graphical representation of Planck's Law expressed as a function of the product λT and normalized with respect to the peak wavelength. The integral referred to the right axis is the integral of the universal curve from zero to each value of λT. The "in band" spectral blackbody exitance is then given by:

$$M(\lambda, T) = f \sigma T^4 \qquad (2.12)$$

where f is the fraction of the exitance contained in a certain bandwidth and takes values from zero to one.
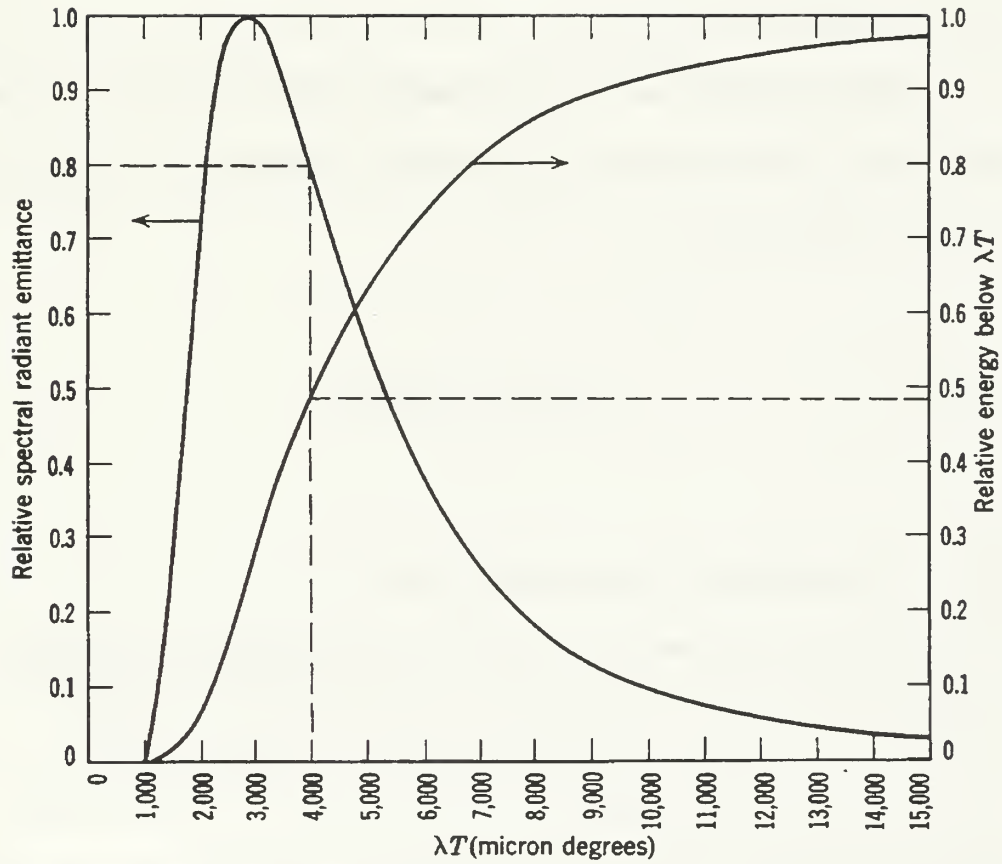
Figure 2.3 Universal Blackbody Curve [Ref. 9]

5.   Lambert's Law

A blackbody with a rough planar surface emits radiation diffusely. Such a surface

is called a Lambertian surface,, and the emitted radiant intensity is given by Lambert's

law, expressed by the following equation:

$$I(\theta) = I(0) \cos(\theta) \tag{2.13}$$

15

where θ is the angle between the normal to the surface and the viewing line of sight, and I(0) is the normal radiant intensity.

From Lambert's law it can be shown that the radiance N radiated from a blackbody Lambertian source into a hemisphere is independent of the viewing angle, and has the value[Ref. 9]:

$$N = M/\pi \tag{2.14}$$

D.   ATMOSPHERIC TRANSMITTANCE

The laws described in Section C give the IR radiometric quantities for vacuum conditions. However, in most practical applications, the atmosphere is the medium through which IR radiation propagates. The atmosphere reduces the radiance reaching the sensor from the source by two main mechanisms: absorption, and non-forward scattering.

The atmospheric absorption is due to individual molecules or aerosol particles such as fog, dust, salt, and others. The transmitted radiation is absorbed whenever it contains photons with energies that match the allowed transitional energies of the molecules or the aerosol particles.

In general scattering can be classified as either forward scattering or non-forward scattering. The non-forward scattering decreases the received radiance, while the forward scattering increases the received radiance. The scattering occurs when the incoming

16

spectral radiation has wavelength components that are in the order of the size of molecules or aerosol particles. Then the incoming radiation is scattered in all directions.

The atmospheric transmittance τ accounts for the effects of radiance reduction by the absorption and the non-forward scattering. The atmospheric transmittance takes values from zero to one and can be calculated by the Lambert-Beer law as follows [Ref. 10]:

$$\tau(\lambda) = \exp(-\mu(\lambda)R) \qquad (2.15)$$

where:

- $\mu(\lambda)$ is the spectral attenuation coefficient, or extinction coefficient which is a function of the wavelength λ.
- R is the path length.

The atmospheric transmittance for a certain bandwidth is calculated by integrating Lambert - Beer's law over the specific wavelengths of the bandwidth. This is done by all the standard atmospheric transmission codes such as LOWTRAN and MODTRAN.

The atmospheric transmittance for one kilometer path range, a midlatitude location, and a rural aerosol, was calculated using LOWTRAN7 and plotted in Figure 2.4 [Ref. 11]. In this figure we see that there are two regions of high atmospheric transmittance of the MWIR and LWIR bandwidths. These regions are called "atmospheric windows" and are from 3.0 μm to 5.0 μm and from 8 μm to 14 μm. Most of

the modern military infrared systems, such as Infra Red Search and Track (IRST) and Forward Looking Infrared (FLIR) operate in these two atmospheric windows of propagation.
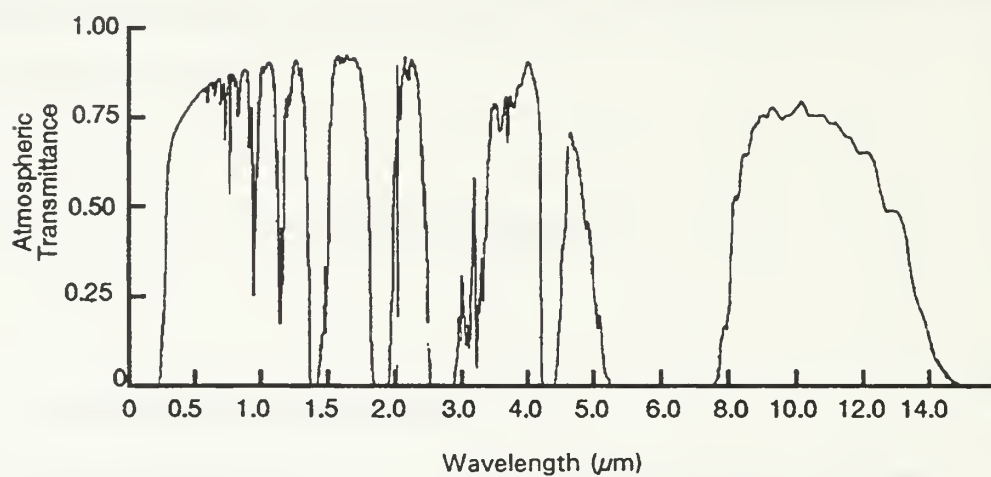
Figure 2.4 Atmospheric Transmittance [Ref. 11].

III.   POLARIZATION OF SEA RADIANCE

The phenomenon of the polarization of sea radiance has been addressed extensively in the existing literature [Ref. 1,2,3,4,5,6,7,12,13]. This chapter presents briefly the theory related to the polarization of sea radiance. The presentation is based on a technical report by C.R. Zeisse [Ref. 8], which accompanies the polarized version of SEARAD model that is evaluated in this thesis.

A.   POLARIZED REFLECTED RADIANCE

In our preliminary analysis the reflection of monochromatic radiation from a flat sea surface will be considered. The sea surface is assumed to be tilted with respect to the horizon. The geometry of the problem is presented in Figure 3.1. In this figure the origin coincides with the point of reflection, the X axis is pointing in the up wind direction, and the Z axis is pointing to the zenith. The subscripts s and r refer to the source and the receiver respectively. The angle φ is the azimuth relative to the upwind direction and the angle θ is the zenith angle. The vector U_r points to the receiver, and U_s points to the source. The unit vector normal to the sea facet is omitted.

The electric vector of the incident and the reflected radiation has two components: the s component which is perpendicular to the plane of incidence and the p component which is parallel to the plane of incidence. The plane of incidence is defined by the unit vector normal to the sea facet, and the direction vector of the incident wave.
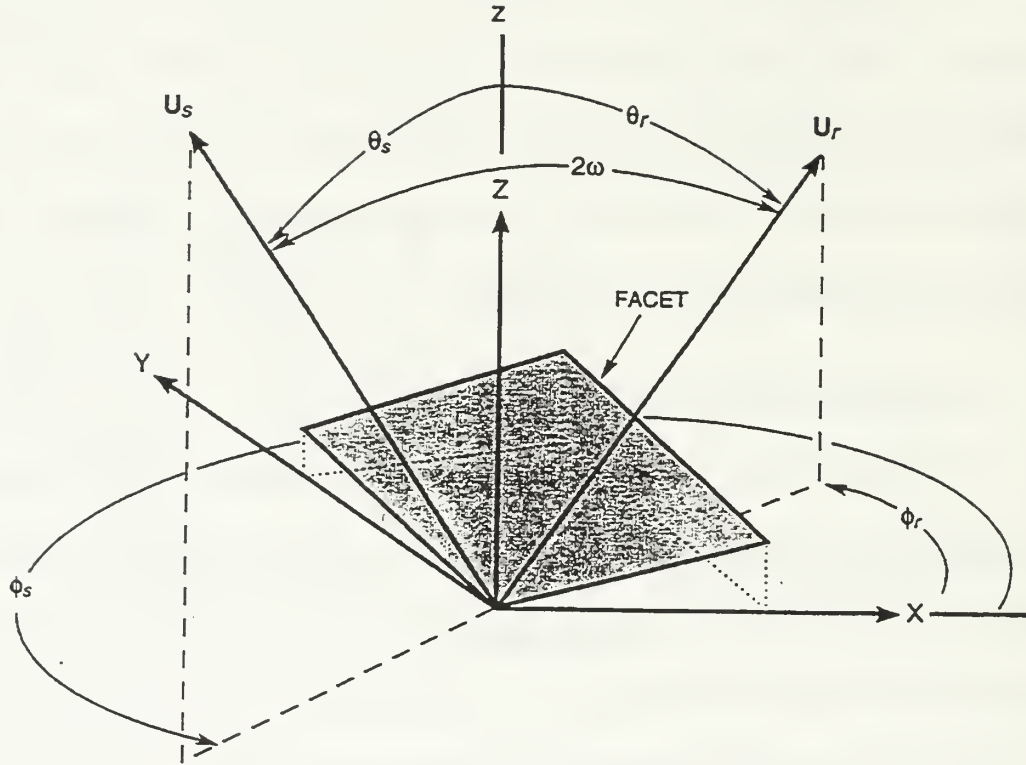
Figure 3.1 The Coordinate System, θ_s is the Zenith Angle of the Source, θ_r is the Zenith Angle of the Receiver, and ω is the Angle of incidence and the Angle of Reflection [Ref. 8].

The Fresnel equations can then be used to derive the reflected components of the electric field E_2 which are:

$$E_{2s} = \rho_s \exp(-i\delta_s)E_0 \sin(\alpha) \tag{3.1}$$

$$E_{2p} = \rho_p \exp(-i\delta_p)E_0 \cos(\alpha) \tag{3.2}$$

20

where:

- E_0 is the magnitude of the electric field of the incident radiation.

- r is the amplitude reflection coeficient and $r^2 = \rho$ is the reflectance.

- δ is the phase of the plane wave.

- α is the angle of arrival (the angle between the E vector and the plane of incidence).

The subscript s refers to the component of the electric field perpendicular to the plane of incidence, and the p refers to the component of the electric field parallel to the plane of incidence, referred to the facet.

The polarizer has an axis called "polarization axis" along which the electric (E) vector passes. The components of the E vector in all other directions are blocked by the polarizer. If the polarization axis is parallel to the plane of the horizon, the horizontal component of the reflected electric vector along U_h in Figure 3.2 passes through the polarizer. On the other, hand if the polarization axis is normal to the plane of the horizon, the vertical component of the reflected electric vector along U_v in Figure 3.2 passes through the polarizer. From Equations 3.1 and 3.2 and by the geometry presented in Figure 3.2, the horizontal E_{2h} and the vertical E_{2v} components of the reflected electric field are:

$$E_{2v} = E_{2p} \cos\beta + E_{2s} \sin\beta \qquad (3.3)$$

$$E_{2h} = E_{2s} \cos\beta + E_{2p} \sin\beta \qquad (3.4)$$

The angle β is the angle between the plane of incidence and the plane of vision. The plane of vision is the one containing the unit vector U_r pointing to the receiver and the unit vector along the Z axis.
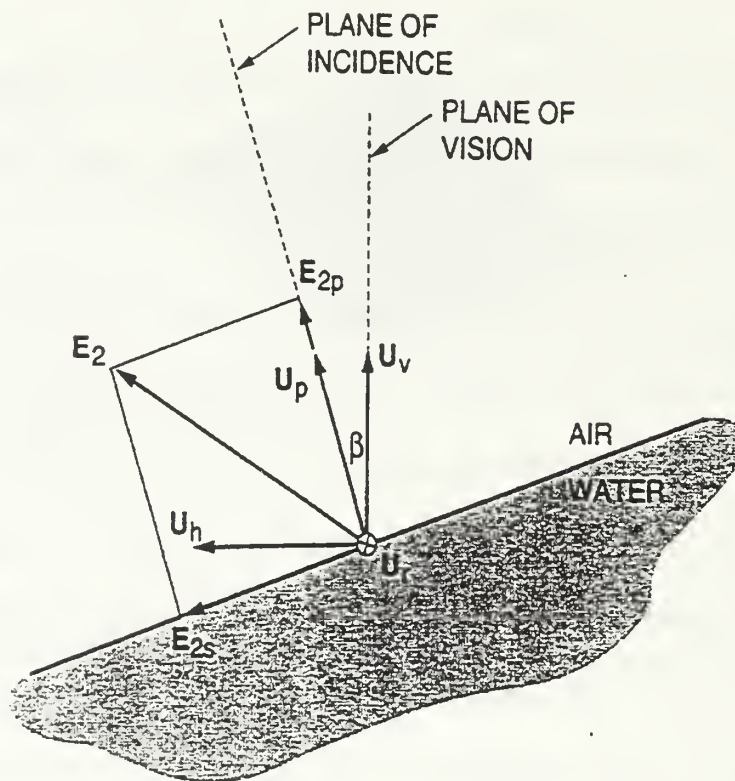
Figure 3.2 Reflected Components of the Electric Field [Ref. 8]

The reflected radiance N^r can be deduced from Equations 3.3 and 3.4, by taking the squared modulus E^*E and assuming natural light as the incident radiation. Then we have the following equations for the reflectance ρ and its polarized components ρ_h and ρ_v [Ref. 8][1]:

$$\rho_h = \frac{N^r_h}{N_0} = \frac{\rho_s}{2}(\cos\beta)^2 + \frac{\rho_p}{2}(\sin\beta)^2 \qquad (3.5)$$

$$\rho_v = \frac{N^r_v}{N_0} = \frac{\rho_p}{2}(\cos\beta)^2 + \frac{\rho_s}{2}(\sin\beta)^2 \qquad (3.6)$$

$$\rho = \rho_h + \rho_v = \frac{N^r}{N_0} = \frac{\rho_s}{2} + \frac{\rho_p}{2} \qquad (3.7)$$

where $\rho_p = r_p^2$ and $\rho_s = r_s^2$ are the reflectances for the p and s components, and N_o is the incident radiance.

B.   POLARIZED EMITTED RADIANCE

When we have radiation incident on the sea surface, part of that radiation will be reflected and part of the radiation will be transmitted into the water. If we consider the water to be thick none of the energy can escape by transmission. The energy is then absorbed by the water causing its temperature to rise. According to Kirchoff's law the emissivity of the sea will be equal to the absorptance of the sea. The emissivity is equal to

---

[1] In Ref. 8 the reflectance ρ is denoted by R, and it is referred to as the "Fresnel reflection coefficient".

N^{sea}/N_{bb} where N^{sea} is the sea emitted radiance and N_{bb} is the blackbody radiance for the same temperature. The emissivity ε is equal to the absorptance α, which is equal to the fraction of the radiant energy that the water absorbs from the incident radiation since there is no transmission: $\varepsilon = \alpha = 1 - \rho$ (Equation 2.6). This Equation also holds for the polarized components i.e. $\varepsilon_s = \alpha_s = 1 - \rho_s$, and $\varepsilon_p = \alpha_p = 1 - \rho_p$,

Finally with an analysis similar to the one of the previous section, the following equations can be obtained for the emitted vertical N_v^{sea}, and horizontal N_h^{sea} polarized sea radiance, as well as the unpolarized N^{sea} sea radiance [Ref. 8][2]:

$$\varepsilon_h = \frac{N_h^{sea}}{N_{bb}} = \frac{\varepsilon_s}{2}(\cos\beta)^2 + \frac{\varepsilon_p}{2}(\sin\beta)^2 = \frac{1}{2} - \rho_h \tag{3.8}$$

$$\varepsilon_v = \frac{N_v^{sea}}{N_{bb}} = \frac{\varepsilon_s}{2}(\sin\beta)^2 + \frac{\varepsilon_p}{2}(\cos\beta)^2 = \frac{1}{2} - \rho_v \tag{3.9}$$

$$\varepsilon = \varepsilon_h + \varepsilon_v = \frac{N^{sea}}{N_{bb}} = \frac{\varepsilon_s}{2} + \frac{\varepsilon_p}{2} = 1 - \rho \tag{3.10}$$

The emissivities ε_s, ε_p, and reflectances ρ_s, ρ_p, for sea water at a wavelength of 10 μm, are shown in Figure 3.3.

---

[2] In Ref. 8 the emissivity ε is denoted by A, and it is referred to as "the Fresnel emission coefficient".
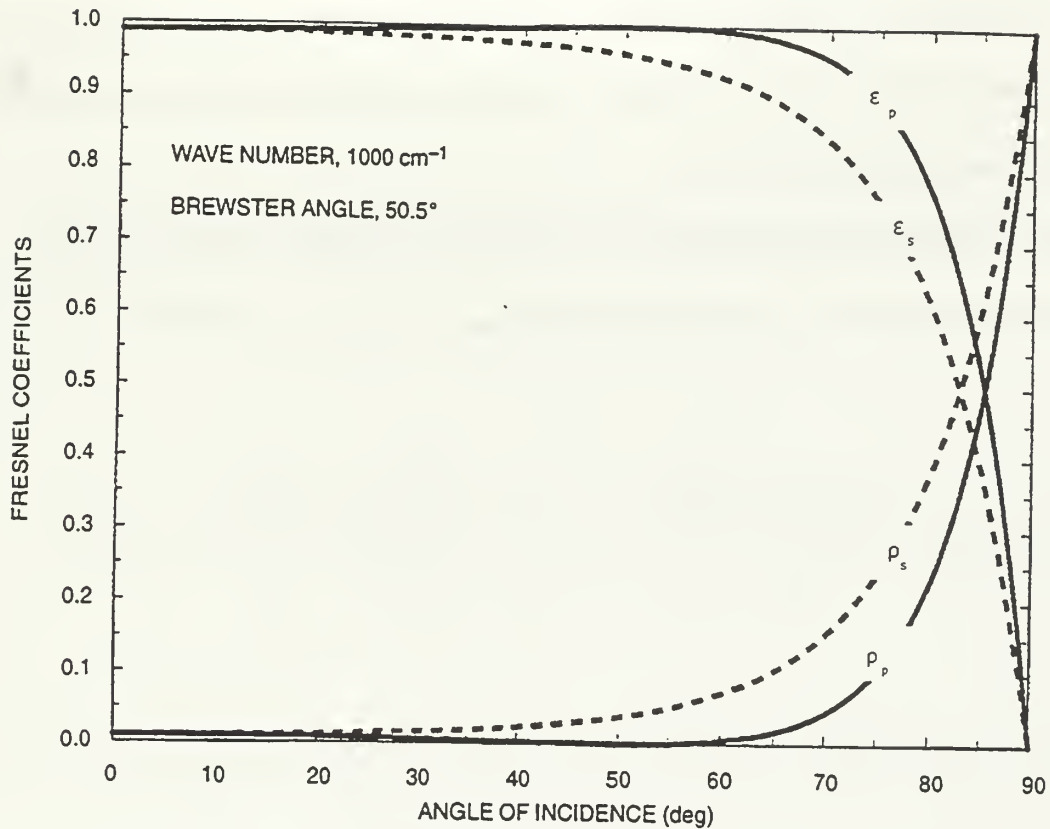
Figure 3.3 Sea Water Emissivities and Reflectances for a Wavelength of 10 μm; s Refers to the Component Perpendicular to the Plane of Incidence, and p to the Component Parallel to the Plane of Incidence [Ref. 8].

C.   TOTAL RECEIVED RADIANCE

The expressions derived in the two previous sections for the polarized reflected and emitted radiance refer to a single wave slope of the sea surface. Integrating over all slopes, and applying a weight for each one of them, it is possible to calculate the radiance leaving the footprint of the sea surface either by reflection or by emission.

Usually the receiver is located a substantial distance away from the footprint. Thus atmospheric attenuation and path radiance must also be taken into account, along with the reflected and emitted radiation. The path radiance N^{path} is unpolarized.

Averaging over all angles of arrival and assuming a perfect polarizer, half of the path radiance will be added to the vertical component, and half to the horizontal component of the received radiance [Ref. 8].

Summarizing the above, the received sea radiance, with the polarizer in the horizontal direction N_h, in the vertical direction N_v, and removed N is:

$$N_h = \left\{ \left\langle N_0 \frac{\rho_s \cos^2 \beta + \rho_p \sin^2 \beta}{2} \right\rangle_r + N_{bb} \left\langle \frac{1 - \rho_s \cos^2 \beta - \rho_p \sin^2 \beta}{2} \right\rangle_r \right\} \tau f + \frac{N^{path} f}{2} \qquad (3.11)$$

$$N_v = \left\{ \left\langle N_0 \frac{\rho_s \sin^2 \beta + \rho_p \cos^2 \beta}{2} \right\rangle_r + N_{bb} \left\langle \frac{1 - \rho_s \sin^2 \beta - \rho_p \cos^2 \beta}{2} \right\rangle_r \right\} \tau f + \frac{N^{path} f}{2} \qquad (3.12)$$

$$N = N_h + N_v = \left\{ \left\langle N_0 \frac{\rho_s + \rho_p}{2} \right\rangle_r + N_{bb} \left\langle 1 - \frac{\rho_s + \rho_p}{2} \right\rangle_r \right\} \tau f + N^{path} f \qquad (3.13)$$

where:

- N_0 is the incident radiance.

- N_{bb} is the emitted blackbody radiance of the sea water.

- ρ_s is the reflectance in the s plane (plane perpendicular to the plane of incidence).

- ρ_p is the reflectance in the s plane (plane parallel to the plane of incidence).

- β is the angle between the plane of incidence and the plane of vision.

- τ is the "in band" transmittance along the path[3].

- f is the "in band" fraction of radiance[4].

The angular brackets in Equations 3.11, 3.12, 3.13 represent the following integral over the slope space:

$$\langle g \rangle_r \equiv \frac{\displaystyle\iint_{\substack{\omega \leq \pi/2 \\ U_r = \text{const}}} g \frac{\cos\omega}{\cos\vartheta_n} p(\zeta_x, \zeta_y, W) d\zeta_x d\zeta_y}{\displaystyle\iint_{\substack{\omega \leq \pi/2 \\ U_r = \text{const}}} \frac{\cos\omega}{\cos\vartheta_n} p(\zeta_x, \zeta_y, W) d\zeta_x d\zeta_y} \tag{3.14}$$

where:

- ω is the angle of incidence and the angle of reflection of the radiation (Figure 3.1).

- θ_n is the zenith angle of the sea facet normal.

- ζ_x is the facet slope in the upwind direction (Figure 3.1).

- ζ_y is the facet slope in the cross wind direction (Figure 3.1).

- $p(\zeta_x, \zeta_y, W)$ is the probability that a wave facet will have a slope within $\pm d\zeta_x/2$ of ζ_x, and $\pm d\zeta_y/2$ of ζ_y, with a wind speed W. This probability is given by a model developed by Cox and Munk [Ref. 14, 15]

---

[3] τ is referred to as the "spectral transmission" in Ref. 8

[4] f is referred to as the "relative spectral responsivity" in Ref. 8

27

D. POLARIZATION CHARACTERISTICS OF SEA RADIANCE

The radiance N_o incident on the sea surface is the sum of radiance coming from the sun and radiance coming from the sky. Equations 3.11, 3.12, and 3.13 can be rewritten in a way such that the contribution of the sun incident radiation and the sky incident radiation is more explicit. By denoting N^{sun} the integrated reflected radiance due to the sun radiation, N^{sky} the integrated reflected radiance due to the sky radiation, and using the h and v subscripts, for the horizontal and vertical components respectively Equations 3.11, 3.12, and 3.13 can be rewritten as follows:

$$N_h = \left\{ N_h^{sun} + N_h^{sky} + N_h^{sea} \right\} \tau f + \left\{ \frac{N^{path}}{2} \right\} f \tag{3.15}$$

$$N_v = \left\{ N_v^{sun} + N_v^{sky} + N_v^{sea} \right\} \tau f + \left\{ \frac{N^{path}}{2} \right\} f \tag{3.16}$$

$$N = N_h + N_v = \left\{ N^{sun} + N^{sky} + N^{sea} \right\} \tau f + \left\{ N^{path} \right\} f \tag{3.17}$$

The degree of polarization P of the observed sea radiance is then defined as:

$$P = \frac{N_h - N_v}{N} = \frac{N_h - N_v}{N_h + N_v} \tag{3.18}$$

A negative value of the polarization indicates vertically polarized radiation. The percent degree of polarization is simply the degree of polarization multiplied by 100.

The problem of predicting the polarization of the observed sea radiance has been addressed in previous studies [Ref. 1,2]. In these studies it has been shown that the reflected sun and sky radiance are predominantly polarized in the horizontal direction. On the other hand the emitted sea radiance has been shown to be vertically polarized. The total degree of polarization of the received sea radiance is given by summing the horizontally polarized reflection terms with the vertically polarized emission term.

Figure 3.4 shows the predicted degree of polarization for the MWIR and the LWIR bands, in the sun glint region. The polarization is plotted, for selected sun zenith angles, as a function of the observer azimuth angle relative to the sun azimuth. In the case of the MWIR band, the polarization appears horizontal (positive) inside the sun glint, and vertical (negative) outside of it, for most sun zenith angles. In the LWIR band, the polarization is vertical both within and outside the sun glint region, for almost all the selected sun zenith angles. The difference in polarization between the two bands is due to fact that the LWIR band contains only 0.1% of the vertically polarized reflected solar radiation [Ref. 2]. The SWIR band, on the other hand, contains 6% of the solar radiation [Ref. 2]; that is why the horizontally polarized reflected sun radiance dominates over the vertically polarized emitted sea radiance, in the sun glint region.

Experimental data analysis [Ref. 2] confirms the predicted degree of polarization
depicted in Figure 3.4. Concluding it can be said that in the LWIR band that is examined
in this thesis, the observed sea radiance is polarized vertically outside the sun glint region,
due to the dominant sea surface emission term of the received radiance.
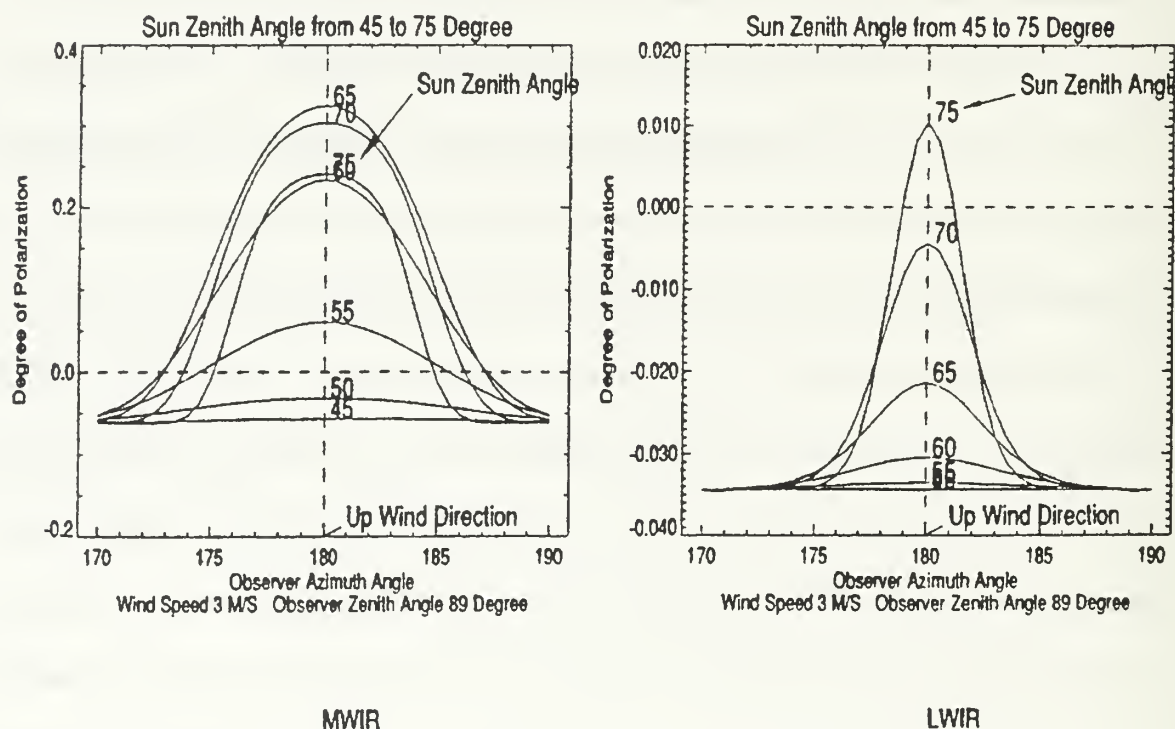
Figure 3.4 Theoretically Predicted Degree of Polarization in the Sun Glint Region, for the
MWIR and LWIR, as a Function of Solar Azimuth and Zenith Angles [Ref. 1].

IV.   DATA ACQUISITION AND ANALYSIS

To examine whether the polarized version of the SEARAD model predicts accurately the polarization effects of sea radiance, a direct comparison with experimental data is needed. Data are available to qualified people in the EOPACE data base in the internet address http://sunspot.spawar.navy.mil/543//eopace/eomain.html. The acquisition of the data was done by Professor A.W. Cooper, W.J. Lentz, LT Britton, Dr. P.L. Walker, the crew of R/V POINT SUR, and the NPS Boundary Layer Meteorology Group by Professor K.L. Davidson and P. Fredrichsen. I performed the data analysis.

A.   EXPERIMENT DESCRIPTION

The EOPACE data analyzed in this thesis were collected during an experiment conducted in April 1996 in San Diego Bay. Infrared images in the LWIR band of the R/V POINT SUR were recorded for two days, 9 and 10 of April, using the AGA-780 thermal imager. Internal polarization filters were employed with the camera to obtain three sets of images, unpolarized, horizontally and vertically polarized, for a certain period of time and position of the ship. The camera was positioned on the tip of Point Loma, inside NRAD building 15, with geographical coordinates 32° 39' 55'' N, 117° 14' 31'' E. It was mounted on a pan and tilt head, extended through the window. The height of the camera was not available from the EOPACE data base. To overcome that, the known position of the camera, which was 32° 39' 55.02'' N and 117° 14' 31.02'' E, was plotted on a nautical chart of the San Diego Bay and the elevation was found to be 90 feet (27.4 m) from mean sea level, using the isoheights on that chart. The ship assumed predetermined

31

positions, with bearings ranging from 135° to 200°, and ranges from 0.5 to 3.0 nautical

miles as indicated in Figure 4.1. In each of the above positions the ship changed its

heading from 280° to 100° turning clockwise. Full meteorological data, including ship

GPS position, heading, and ship temperatures, were recorded on the R/V POINT SUR,

for the two days of the measurements.
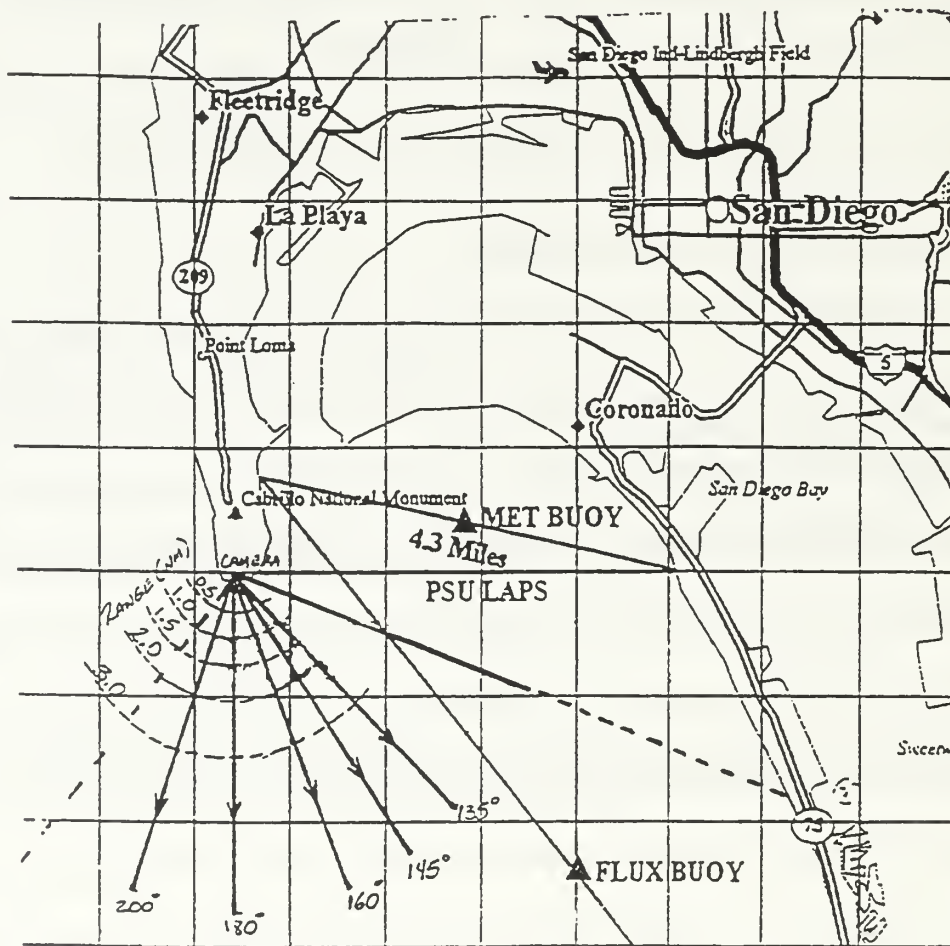
Figure 4.1 Experiment Location Map Depicting the Positions Assumed by R/V POINT SUR.

B.   INSTRUMENTATION

1.   The AGA 780 Thermovision Thermal Imaging System

The AGA 780 is a dual band infrared scanner. It can operate in the MWIR band from 3 to 5.6 µm using an InSb detector, and in the LWIR band from 8 to 12 µm using a HgCdTe detector. The cooling of the detectors is accomplished by the use of liquid nitrogen at 77° K. The AGA scanner unit uses two rotating prisms, one vertical and one horizontal, producing one interlaced frame consisting of four fields each having 70 active image lines. There were two types of input lens used with the camera in the experiment, 7° x 7° and 3.5° x 3.5° field of view lenses. The geometrical resolution achieved by the AGA 780 is 1.1 mrad for the 7° x 7° lenses and 0.5 mrad for the 3.5° x 3.5° lenses [Ref. 16] The aperture was set to f/1.8 for the duration of the experiment. The arrangement of electro-optical components of the camera is presented in Figure A1 in Appendix A.

The camera's measure of the received radiance, is called the Thermal Value [Ref. 16: p. 10.1]. It is measured in arbitrary Isotherm Units. The Thermal Value is proportional to the incident photon radiation flux. On the other hand, the relation between the Thermal Value and the apparent temperature of an object is not linear. The latter relation can be obtained by the means of laboratory calibration curves that give the Thermal Value as a function of blackbody temperature as shown in Figure A.2 in Appendix A.

2.   Internal Polarization Filters

The polarization filters used in the experiment were manufactured by Graseby Specac, and consisted of an aluminum grid on a round KRS-5 substrate. The specifications of the filters predicted 85% transmission efficiency for wavelengths from 1

to 12 μm. The effectiveness of polarization was given as 98%. The performance curves for the two filters are depicted in Figures A.3 and A.4 in Appendix A. As we can see from the two Figures the performance of the two filters is nearly identical.

The filters were positioned in the internal filter wheel mounting of the AGA, which has seven positions, selectable from the filter control knob, as shown in Figure A.1 in Appendix A. The positioning of the two filters was done in such a manner that one filter would pass the horizontal incident radiation, and the second one the vertical incident radiation. Thus by changing the position of the knob periodically, three sets of images of the R/V POINT SUR were recorded:

- horizontally polarized images, in position 4
- vertically polarized images, in position 5
- unpolarized images, in position 6, with no filter.

For each of the above positions a calibration procedure was performed in the laboratory, (by E.C. Crittenden on 3-21-96), using the NOSC LW Head. He recorded the AGA thermal level of a blackbody for various temperatures. Then by a curve-fitting process, a calibration curve was obtained for each of the three positions, 4, 5, and 6, as shown in Figure 4.2. The curve fitting equation is:

$$I = \frac{A}{C * \exp(B/T) - 1} + OS \tag{4.1}$$

where:

34

- I = Thermal value corresponding to temperature T (Isotherm Units)

- T = Temperature in K

- OS = Offset

The constants A, B, C depend on the filter position set on the camera 4, 5, or 6, as shown on Figure 4.2

Figure 4.2 Calibration Curves for Filter Positions 4,5,and 6.

NRAD (NOSC) Head. LW

Internal Polarizers, 3/21/96

POS 4 OR 5 A=1675,B=1348, OS=39

POS 6,A=6808,B=1511,OS=12

CAVITY BLACK BODY TEMPERATURE

+ Position 5   ◊ Position 6   × Position 4
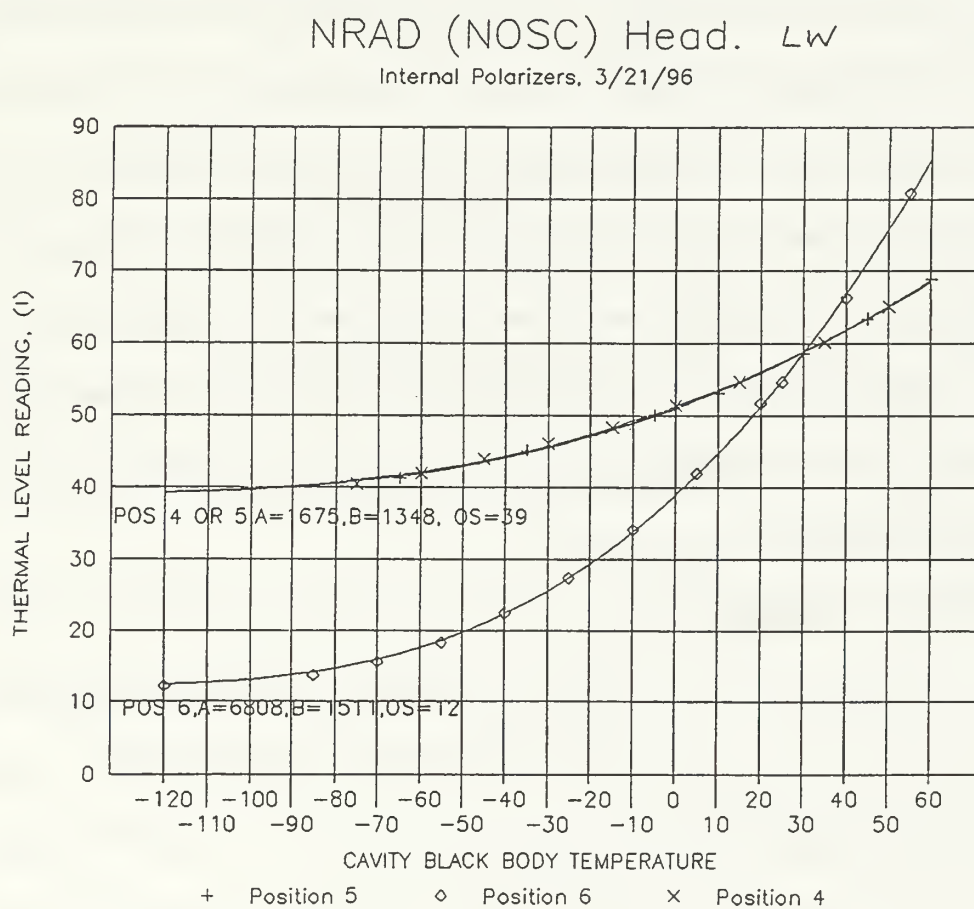
3. R/V POINT SUR

The R/V POINT SUR is a ship 135 feet long, which is owned by the National Science Foundation and operated by the Moss Landing Marine Laboratories. In the San

Diego experiment on April 96 it was used as an infrared target. The ship's equipment was used to record meteorological data, and GPS position, and a thermistor set installed by NPS measured spot temperatures of its hull.

C. ORIGINAL DATA

1. Recording Software

The experiment data were recorded using a program called PTRWIN developed by the French company CEDIP. This software employed five hardware cards, the PTR card, the DSP card, the RANGEL card, the TOPAZE card, and the VGA card, installed in the docking station of an NEC laptop computer for the recording of the data. These acquisition boards allowed the interface with the AGA 780. Of these cards the one labeled PTR by the manufacturer allowed digitization of the analog video of the scanner into 12 bit integers which are referred to as the Digital Level. Besides being used as a recording software, PTRWIN is also able to perform some limited analysis of the data under the Windows operating system.

2. Images

As mentioned above, three sets of images were recorded for a specific position and heading of R/V POINT SUR: horizontally polarized, vertically polarized and, unpolarized images. For each polarization case there is a series of images recorded, usually 26. A sample set of these images is contained in Appendix B. The polarized frames are recorded together in one file, and the unpolarized ones are recorded in a separate file. Each file begins with a main header which contains general information, such as day and time data, scanner parameters etc. The main header is then followed by

the image frames. Each frame consists by a frame header and the four fields of an image as shown in Figure 4.3

| Main Header |
| First Frame header |
| 1st field of first frame |
| 2nd field of first frame |
| 3rd field of first frame |
| 4th field of first frame |
| |
| 1st field of last frame |
| 2nd field of last frame |
| 3rd field of last frame |
| 4th field of last frame |

Figure 4.3 Structure of the Image Files

Each field is made up of 64 lines. A line has 125 pixels. There are four fields per frame, so the frame is an array of 4(64)=256 by 125 pixels.

3.   Geographical and Meteorological Data

The geographical data were recorded using the ship's GPS system located in the electronics laboratory. For the collection of the meteorological data, two meteorological towers were installed on the ship. One was positioned over the bridge, and the other on the bow. The measurements from these towers were averaged over periods of 30 seconds and recorded along with the GPS position and heading into two different sets of files, the

37

METOC 1 and METOC 2 format files. The exact structure of those files is given in Appendix C

4. External Ship Temperatures

To measure the external temperatures of the ship, 16 thermistors were installed on her hull by NACIT- NPS. The thermistors were connected to a computer and their outputs were recorded along with time information in special "skin" files, for the duration of the experiment. The temperatures were recorded in 20 second intervals. The positions of the thermistors are shown in Figure D1 in Appendix D. The format of the files, in which the data were recorded, is also given in Appendix D.

D. DATA ANALYSIS

1. Data Processing

I used programs written in Interactive Data Language (IDL) to process the data and bring them into a format suitable for analysis.

a) Images

The original image files with a PTW extension had to be converted to a different format with a PTE extension. The reason for that conversion was that the original files were too large, and contained information unnecessary for the purpose of this study. Furthermore the polarization cases were separated into two different files, one for the horizontal and vertical polarization and one for the unpolarized case. The IDL program used to perform this conversion, called CONVERT.PRO, is based on an existing program BASEGEN.PRO written by M.C. Pontes [Ref. 17].

38

Another problem that arose with the original images was the fact that each pixel of the image was recorded in Digital Level. A pixel in the image occupies two bytes, but only twelve bits were used, giving Digital Level numbers from 0 to 4096. The Digital Level (DL) is an arbitrary unit of measurement which is linearly proportional to the received radiance. The existing calibration curves for the AGA 780 relate the isotherm units (IU) to temperature. Therefore, there is a need to convert from DL to IU, so that we can extract apparent temperature and radiance from an image.

The relation between the DL and IU is not given by the existing PTRWIN documentation. There is however a feature in the analysis part of the PTRWIN program that allows the conversion from DL to IU for a single pixel. This is done by using information about the thermal range and thermal level settings of the AGA 780, at the time of recording. The thermal range is selected by a knob on the camera, as shown in Figure 4.4, and corresponds to different scales depending on the variation of intensity of the received radiation. The thermal level is also selected by the user in order to display both the lowest and the highest temperatures of the object. Both of these settings were recorded automatically for each frame in the original data, through the card labeled RANGEL by the manufacturer, in the NEC docking station.
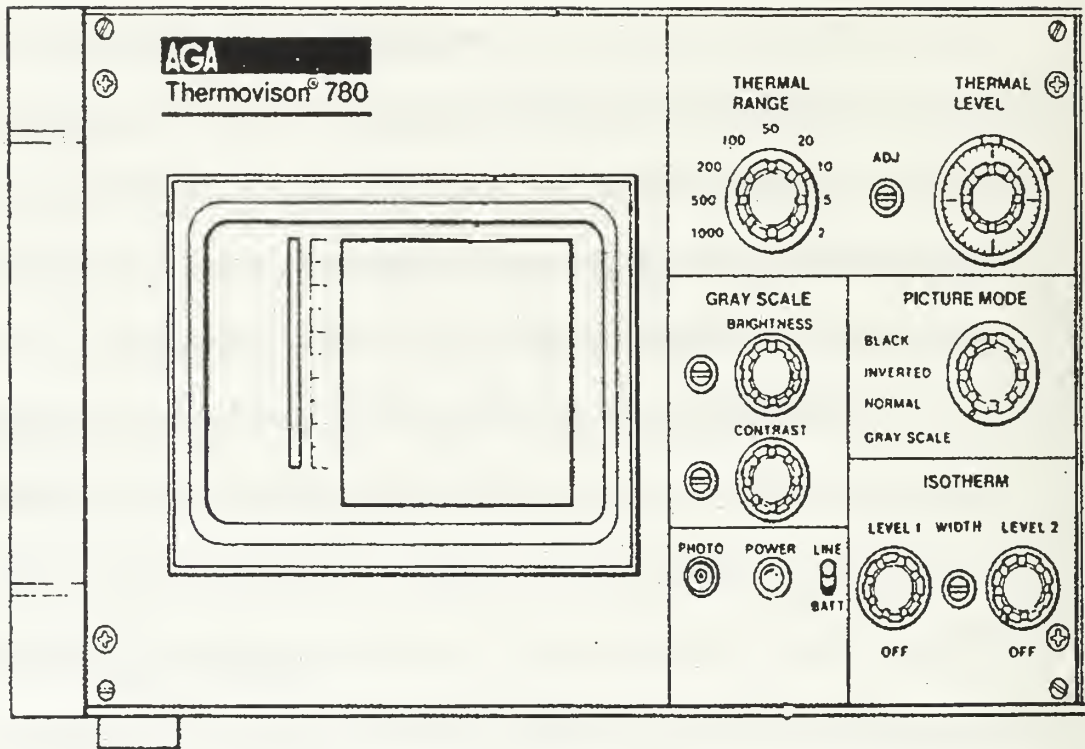
Figure 4.4 Thermal Range and Level Controls [Ref. 16]

The desired relation between DL and IU can be obtained by plotting the IU against DL for a large number of pixels taken from the same frame. Then a line fitted to the points gives the conversion relation for that frame, as we can see in Figure 4.5.

After processing frames having different thermal ranges and levels it was concluded that a linear dependence exists between the DL and IU. This linear dependence is expressed by the following relation:

$$IU = a\,(DL) + b \qquad\qquad (4.2)$$

where a and b depend on the thermal range and level as shown in Table 4.1. This process can be applied for each frame set used. The values a and b are constant between frames that were recorded with the same thermal range and level settings.
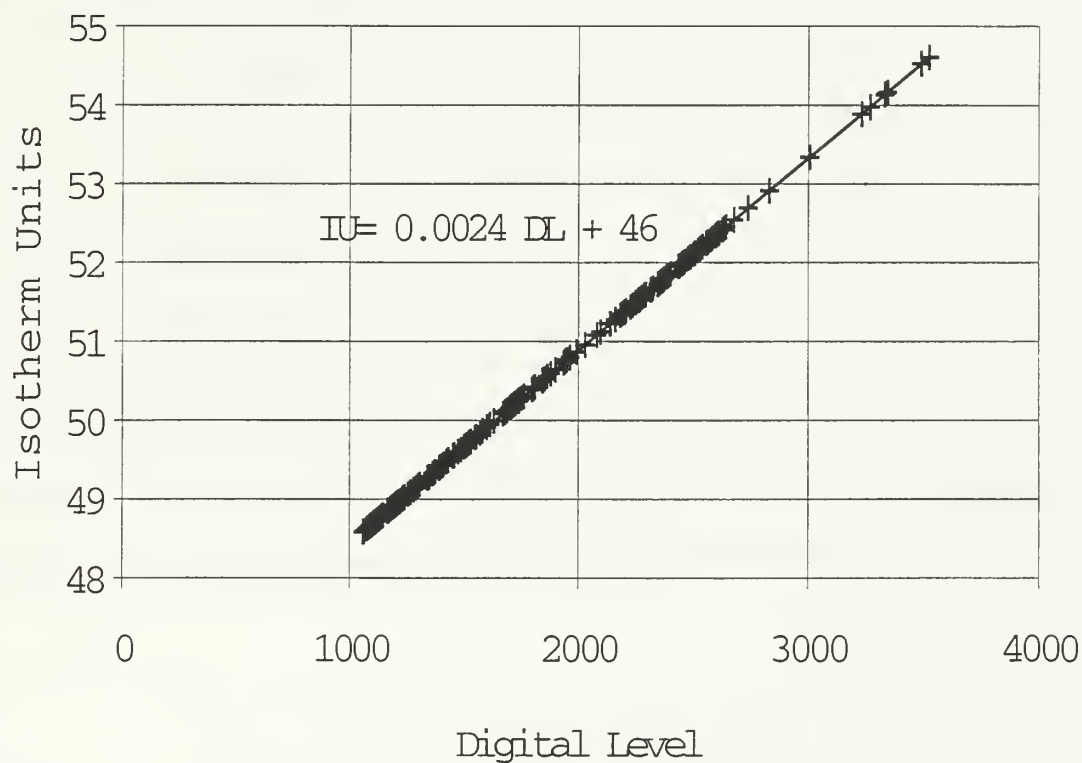
Figure 4.5 Plot of Isotherm Units against Digital Level.

Thermal Range	a	b
5	0.001221	Thermal Level-2.5
10	2x0.001221=0.002442	Thermal Level-2(2.5) = Thermal Level-5
20	4x0.001221=0.004884	Thermal Level-4(2.5) = Thermal Level-10

Table 4.1 Values of the a and b Coefficients

b)   *Geographical and Meteorological Data*

The original METOC data were recorded in GMT time, while the images were recorded in PST time, so the geographical and meteorological had to be converted to PST time, to be able to correlate them with a specific frame. Furthermore not all the information in the original files was useful for the present study, so a new file was created, called GEOMET.PTE containing only the parameters needed. Those parameters are listed in Table 4.2.

c)   *Ship Temperature Data*

As mentioned in the previous section the ship's external temperatures were recorded through the use of thermistors, in special "skin" temperature files. The first column, out of seventeen, of the original skin data files represents the time in seconds that has elapsed from the initial recording time as shown in Appendix D. There is not,

however, an indication inside the temperature files, or the files that accompany them, as to whether this time is local Pacific Standard Time or GMT time.

Parameter	Units
Time elapsed from 00:00 PST	Sec
Latitude of the ship	Min
Longitude of the ship	Min
Antenna height	Meters
Air temperature	Degrees C°
Relative Humidity	Percent %
Air Pressure	Mbar
Wind speed	meters/second
Wind Direction	Degrees relative to North
Temperature of the Sea Surface	Degrees C°

Table 4.2 Parameters used in the GEOMET.PTE file

To clarify this discrepancy, and be able to correlate the temperatures with the image frames, a direct comparison with the meteorological data was performed. Thermistor number three had been positioned in the water surface underneath the stern of R/V POINT SUR as depicted in Figure D.1. The temperature of the sea surface was also recorded by the meteorological stations. The two temperatures were plotted together for the 9th of April assuming that the thermistor temperatures were recorded in Pacific Standard Time (PST). This plot is shown in Figure 4.6.

43

The variation of the two temperatures over time, on Figure 4.6 is very similar, leading us to the conclusion that the ships hull temperatures were indeed recorded in PST time.
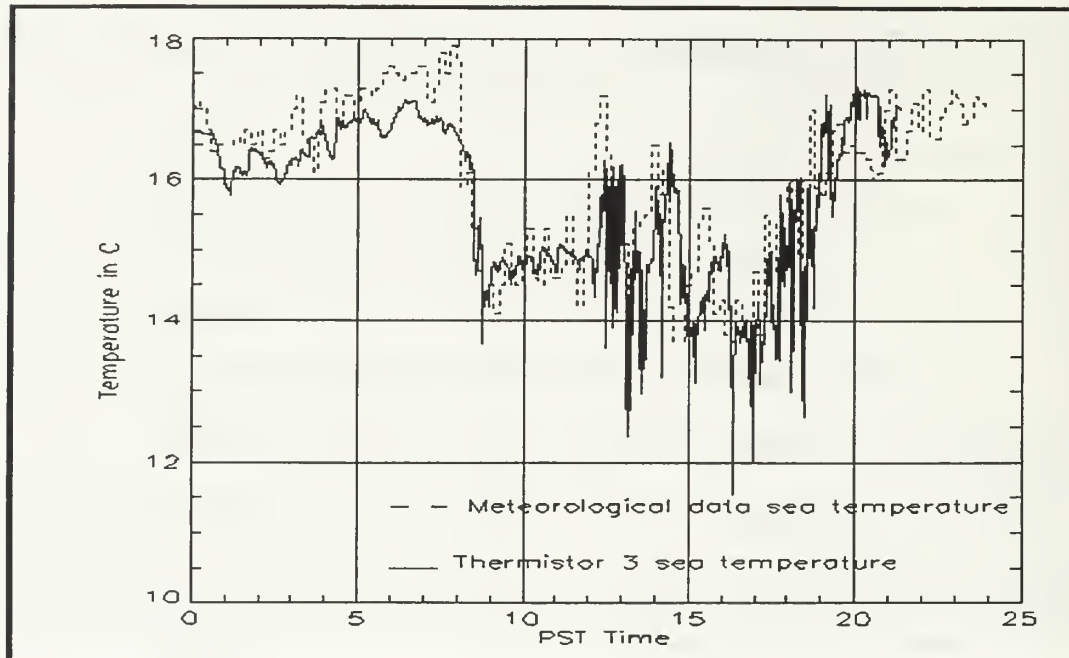
Figure 4.6 Comparison of the Meteorological Data Sea Temperature and Thermistor 3 Sea Temperature, to Clarify in which Time Zone were the "Skin " Data Recorded

2. IDL Programs

The analysis of the experimental data was performed by using primarily programs written in the Interactive Data Language (IDL). IDL is an array oriented language which provides many mathematical analysis tools and techniques for graphical display. Compared to other programming languages such as FORTRAN or C, it is significantly faster because its operators work on entire arrays. Moreover it provides means of

44

visualization of the data. Finally its input and output capabilities allow the manipulation of any data file format.

The purpose of the IDL programs written in this study was to take the original images, correlate them with the existing geographical, meteorological, and temperature data; and produce proper input for use by the SEARAD model. In that way a direct comparison can be made between the experimental data and the theoretical predictions of the polarized version of SEARAD, about the polarization effects from the sea surface.

Some IDL programs of particular interest are described below. The code for these programs is given in Appendix E

a) *Geography.pro*

The SEARAD model requires as an input the relative geographical position of the observation point and the point on the sea we are interested in, which is called the footprint. Geography.pro takes as input the GPS position, and the height of the camera, as well as the GPS position, and the height of the ship which are recorded in the METOC data. Then based on that input, it calculates the slant path distance from the camera to the ship, the true azimuth of the ship, and the zenith angle of the line of sight to the ship, as shown in Figure 4.7.

b) *Data.pro*

Data.pro uses the recorded time on each image frame to interpolate the meteorological data, the position data given by Geography.pro, and the ship temperature data. After the interpolation a new file is created that has additional information about the

image including the thermistor temperatures. This additional information is inserted in the form of a matrix at the end of each image matrix. The contents of the matrix is laid out in Table 4.3.
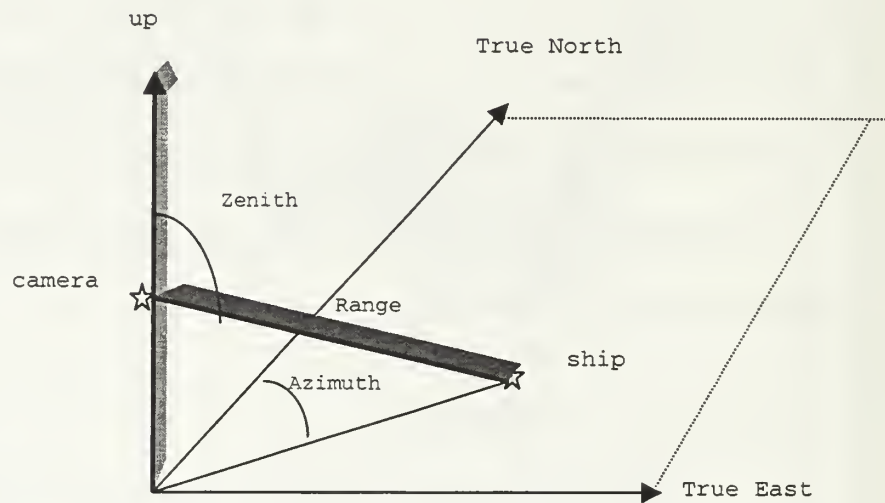
Figure 4.7 Position Data given by Geography.pro

c) *Tape5ship.pro*

Tape5ship.pro reads the geographical and meteorological data created by Data.pro that correspond to a specific image frame. Then it produces a Tape5 file, which is an input file for the SEARAD code, for the position where the ship was for a specific time. The reason we need this file is that we want to know what the transmittance and the path radiance were for that position of the ship. We can get that information when we run

SEARAD with the Tape5 file that Tape5ship.pro produces, as input. A sample of the Out file that SEARAD creates is given in Appendix F.

1	Frame time elapsed in sec	17	Temperature from thermistor 1 in C
2	Latitude of the ship in min	18	Temperature from thermistor 2 in C
3	Longitude of the ship in min	19	Temperature from thermistor 3 in C
4	Ship height in meters	20	Temperature from thermistor 4 in C
5	Air temperature in C	21	Temperature from thermistor 5 in C
6	Relative Humidity in %	22	Temperature from thermistor 6 in C
7	Air Pressure in mbar	23	Temperature from thermistor 7 in C
8	Wind speed in m/s	24	Temperature from thermistor 8 in C
9	Wind Direction relative to North	25	Temperature from thermistor 9 in C
10	Latitude of the camera in min	26	Temperature from thermistor 10 in C
11	Longitude of the camera in min	27	Temperature from thermistor 11 in C
12	Height of the camera	28	Temperature from thermistor 12 in C
13	Slant path range from the camera to the ship in m	29	Temperature from thermistor 13 in C
14	Zenith angle from the camera to the ship in min	30	Temperature from thermistor 14 in C
15	True Azimuth angle of the ship in minutes	31	Temperature from thermistor 15 in C
16	Stack temperature given by the average of thermistors 12 and 14	32	Temperature from thermistor 16 in C

Table 4.3 Information Matrix generated by Data.pro

d) *Input.pro*

Input.pro can be considered as the main analysis program in this study. It employs many other programs -functions to extract input information for SEARAD, from a specific set of images which consists of a horizontally polarized image, a vertically polarized image and an unpolarized image.

It begins by using the following programs, written by M.C. Pontes [Ref. 17] and modified for the needs of this thesis:

- Hotspot.pro: Finds the point on the ship's stack with the greatest temperature (hotspot).

- Horizon.pro: Provides the equation of the horizon in an image.

- Elements.pro: Generates an array that has the same dimensions as the image array, but the values in this array are ones where there is a sea pixel, and zeros everywhere else (ship and sky). This array is called a mask.

The program continues by sampling the selected image every nine pixels horizontally and every nine pixels vertically. This action corresponds to sampling the image every half degree vertically and every one fourth of a degree horizontally, because the image is an array of 125 by 256 pixels and the field of view of the camera is 7° x 7°. So 9 pixels vertically are equivalent to $7^{\circ}/125(9) = 0.5^{\circ}$, and 9 pixels horizontally are equivalent to $7^{\circ}/256(9) = 0.25^{\circ}$.

Input.pro then retrieves information about the zenith and azimuth angles of the reference point on the ship, and calculates the zenith and azimuth angles at every point that is sampled, by determining the relative position of the sampling point and the reference point. This is better understood by looking at an example. Suppose that at the

reference point the zenith angle is $91°$, the azimuth angle is $100°$, and the data coordinates are 50 and 130. One sample point has data coordinates 60 and 240. Then at the sample point the zenith angle is $91° + (60-50)/9(0.5°) = 91.56°$ and the azimuth angle is $100° - (240-130)/9(0.25) = 96.95°$.

Not all the sampled points correspond to sea pixels. To eliminate the unwanted points we multiply them by the mask matrix, obtained by the Elements.pro program. The mask matrix has ones where we have sea pixels and zeros everywhere else. After the multiplication process we are left solely with sea pixels, which are the ones we are interested in.

Finally, Input.pro provides information about the wind speed, the wind direction relative to the LOS at each point, sea surface temperature, and time of each frame. These data along with the zenith and azimuth angles of each point are the only information needed for SEARAD to predict the radiance from a specific point at sea.

e) *Isotherm.pro, Radiance.pro, Invrad.pro, Offset.pro, and Temp.pro*

The task of providing SEARAD with inputs is accomplished by Input.pro as described above. However to be able to perform a direct comparison between the output apparent temperatures of SEARAD and the experiment, we need to have an apparent temperature for each of the sampling points.

The data as mentioned earlier in this chapter were recorded in units of Digital Level. Isotherm.pro converts the digital level to isotherm units, using the linear

relations between the two, which depend on the thermal range and thermal level of the camera.

The conversion from isotherm units to temperature can be achieved through the use of the calibration curves for each of the polarization filters. These curves, however, correspond to zero range measurements, so to use them, we must also bring the experiment measurements to zero range. The recorded isotherm units for each pixel in the image have the following components:

- The radiance due to the temperature of the body multiplied by the transmittance for the range from the object to the camera.

- The reflected radiance from the object surroundings multiplied by the transmittance for the range from the body to the camera.

- The path radiance.

For the case of the stack (hotspot) we know the temperature from the ship's thermistors, and SEARAD can calculate the transmittance as well as the path radiance from the camera to the ship having as an input the Tape5 file created by Tape5ship.pro.

Radiance.pro calculates the radiance emitted by the hotspot using the Stefan-Boltzmann law:

$$M(T) = \sigma T^4 \qquad (4.3)$$

where:

50

- M(T):is the total radiant exitance from a black body surface

- σ : is the Stefan-Boltzmann constant $= 5.6697 \times 10^{-12}$ Watts-cm^{-2} K^{-4}

- T: is the black body's temperature

Then the radiance is:

$$N = \frac{M}{\pi} f \qquad (4.4)$$

where:

- N: is the "in band" Radiance

- f: is the "in band" fraction of radiance in the 8 to 12 μm range. It is obtained from the universal blackbody curve [Ref. 9].

The calculated black body radiance for the hotspot is then multiplied by the transmittance, and the path radiance is added to the result giving us the total radiance that the camera receives at a specific ship-camera range. In the previous procedure the reflected radiance originating from the object surroundings is not taken into account, because there is not enough information to do so. Nonetheless its contribution is not considered very big, because the stack is much hotter than its surroundings, has an emissivity close to one, and moreover, this reflected radiance is multiplied by the transmittance and thus its weight is greatly reduced.

Invrad.pro uses the total apparent radiance calculated by Radiance.pro, and finds an apparent temperature by employing the Stefan-Boltzmann law once more. This

temperature is the apparent temperature of the stack which includes the effects of atmospheric absorption and path radiance.

The process of correcting the stack temperature can be expressed by the following equation:

$$T_{final} = (\frac{f\sigma T_{initial}^4 \tau / \pi + N^{path}}{f\sigma}\pi)^4 \qquad (4.5)$$

where:

- T_{final}: is the corrected temperature of the stack.

- $T_{initial}$: is the temperature of the stack recorded by the thermistors.

- f: is the "in band" fraction of Radiance in the 8 to 12 μm range.

- σ : is the Stefan-Boltzmann constant $= 5.6697 \times 10^{-12}$ Watts-cm^{-2} K^{-4}.

- τ: is the "in band" atmospheric transmittance.

- N^{path}: is the "in band" path Radiance.

Offset.pro employs the corrected apparent temperature along with the known isotherm unit (IU) value on the stack to calculate the offset OS by using Equation 4.1 as shown below:

$$OS = I - \frac{A}{C\exp(B/T) - 1} \qquad (4.6)$$

Since the offset has been calculated, the calibration curves for the AGA 780 can now be used. With the IU and the offset known for every sampling point,

Equation 4.1 can be solved to give us the apparent temperature of every point. The above procedure is performed by Temp.pro. There is however an approximation involved. The range of the different points at sea to the camera is either smaller or greater than the distance from the camera to the ship. This difference in range affects the transmittance and the path radiance and subsequently the offset, giving a different offset for every range. Nevertheless to calculate these different offsets we need to have a reference temperature at every distance, such as the stack temperature. Unfortunately we do not have these reference temperatures, so we use the offset calculated for the ship-camera range, making the necessary assumption that the offset does not change significantly for the ranges involved.

f) Tape5.pro, Out.pro

Tape5.pro has the task of gathering information from Input.pro and other programs to write formatted Tape5 files, ready to be input by SEARAD. Every sampling point in an image corresponds to a different Tape5 file.

After SEARAD is run for the different Tape5 files a number of output files called Out are generated. These files are read by Out.pro which also makes the comparison of the SEARAD and experimental received sea radiance and degrees of polarization. These results will be presented in the next chapter.

3. Polarized Version of the SEARAD Code

The polarized version of SEARAD, developed by C.R. Zeisse at SPAWAR-SYSCEN NRAD, is a modification of the standard atmospheric propagation code MODTRAN 2. Besides the classic results of MODTRAN, the polarized version of

53

SEARAD predicts the polarization components of the received sea radiance. The way this is done is explained in Chapter III, and summarized briefly by C.R. Zeisse, as follows [Ref. 8: p.1]:

> The Fresnel coefficients are applied to the reflection of unpolarized monochromatic radiation by a sea water capillary wave facet. The result for a single tilted facet is integrated over all possible tilts and wave numbers to predict the polarization dependence of radiance received from the wind-ruffled ocean surface.

The SEARAD model uses an input file called Tape5 to compute the received radiance from the sea surface. An example of such a file is given in Appendix F. The Tape5 contains all the necessary meteorological and geographical information to calculate the sea radiance. Each line in this file is called a "card". The description of the significance of each number in the cards is explained in the LOWTRAN 7 User Instructions [Ref. 18]. The differences of SEARAD from these instructions are contained in the "Notes" file which accompanies the polarized SEARAD model.

The methodology followed for creating the Tape5 files, using IDL programs, was described above. Generally the following parameters were used:

- Midlatitude Summer atmospheric model.

- Slant path to space from the camera height to the sea.

- Program execution in thermal radiance mode.

- Navy maritime aerosol model.

- Air mass parameter 3.

- Wind speed and relative wind direction from METOC data

- Sea temperature from METOC data

- Camera position, zenith and azimuth and time data, from the processed METOC data.

After creating the necessary Tape5 files for all the sampled sea points in an image, a batch file was used to run the program sequentially. The approximate number of Tape5 files per image was 160.

After SEARAD is executed several output files are created. Those are the Tape6, Tape7, Tape8, Path, Sky, Sun, and Out files. For the purpose of the present study the Out file was chosen for the analysis, because it describes adequately the received sea radiance and its polarized components. An example of such a file is given in Appendix F. As can be seen in this file, the received sea radiance and the polarization are provided for zero and full range. The full range results include the path attenuation and the path radiance. Since the received experimental sea radiance was recorded at a certain range, the full range results of SEARAD were chosen for the comparison between theory and actual data. The results of this comparison are laid out in the next chapter.

V.   RESULTS

In this chapter all the experimental results will be compared directly, whenever this is possible, to the predictions of the theoretical model used by the polarized version of the SEARAD code. The comparison will include the apparent received sea radiance, the degree of polarization, and the azimuth dependence of the polarization.

A.   APPARENT RECEIVED RADIANCE

The main concern when trying to compare apparent received radiance is to determine what the offset is in Equation 4.1, so that the conversion from IU to temperature can be accurate. Ideally we need a blackbody for every range and every polarization filter to obtain a point on the calibration curve, and thus acquire the offset. As mentioned in Chapter IV, we only have one such point, the ship's stack. Therefore the offset is correct only for the range from the ship to the camera, and approximately correct for sea pixels in the same image at a distance around this range.

Furthermore, in the case of images recorded with the use of polarizers we cannot use the calibration method analyzed in Chapter IV. This is because, in this case, the hotspot temperature corresponds to a polarized radiance which is a fraction of the total radiance. There is no method by which we can compute what this fraction is. The only way we could obtain the offset for the polarized cases, would be if we had a calibration curve at a specific range, for each of the polarizers used by the camera (vertical or horizontal).

Summarizing, due to calibration restrictions, the comparison between the observed sea radiance from the experiment and the calculated sea radiance from SEARAD was done only for the unpolarized case. A set of 34 images was used, in which the ship-camera distance varied from 0.5 to 1.5 nautical miles and the plots created are presented in Appendix F1. An example of such a plot is shown in Figure 5.1. The experimental and the SEARAD radiance are plotted against the zenith angle. The zenith angle was defined in Chapter IV in Figure 4.5. It is the angle between the Line Of Sight (LOS), which is the line from the camera to a specific point in the sea, and the line that points vertically from the position of the camera. Different zenith angles correspond to different slant ranges. The bigger the zenith angle the smaller the slant range.

Figure 5.1, as well as all the other figures in this Appendix F1, was created by taking approximately 160 points from the unpolarized image and by running SEARAD as many times. Each time SEARAD was run the combination of azimuth angle, zenith angle, and relative sea wind was changed to correspond to the conditions of the experiment, and the target point that was chosen. All the other meteorological conditions were kept the same for each image.

By examining Figure 5.1 and the other plots in Appendix F1, we observe that there is a good agreement between the experimental and the predicted sea radiance. In fact for this particular case, where the ship camera slant range is 1399 m, the average absolute error is 0.36 $Wm^{-2}sr^{-1}$ (about 1.2% of the experimental radiance) and the standard deviation is 0.26 $Wm^{-2}sr^{-1}$.
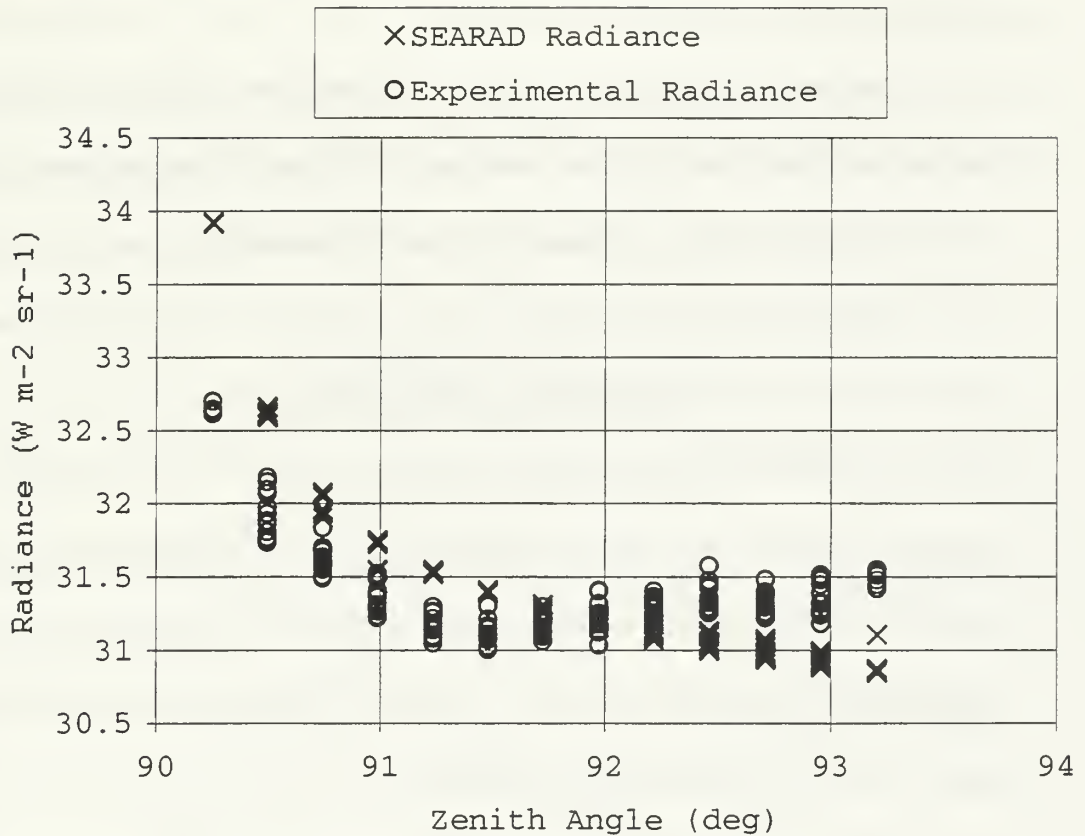
Figure 5.1 Experimental and SEARAD Sea Radiance as a Function of the Zenith Angle. Different Values of Radiance for the Same Zenith Angle Correspond to Different Azimuth Angles.

Figure 5.1 includes equal numbers of experimental and computed values at each zenith angle. We also observe that, for a specific zenith angle we have various values of the radiance. The different values correspond to different azimuth angles from the camera to the target point. The azimuth angle is also defined in Figure 4.3; it is the angle between the projection of the LOS to the earth and the true North. The variation in radiance is to be expected, because when the azimuth changes, the wind direction relative to the LOS, and the relative position of the sun both change, facts that change the total received

radiance [Ref. 1,14, 15]. It is important to the assessment of its accuracy, that SEARAD is actually sensitive to these kinds of changes.

However, the experimental variation in radiance is bigger than the SEARAD variation in radiance for the same zenith angle. In Figure 5.2 the radiance is plotted as a function of azimuth relative to the solar azimuth. For clarity only two zenith angles have been selected. We see in this figure that the variation of the experimental radiance appears random, which may be due to data analysis errors. On the other hand the SEARAD predicted radiance generally decreases when we get away from the sun's azimuth as one might have expected, because then the solar reflected component of the apparent sea radiance becomes less intense. From Figure 5.2 we also see that the variation of the SEARAD radiance is smoother in greater zenith angles (smaller distances), and bigger in small zenith angles (greater distances).

In the other plots of Appendix F1 the agreement between SEARAD and experimental results is not as close as in Figure 5.1. The reason for the increasing differences between the two could be attributed to the fact that an accurate camera elevation is not available. This factor affects the calculated zenith angles, and thus distances from the camera to the different points at sea. Different distances mean that we have different path radiance, and different path attenuation. It is guessed that the mistakes made in these two elements of the total sea radiance cancel each other in the case of Figure 5.1. That may be the reason the results in that case give such a good agreement between theory and experiment.

Finally another factor affecting the quality of the results is the accuracy of the offset calculation. It is known that the offset changes as the experimental conditions, such as the wind, air temperature, and time of day, change. That is why the offset was calculated on a frame by frame basis. Furthermore it is suggested from the analysis of the data that the offset may also be a function of distance.
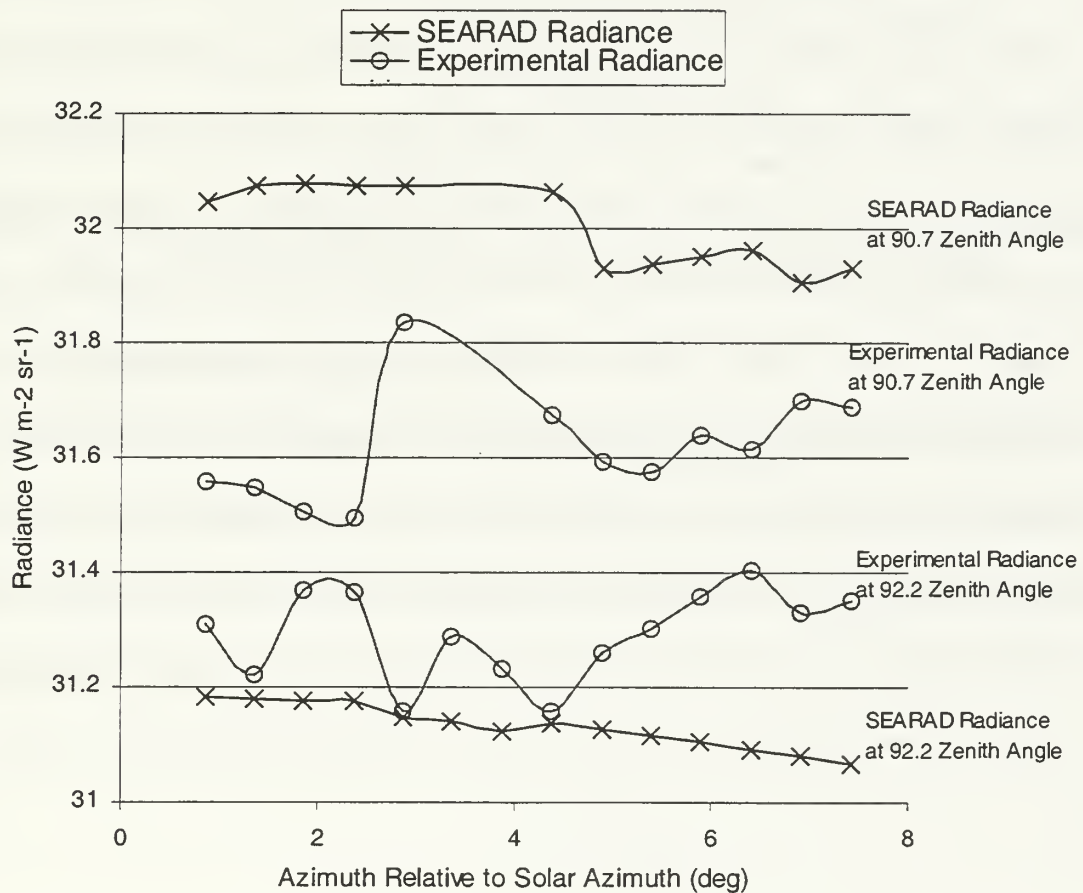

Figure 5.2 Experimental and SEARAD Radiance as a Function of the Azimuth Angle Relative to Solar Azimuth. The Radiance is Plotted for Two Different Zenith Angles, 90.7, and 92.2 Degrees.

In Figure 5.3 the calculated offset is plotted against the slant path range from the camera to the ship. We see from this figure that the offset decreases exponentially as the distance increases. The apparent temperature T and the radiance increase as the offset decreases (Equation 4.5). So the apparent radiance increases with increasing distance (decreasing zenith angle).

Note in Figure 5.1 and in Figures G1.1 through G1.5 that the SEARAD radiance varies with zenith angle which corresponds to a distance change, while the experimental radiance almost levels out at about 91°. These figures were plotted assuming the offset does not change in a particular frame. If based on the analysis of the previous paragraph the offset does change with distance then the plotted experimental radiance would be bigger in the small zenith angles and smaller in the bigger zenith angles. This would change the shape of the curve for the experimental radiance and probably make it look like the shape of the SEARAD radiance. Unfortunately, as mentioned above the offset is also a function of the experimental conditions; thus it was not possible to extract a reliable equation for the offset as a function of zenith angle, because the data points in Figure 5.3 were extracted from different images recorded at various times of the day.
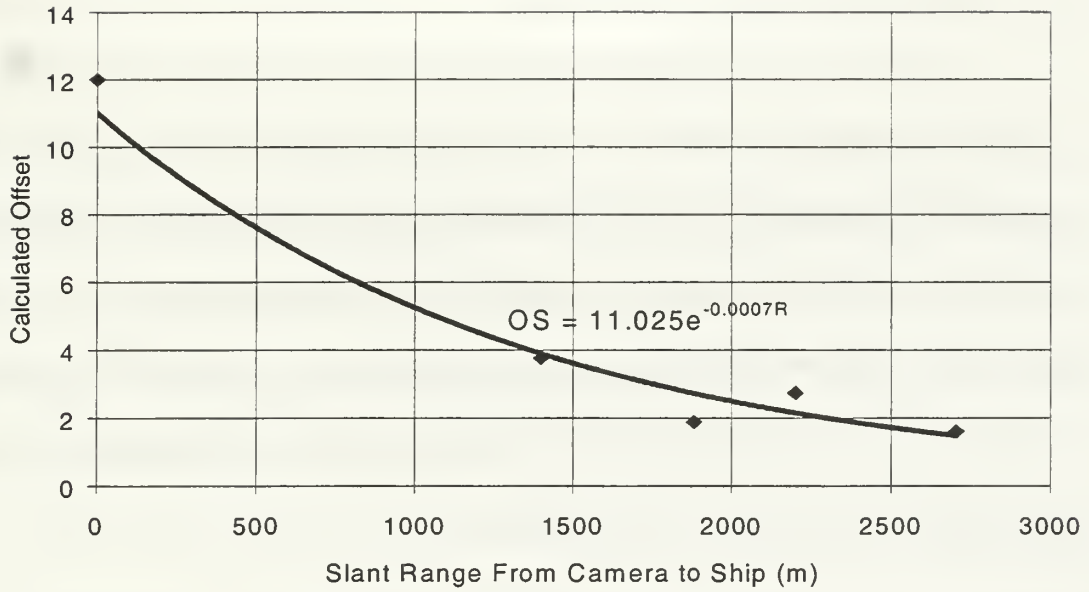
Figure 5.3 Plot of the Calculated Offset as a Function of the Ship Camera Distance. Data Points were Extracted for Different Scenes and Experimental Conditions.

B.   DEGREE OF POLARIZATION

The degree of polarization P is, as discussed in Chapter III, the ratio of the difference of the horizontal and the vertical components of the radiance, divided by the total radiance. To get the degree of polarization per cent, P′, we multiply the degree of polarization by 100:

$$P^{'} = 100 \frac{N_h - N_v}{N} \qquad (5.1)$$

where:

- N_h is the horizontal component of the radiance

- N_v is the horizontal component of the radiance

- N is the total received radiance

To determine the polarization from SEARAD, the Out file was used, an example of which is contained in Appendix D. The Out file explicitly determines what the vertical and horizontal components of the radiance are, as well as what the total radiance is. In the case of the experimental data we do not have the radiance recorded, but we do have the IU values, which are directly proportional to the radiance. By assuming that the set of vertically and horizontally polarized images are recorded simultaneously the degree of polarization per cent is calculated as follows:

$$P^{.} = 100 \frac{IU_h - IU_v}{IU_h + IU_v} \tag{5.2}$$

In Equation 5.2 it is assumed that the total unpolarized sea radiance is the sum of the horizontal and vertical components of the sea radiance [Ref. 8:p.19]. It is mandatory to make that assumption, because the IU values in the unpolarized image have a different offset from the polarized images. Therefore the unpolarized IU can not be compared directly with the IU in the vertically and horizontally polarized images, which have equal offsets, as is shown in Figure 4.2.

Taking approximately 160 points in each polarized image, that have different zenith and azimuth angles, and by running SEARAD for each of these points, we obtain plots like the one presented in Figure 5.4 where the degree of polarization per cent is plotted against the zenith angle. The different values of degree of polarization, observed in Figure 5.4, for the same zenith angle correspond to different azimuth angles. Negative

64

values of polarization correspond to vertically polarized radiation. The full range of plots for different ship-camera slant ranges is presented in Appendix F2.

In Figure 5.4 the average absolute error is 0.17 % and the standard deviation is 0.26 %. The results for the average absolute error and the standard deviation, in the cases included in Appendix F2, give the same order of agreement between SEARAD and experiment. It is therefore concluded that the polarized version of SEARAD is a reliable model for calculating the sea polarization.

Note in Figure 5.4 that the degree of polarization is reduced at small zenith angles which correspond to greater distances. The degree of polarization decreases with increasing distance because the polarized reflected and emitted components of sea radiance are attenuated through the atmosphere, and unpolarized path radiance is accumulated in the apparent radiance causing the degree of polarization to be reduced [Ref.8].

Combining the results of this section with the results of Section A, the experimental received radiance for either the vertical or the horizontal polarization can be calculated [Ref. 1,2]:

$$N_h = N\frac{1+P}{2} \qquad (5.3)$$

$$N_v = N\frac{1-P}{2} \qquad (5.4)$$

where:

65

- N_h is the horizontal component of the radiance

- N_v is the vertical component of the radiance

- N is the total received radiance

Using the above equations, the problems of the polarized calibration can be overcome, provided that SEARAD is considered reliable.
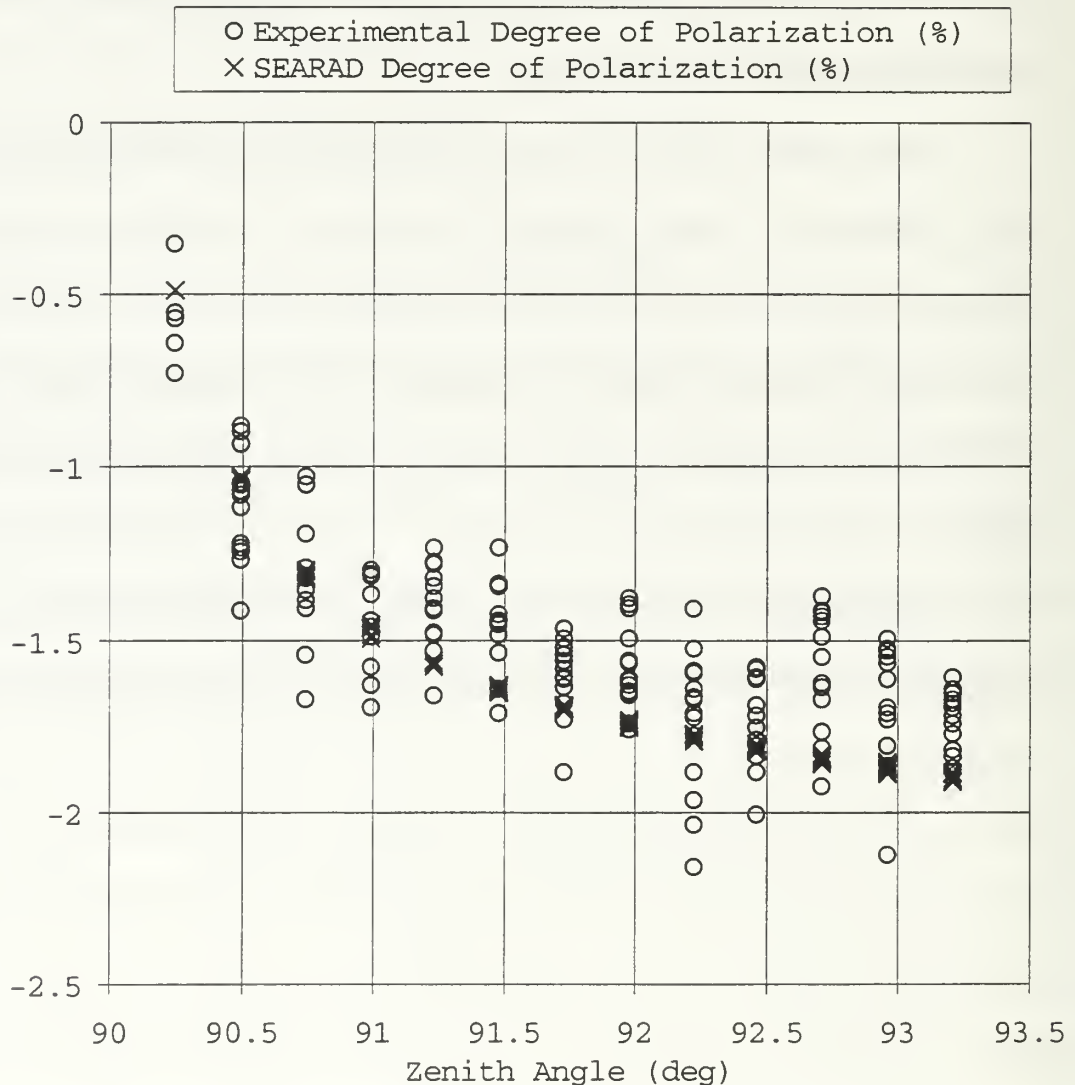

Figure 5.4 Comparison of the SEARAD and Experimental Degrees of Polarization Different Values of Polarization for the Same Zenith Angle Correspond to Different Azimuth Angles.

C. AZIMUTH DEPENDENCE OF POLARIZATION

The results presented in the previous sections indicate that there is an azimuth dependence of the degree of polarization of the total received sea radiance. Using the same assumptions and the same procedures as in the previous section, the experimental and the SEARAD values of the degree of polarization were plotted. This time instead of plotting the degree of polarization against the zenith angle, it was plotted against the azimuth angle relative to the sun. This angle is defined as the angle between the true azimuth of the LOS and the true azimuth of the sun. The angle calculation was based on the subsolar longitude and latitude given by SEARAD in the Out files (Appendix F), the camera's geographical position, and the position of the sampled points of the sea surface. An example of such a plot is Figure 5.5

It can be seen from Figure 5.5 that, for the chosen zenith angle, SEARAD predicts that the polarization will change slightly when going away from the sun direction, and it will become more negative i.e. more vertical. The fact that the received radiation is less vertically polarized in the region close to the sun has been observed in previous studies [Ref. 1,2]. In the region of sun glint the horizontally polarized solar reflected component of the total sea radiance becomes stronger as explained in Chapter III. Thus the observed radiance is less vertically polarized when approaching the sun azimuth.

The experimental degree of polarization, however does not seem to change as regularly as the one from SEARAD does. In fact it appears to be random. The sea footprint, i.e. the patch of sea surface that the camera sees, is 2.8 km^2 or 0.82 nm^2 for the image examined in the two previous sections. The sea footprints, for the rest of the

images are in the same order of magnitude. Based on the size of the footprint we may

conjecture that this irregularity of the experimental polarization is attributable to the fact

that the wind direction and strength are not correlated in the entire scene of the footprint.

A change in the wind parameters changes the probability that a sea wave facet will occur

within a specific slope, given by Cox and Munk [Ref.14, 15], and subsequently the final

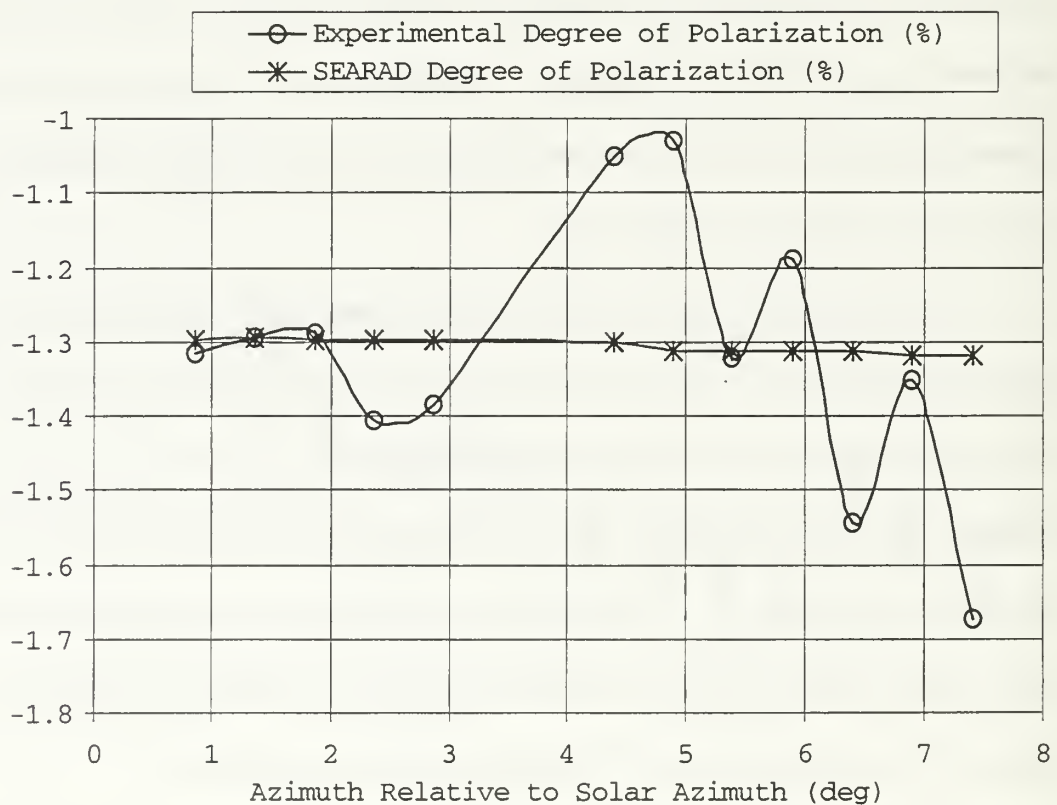polarization of the observed radiance. (Equations 3.11, 3.12, 3.13, 3.14).

Figure 5.5 Azimuth Dependence of Polarization

In the analysis of the experiment, when calculations were made using SEARAD

the conjectured variation of the wind parameters was not taken into account. The reason

for assuming the same wind conditions throughout the image is that the meteorological

data were only recorded in the ship's immediate area.

VI.   CONCLUSIONS AND RECOMMENDATIONS

The primary research objective of this study was to determine whether the polarized version of the SEARAD model predicts accurately the apparent sea radiance, and the related degree of polarization, when compared with the EOPACE experimental data.

The comparison of the unpolarized radiance calculated by SEARAD, with the experimentally recorded radiance showed that there is approximate agreement between the two, within 5%. More specifically the total average absolute error for all the selected images was 1.57 $Wm^{-2}sr^{-1}$ which is approximately 5 % of the experimental radiance. This error may be attributed, in part, to measurement uncertainties and calibration limitations. Overall the level of agreement between the SEARAD code and the experimental unpolarized radiance is considered satisfactory.

The degree of polarization of the received sea radiance predicted by SEARAD agrees to a great extent with the value extracted from the experimental data. The total average magnitude of the difference between the two $\left| \; P'_{SEARAD} - P'_{Experimental} \; \right|$ was only 0.51 %. The results in this case were not affected by calibration limitations as in the radiance case. One possible cause of the error may be the fact that the selected experimental images were not recorded simultaneously, but with a delay of about five seconds one from the other.

Summarizing, the analysis of the experimental data from the EOPACE database shows that the polarization version of SEARAD adequately predicts the received sea

radiance and its polarized components. Thus the polarization version of the SEARAD model is validated.

The results of this thesis indicate that the observed sea radiance in the LWIR is polarized in the vertical direction, outside the sun glint. Therefore the results from previous studies by NPS, on the subject of the polarization of the sea radiance [Ref. 1, 2, 3, 4, 5, 6, 7], indicating a suppression of the sea background through the use of polarizers are validated.

The plots of the experimental and the SEARAD degrees of polarization suggest that the degree of polarization is reduced when the distance between the sea footprint and the sensor increases. Thus the contrast improvement with the method of polarization filtering of the sea radiance is maximized in small distances.

In conclusion, the polarization version of SEARAD is considered a reliable model for the further study of the polarization effects of the sea radiance. This model could be used to identify the conditions under which polarization filtering gives the maximum background suppression and contrast improvement. A new experiment may then be designed to fit those particular conditions when that is possible. SEARAD could also be used in the development of a new generation of IR systems exploiting the polarization effects on the sea environment.

APPENDIX A

AGA 780 THERMOVISION AND POLARIZATION FILTERS PERFORMANCE CURVES

Figure A1 depicts the arrangement of electro-optical components inside the AGA 780 [Ref. 16]. Figure A2 provides typical calibration curves for the camera, using various apertures, in Isotherm Units versus Temperature.

Figures A3 and A4 present the performance curves of the two polarization filters used in the EOPACE April 96 experiment. In each of these Figures there are three curves. Curve one provides the transmittance of the filter with the grid normal to the incident electric field. Curve two shows the transmittance of the filter with the grid parallel to the incident electric field. Finally curve three gives the transmittance when the two filters are placed perpendicular to each other (i.e., crossed). The horizontal axis shows the wavelength and the vertical axis the transmittance. These curves were provided by the manufacturer.

DEWAR FLASK

LIQUID NITROGEN COOLANT

SELECTABLE APERTURE

SELECTABLE FILTER

HORIZONTAL SCANNING PRISM

APERTURE CONTROL

FILTER CONTROL

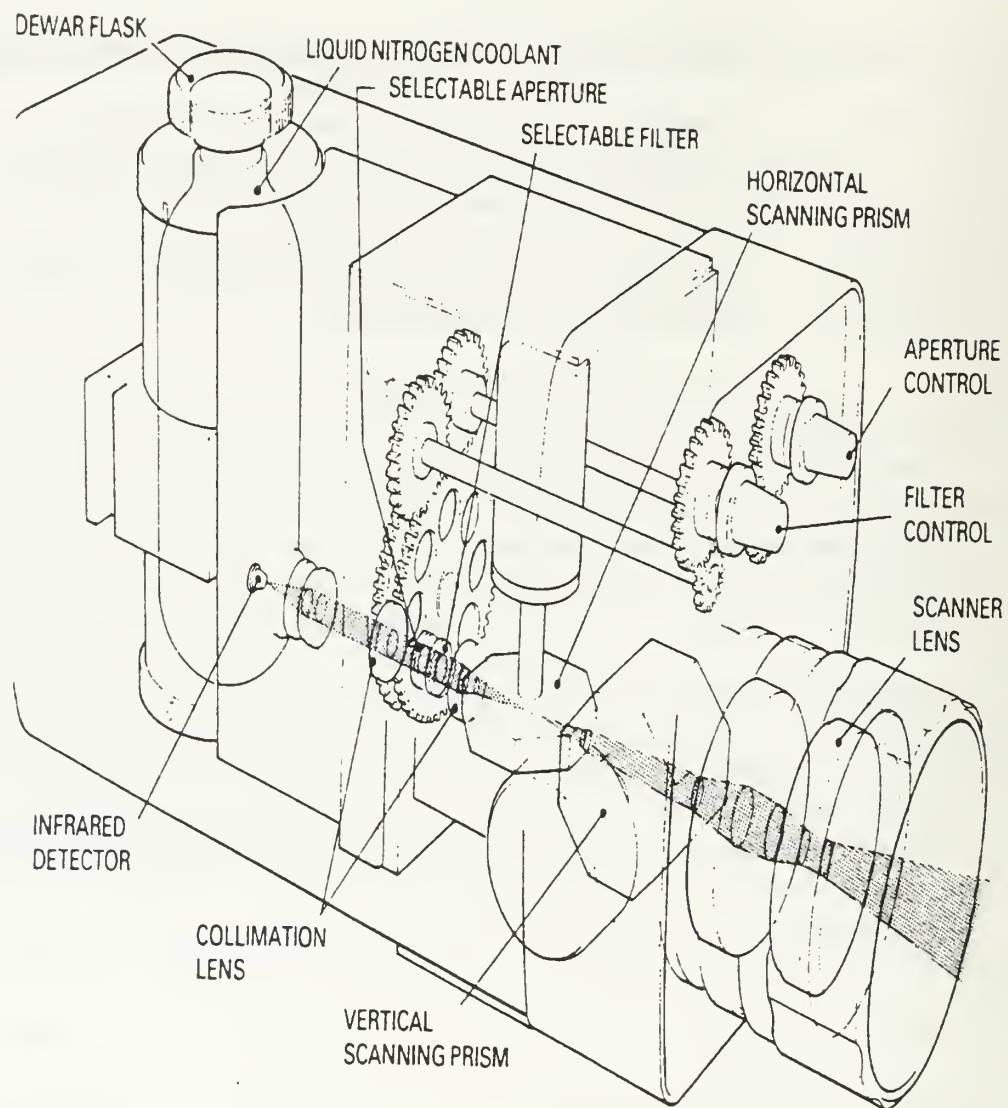SCANNER LENS

INFRARED DETECTOR

COLLIMATION LENS

VERTICAL SCANNING PRISM

Figure A.1 Arrangement of electro-optical components inside AGA 780. [Ref. 16]
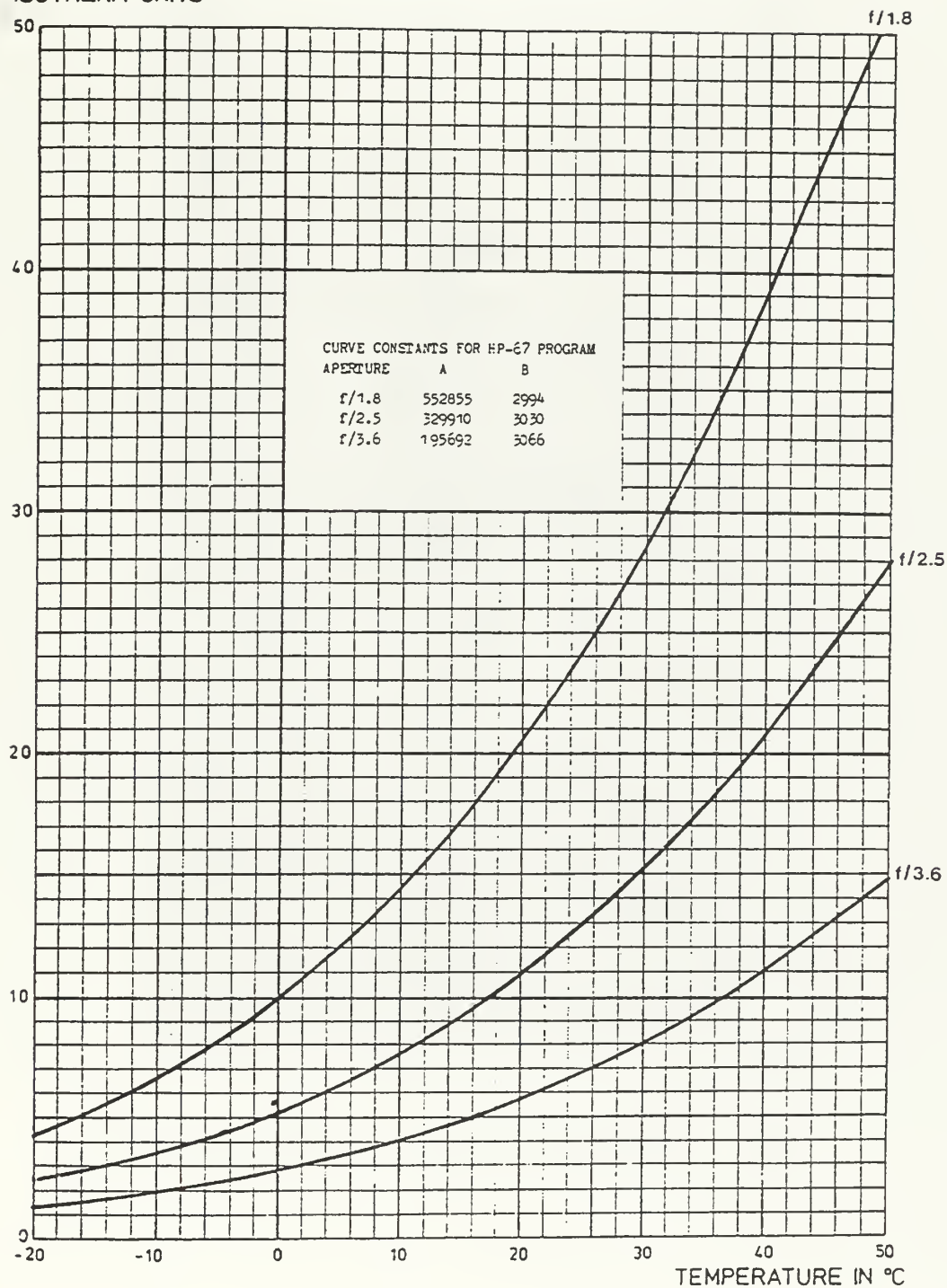
Figure A.2 Calibration curves for the AGA Thermovision 780 in the LWIR. [Ref. 16]
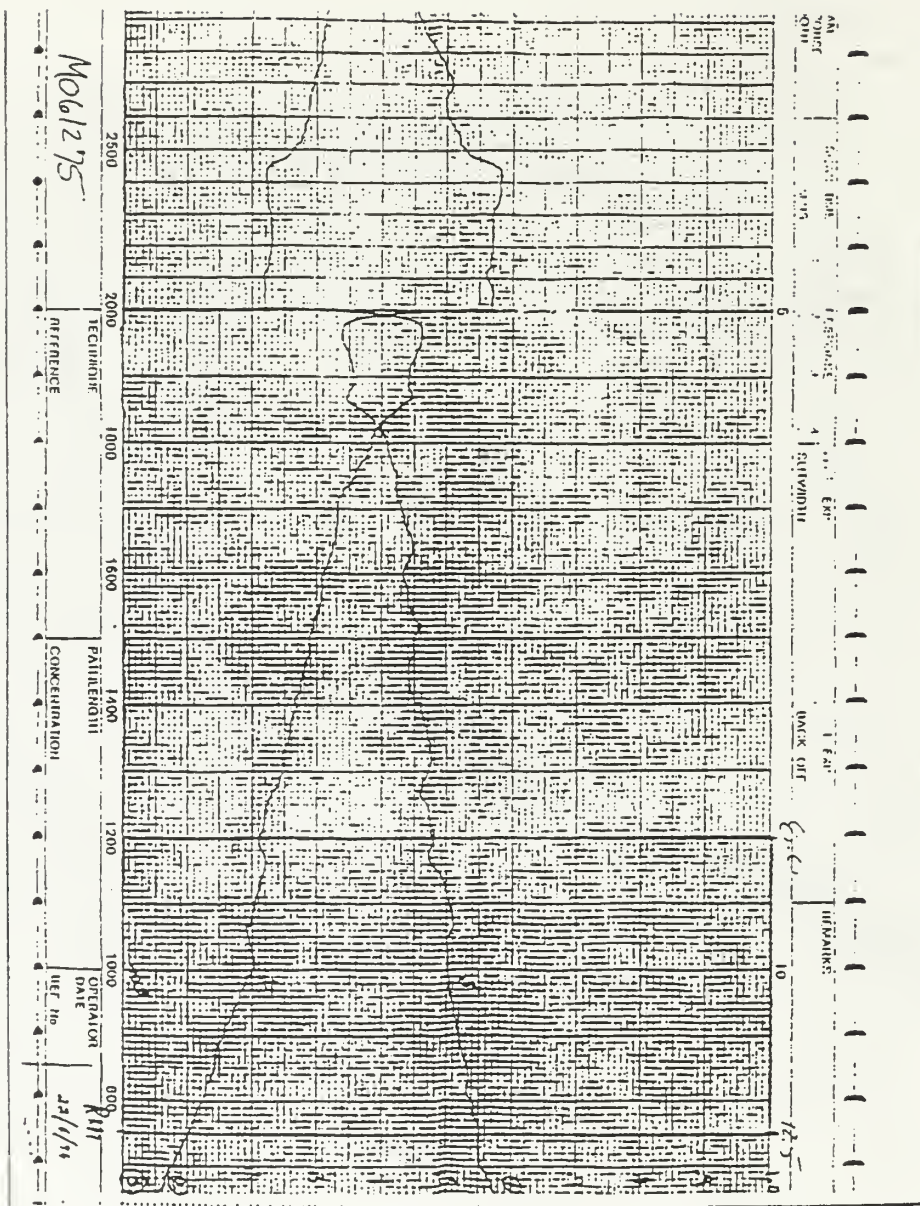
Figure A.3 Performance Curves for the First Polarization Filter
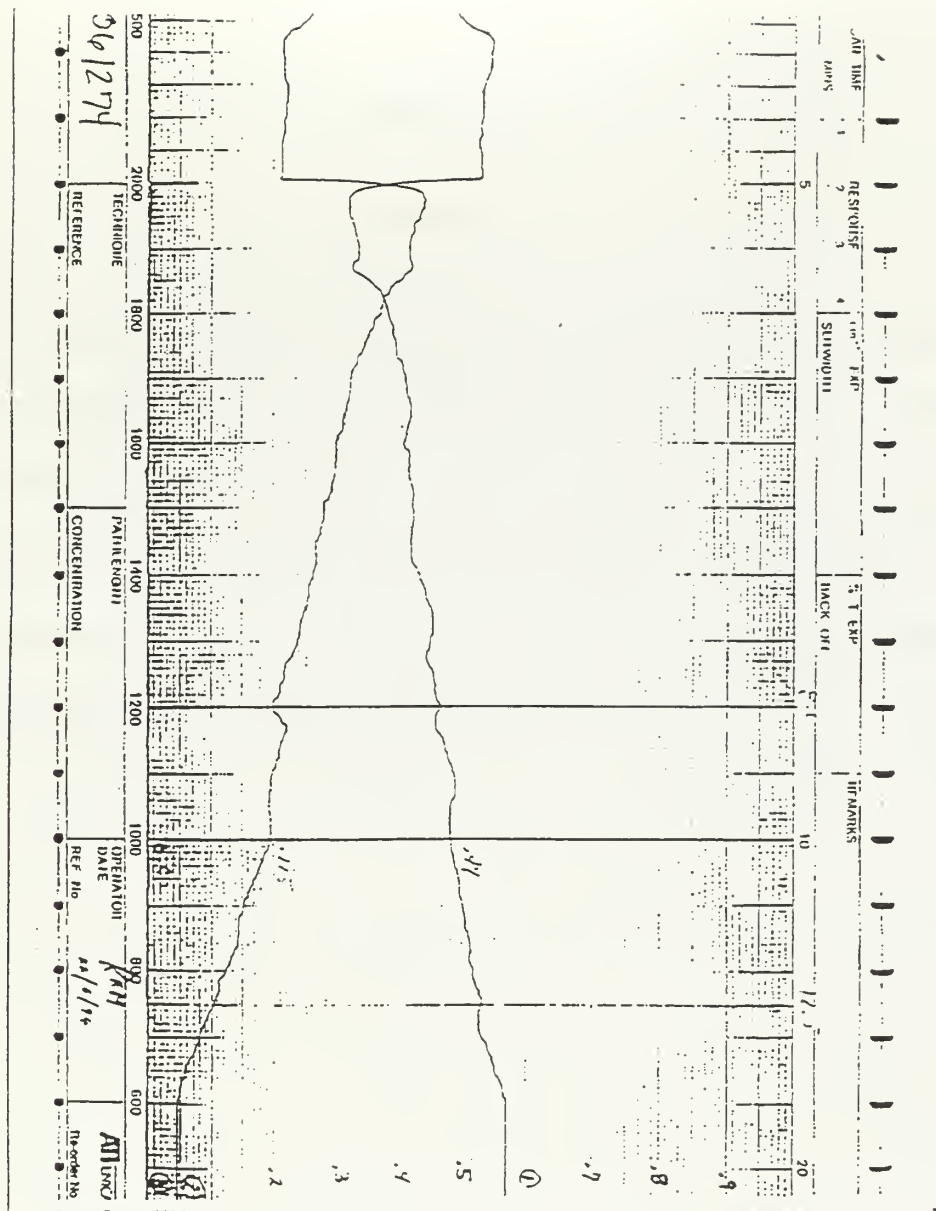
Figure A.4 Performance Curves for the Second Polarization Filter

APPENDIX B

IMAGES

Three images are presented in this Appendix. In the first image the received radiation is horizontally polarized, in the second one the received polarization is vertical, and in the third one the received radiation is unpolarized. Note the improved contrast of ship over sea in Figure B.1. Figure B.1 shows much higher contrast than Figure B.2 or Figure B.3. because the background sea radiance is vertically polarized and by filtering out the vertical component of the radiance the contrast is improved.

Figure B.1 AGA 780 Image with the Polarizer in the Horizontal Position. The Hotspot Appears as a White Spot in the Image. Progression Through the Color Spectrum Indicates Increasing Temperature.

Figure B.2 AGA 780 Image with the Polarizer in the Vertical Position. The Hotspot Appears as a White Spot in the Image. Progression Through the Color Spectrum Indicates Increasing Temperature.

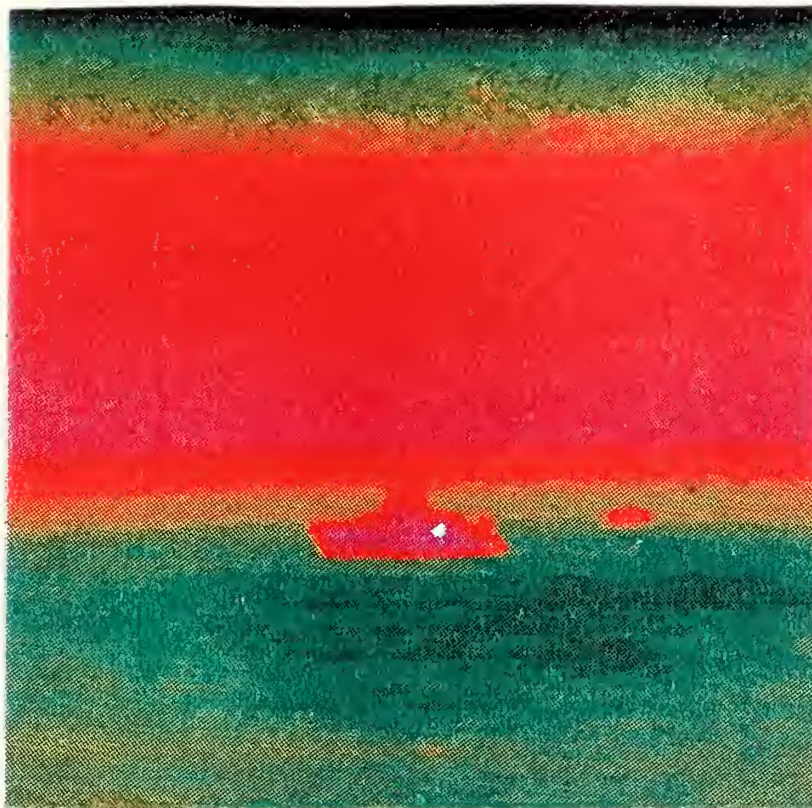
Figure B.3 AGA 780 Image with the Polarizer Removed. The Hotspot Appears as a
White Spot in the Image. Progression Through the Color Spectrum Indicates Increasing
Temperature.

APPENDIX C

METEOROLOGICAL FILES

This Appendix presents the format description of the meteorological –
geographical files used in the analysis of this study. The files were recorded in two
formats, the METOC01, and the METOC02 format. The storage format description
included in this Appendix was provided by the NPS meteorological department.

STORAGE FORMAT FOR METOC01 (DASC) DATA

The data is stored in a set of files with the names "eopace.*" and "30sec.*". The extension for the file names is the Julian date the file was started on. A new pair of files is started every day at 00:00 GMT. The time data in the files are all GMT. The eopace files have the data averaged over 10 minutes. The 30sec files have the GPS data averaged over 30 seconds and the last set of data from the Campbell. In the 30sec file, the Campbell data are not averaged. The data format for both files is the same. Each file has a header which tells when the file was started. Each file also has a footer that tells when the file was finished. Some files may also have additional start and stop times interspersed with the data, depending on whether data logging was turned off or the program was stopped before the end of the day. The data are arranged in fields separated by spaces across a line of text. A carriage return character and a line feed character are at the end of each line. Each new reading is on a new line. The fields are in the order below. The numbers before the fields are not in the data. They serve to make identifying the fields easier.

01 number of readings in this average, nn
02 year, yyyy
03 Julian date, ddd
04 hours & minutes, hhmm
05 seconds, ss
06 Relative Wind Speed, m/s, mmm
07 Relative Wind Direction, degrees, ddd
08 Ship Speed, knots, at present always 0
09 Ship Direction, degrees, at present always 090
10 True Wind Speed, m/s, mmm
11 True Wind Direction, degrees, ddd
12 T air, degrees C, tt.t
13 RH, per cent, pp
14 Pressure, millibars, pppp.p
15 Sea Surface Temperature, degrees C, tt.t
16 GPS time, hhmmss
17 GPS Latitude, ddmm.m
18 GPS North/South Indicator, either 'N' or 'S'
19 GPS Longitude, dddmm.m
20 GPS East/West Indicator, either 'E' or 'W'
21 GPS Speed Over Ground, knots, kk.k
22 GPS Course Over Ground, degrees, ddd.d
23 GPS Antenna Height, meters, mm.m

Here is a sample of the data:
```
   30    1996    99   1103    28    5   009    0   090    3   323   12.3    91  1013.9
20.3  110838  3306.2 N 11806.0 W    0.0   90.0   189.6
```

STORAGE FORMAT FOR METOC02 DATA

The METOC02 system had two additional temperature sensors and two additional RH sensors. The data are arranged slightly differently than the METOC01 system. The data is stored in a set of files with the names "eopace.*" and "30sec.*". The extension for the file names is the Julian date the file was started on. A new pair of files is started every day at 00:00 GMT. The time data in the files are all GMT. The eopace files have the data averaged over 10 minutes.

The 30sec files have the GPS data averaged over 30 seconds and the last set of data from the Campbell. In the 30sec file, the Campbell data are not averaged. The data format for both files is the same. Each file has a header which tells when the file was started. Each file also has a footer that tells when the file was finished. Some files may also have additional start and stop times interspersed with the data, depending on whether data logging was turned off or the program was stopped before the end of the day. The data are arranged in fields separated by spaces across a line of text. A carriage return character and a line feed character are at the end of each line. Each new reading is on a new line. The fields are in the order below. The numbers before the fields are not in the data. They serve to make identifying the fields easier.

01 number of readings in this average, nn
02 year, yyyy
03 Julian date, ddd
04 hours & minutes, hhmm
05 seconds, ss
06 Relative Wind Speed, m/s, mmm
07 Relative Wind Direction, degrees, ddd
08 Ship Speed, knots, at present always 0
09 Ship Direction, degrees, at present always 090
10 True Wind Speed, m/s, mmm
11 True Wind Direction, degrees, ddd
12 T air, degrees C, tt.t
13 RH, per cent, pp
14 Pressure, millibars, pppp.p
15 Sea Surface Temperature, degrees C, tt.t
16 T air A, degrees C, tt.t
17 RH A, per cent, pp
18 T air B, degrees C, tt.t
19 RH B, per cent, pp
20 delimiter between Campbell data and GPS data, "***"
21 GPS time, hhmmss
22 GPS Latitude, ddmm.m
23 GPS North/South Indicator, either 'N' or 'S'
24 GPS Longitude, dddmm.m
25 GPS East/West Indicator, either 'E' or 'W'
26 GPS Speed Over Ground, knots, kk.k
27 GPS Course Over Ground, degrees, ddd.d
28 GPS Antenna Height, meters, mm.m

Here is a sample of the data :
```
    18  1996   99  0319   28    2  090     0  090     3   263  12.2    96 1012.3  16.4
12.2  96.9  12.7  95.7*** 031908 3322.3 N 11836.9 W   5.0  126.3  25.7
```

APPENDIX D

THERMISTOR LOCATIONS AND TEMPERATURE FILES

This Appendix presents the location of the thermistors placed on R/V POINT SUR, to measure the external "skin" temperatures of the ship. The temperature data from the 16 external thermistors were recorded by NPS – NACIT in special "skin" temperature files along with time information. The description of the format of these files, and a sample of them, is also contained in this Appendix.

THERMISTOR LOCATION

Flir 13 April 1, 1996
PT Sur
Channel # Location
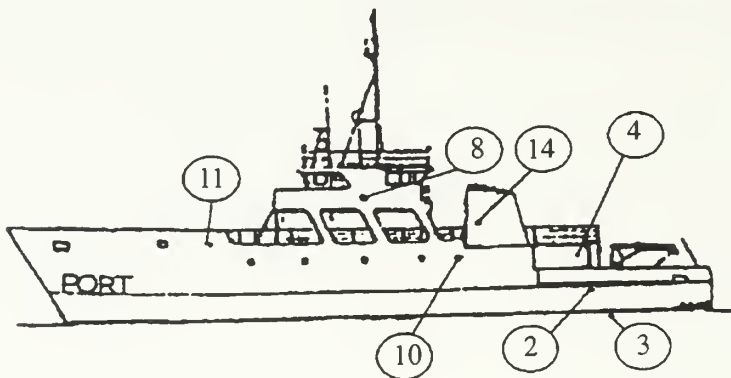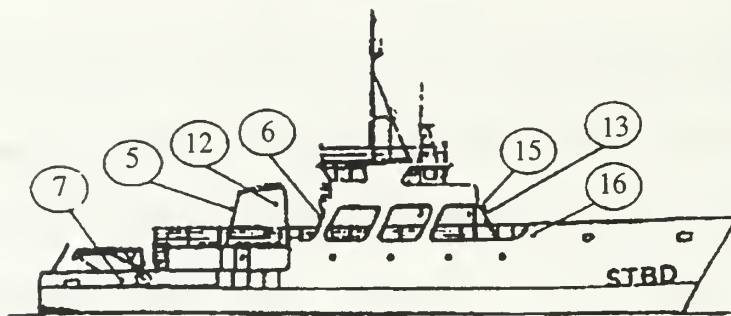
1	Reference 25.0 C
2	Aft Port
3	Aft water probe
4	Aft of Stack
5	Aft On Stack
6	Aft Boathouse
7	Aft Starboard
8	Port Boathouse
9	Reference 25.0 C
10	Port Below Stack
11	Port Bow
12	Starboard Stack
13	Air
14	Port Stack
15	Bow Boathouse
16	Starboard Boathouse

"SKIN" TEMPERATURE FILE FORMAT

Data Format: Header - self explanatory Time in seconds, Channel 1 reference (25.001, channel2,3,4,5,6,7,8,Channel 9 reference (25.001),10,11,12,13,14,15,16
april1.1
Mon,Day,Year= 4 1 1996
Hour,Min,Sec= 20 8 6
volts,istart,istop,nsam,iref 1.49939 1 16 100 1
72486 25.001 12.863 14.185 12.883 14.996 14.756 12.581 13.813 25.001 13.034 13.182 18.452 18.542 13.949 13.425 13.243
72506 25.001 12.865 14.188 12.886 15.001 14.757 12.584 13.813 25.001 13.038 13.187 18.461 18.546 13.951 13.423 13.246
72526 25.001 12.868 14.140 12.888 15.006 14.756 12.588 13.817 25.001 13.039 13.189 18.432 18.551 13.953 13.425 13.245
72546 25.001 12.873 14.113 12.892 15.005 14.756 12.588 13.820 25.001 13.043 13.197 18.445 18.557 13.958 13.424 13.243
72566 25.001 12.877 14.118 12.896 15.003 14.755 12.590 13.822 25.001 13.045 13.201 18.433 18.560 13.963 13.424 13.240

APPENDIX E

IDL PROGRAMS

This Appendix presents some of the most important IDL programs used in the analysis of the experimental data.

GEOGRAPHY.PRO

```
;************* LTJG PANAGIOTIS KARAVAS HELLENIC NAVY****************
;********************* THESIS RESEARCH******************************
;***VALIDATION EVALUATION OF THE POLARIZATION VERSION OF SEARAD******
;PROGRAM NAME :Geography.pro
; Purpose: Calculates position of the ship relative to the camera
function Geography, gpsship, gpscam
; dimensions & initial values
aux1 = size(gpsship)
aux2 = size(gpscam)
; return if error
if (aux1(2) ne aux2(2)) then return, 'input error'
; dimensions & definitions
ncol = 3
nlin = aux1(2)
latship = gpsship(0,*)
lonship = gpsship(1,*)
hship = 7.3 ;estimated height above sea level of the ship
latcam = gpscam(0,*)
loncam = gpscam(1,*)
hcam = gpscam(2,*)
pi = 3.1416
fi = fltarr(1,nlin)
; latitude variation   = latidude distance in nmi
dlat = latship-latcam
latdist = dlat*1852.0          ; convert nmi to m
; longitude variation
dlon = lonship-loncam
; altitude variation
dh = hcam- hship
; midlatitude
mlat = (latship+latcam)/2.0
; transform midlatitude to radians
mlat = mlat*pi/(60.0*180.0)
; longitude distance
londist = dlon*cos(mlat)*1852.0    ; converted nmi to m
; calculate fi angle
for i = 0, nlin-1 do  if (dlat(i) ne 0.0) then fi(i) =(-1)*atan(londist(i)/latdist(i))*(dlat(i) gt 0)+((-
1)* atan(londist(i)/latdist(i))+pi)*(dlat(i) lt 0) else fi(i) = (pi/2)*(dlon(i) le 0) + (1.5*pi)*(dlon(i) gt
0)
; calculate range R
R =sqrt(dh^2+latdist^2+londist^2)
; calculate theta angle
theta = pi-acos(dh/R)
; return
saida = [R,theta,fi]
return, saida
end
```

DATA.PRO

```
;PROGRAM NAME :Data.pro
;Purpose : Interpolate meteorological and geographical data into images creating a new image
;array with additional information
pro Data
basepath ='c:\Thesis\data\basic\'    ; where is the BASEN.PTE
filename = pickfile(/read, path = basepath , filter = '*.pte', title='Select file to Analysis')
; Get Information
info = leia_pte(filename, 'info',0)
npol = info(7)
ncol = info(8)
nlin = info(9)
nfra = lonarr(npol)
for i = 0, npol - 1 do nfra(i) = info(10+i)
; Size of elements (variables) in *.pte (in bytes)
resuoff = lonarr(npol)             ; offset for each result matrix (case)
stime  = nfra*2*4              ; 2 bytes per integer element
slrange=nfra*2*2
simag  = nfra*ncol*nlin*2
sresu  = (nfra+1)*4*100            ; 4 bytes per float element / 100 colunms
; offsets
timeoff  = long(40+2*npol)           ; offset for first time matrix
lrangeoff=long(timeoff + total(stime))
imagoff = long(lrangeoff + total(slrange))  ; offset for first image matrix
resuoff(0) = long(imagoff + total(simag))     ; offset for file result matrix
for i = 0, npol - 2 do resuoff(i+1) = resuoff(i) + sresu(i)
; Calculations
     for n = 0,npol-1 do begin
        ; create result matrix
        result = fltarr(100,nfra(n)+1)
        print, 'POLARIZATION CASE : '+strtrim(string(n),1)
        ; elapsed time for each frame
        time = leia_pte(filename, 'tempo',n)
        etime = deltat(time)        ; calculate elapsed time
        inclua, etime, result, 0
        ; metdata
        info = leia_pte(filename, 'info',n)
        time = leia_pte(filename, 'tempo',n)
        metoc = meteoro (info,time)                  ; interpolates metoc data
        ; position data
        gpsship = metoc(0:2,*)                       ; GPS position of the ship
        camera = [1959.917,7034.517,27.439] ; lat, lon, alt. of the camera in minutes
        auxones = make_array(1,nfra(n),/float, value=1.0)
        gpscam = camera#auxones
        position = Geography(gpsship,gpscam)
        ; skindata
        info = leia_pte(filename, 'info',n)
        time = leia_pte(filename, 'tempo',n)
```

```
      skin = skintemp(info,time)                    ; interpolates skintemp data
      ; include results in Result matrix
      inclua, metoc, result, 1
      inclua, gpscam, result, 10
      inclua, position, result, 13
      inclua, skin, result, 16
      ; open file, localize pointer and save matrix
      escreva, result, filename, resuoff(n)
   endfor
end
```

TAPE5SHIP.PRO

```
;************* LTJG PANAGIOTIS KARAVAS HELLENIC NAVY*****************
;********************* THESIS RESEARCH*****************************
;***VALIDATION EVALUATION OF THE POLARIZATION VERSION OF SEARAD******
;PROGRAM NAME :Data.pro
        ;Purpose : This program writes formatted input files tape5 files for the
        ; specified geographical positions we choose
        pro tape5ship
        ; define variables
        a1=intarr(13)
        b1=fltarr(2)
        a2=intarr(6)
        b2=fltarr(5)
        a2a=fltarr(3)
        b2a=intarr(1)
        a2b=fltarr(3)
        a2c=intarr(3)
        b2c=strarr(18)
        a2c1=fltarr(6)
        b2c1=strarr(15)
        a2c2=fltarr(8)
        b2c2=fltarr(8)
        a2c3=fltarr(3)
        b2c3=intarr(5)
        a2d=intarr(4)
        a2d1=fltarr(1)
        b2d1=strarr(18)
        a2d2=fltarr(4)
        b2d2=fltarr(4)
        c2d2=fltarr(4)
        d2d2=fltarr(4)
        a3=fltarr(7)
        a3a1=intarr(4)
        a3a2=fltarr(8)
        a3b1=intarr(1)
        a3b2=fltarr(6)
        b3=intarr(1)
        c3=strarr(1)
        a4=intarr(5)
        a5=intarr(1)
        ;pick the file of interest
        basepath = 'c:\Thesis\data\basic\'    ; where is the BASEN.PTE
        filename = pickfile(/read, path = basepath , filter = '*.pte', title='Select file to Analyse')
        ask1=0
        read, ask1, prompt = 'CHOOSE POLARIZATION CASE HORIZONTAL = 0 VERTICAL =1
        UNPOLARIZED =2 : '
        if ((ask1 ne 0 )and (ask1 ne 1) and (ask1 ne 2) ) then return
        ;get the information matrix for the specific image
        A=leia_pte(filename,'imagem',ask1)
        ; dimensions & initial val
```

```
aux1 = size(A)
; Assign dimensions
nima = 1
if (aux1(0) eq 3) then nima = aux1(3)
;choose desired frame to analyze
print,'THE NUMBER OF FRAMES FOR THIS POLARIZATION CASE IS:'
print,nima
read, ask2, prompt = 'CHOOSE NUMBER OF FRAME TO ANALYZE'
;choose desired frame to analyze
val=input(filename,ask1,ask2)
;get the name for the tape5 file
N = ''
read, N, prompt = '?PTE : Sequential number to store ship tape5 file (t__.std) : '
f=strtrim(string(fix(ask1)),1)          ;number that gives the polarization
datapath = 'c:\Thesis\data\tape5\'+N+'\ship\' ;where the tape 5 files will be written
;write the ship tape5 file
;card 1 inputs
a1(0)=2 ; Mid-Latitude summer
a1(1)=2 ;slant path between to space
a1(2)=2 ; Radiance mode with solar/lunar scattered radiance included
a1(3)=1 ; multiple scattering
a1(4)=0 ; default
a1(5)=0 ; default
a1(6)=0 ; default
a1(7)=0 ; default
a1(8)=0 ; default
a1(9)=0 ; default
a1(10)=0 ; default
a1(11)=0 ; normal operation(IM)
a1(12)=0 ; normal operation (NORT)
b1(0)=273.15+val(5);Tbound
b1(1)=0 ; SALB=0 assumes the surface is blackbody
; card2 input
a2(0)=3 ; Navy maritime extinction model
a2(1)=0 ; Defaults to seasons of selected model'
a2(2)=0 ; Default to stratospheric background'
a2(3)=3 ; Air mass parameter
a2(4)=0 ; No clouds or rain
a2(5)=0 ; IVSA not used
b2(0)=0  ; meteoroligical range
b2(1)=val(3)  ; current wind speed
b2(2)=4.481 ; 24 hour average wind speed from metoc 2 data'
b2(3)=0 ; rain rate
b2(4)=0 ; ground altitude
;card3 input
a3(0)=0.027 ; camera altitude 90 ft 27.4meters
a3(1)=0.007        ; point altitude
a3(2)=val(2)       ; zenith angle of point
a3(3)=0; range ,we do not need to specify it
a3(4)=0            ; no need to specify it
a3(5)=0 ; earth radius set to default
b3=0 ; normal operation
```

```
a3(6)=val(4); wind azimuth relative to  LOS
c3='T' ;seaswitch
;card3a1 input
a3a1(0)=1 ; IPARM defines card3a2
a3a1(1)= 2; MIE generated data base of aerosol phase functions for lowtran models
a3a1(2)=val(6);Julian day
a3a1(3)=0 ; sun as source of radiance
;card3a2 input
a3a2(0)=32.665 ; observer latitude (+ means North)
a3a2(1)=117.242 ;observer longitude (0 to 360)
a3a2(2)=0
a3a2(3)=0
a3a2(4)=val(7);Greenwich time in decimal hours
a3a2(5)=val(1)     ; path azimuth
if (val(7) gt 24.0) then begin
    a3a2(4)=a3a2(4)-24.0
    a3a1(2)=a3a1(2)+1
 endif
;card4 input
a4(0)=833 ; initial frequency (wavenumber cm-1 )
a4(1)=1250 ; final frequency(wavenumber cm-1 )
a4(2)=10 ; frequency increment (or step size) (cm-1)
a4(3)=5 ; IFWHM
;card5 input set to default mode i.e. end program
; write input cards
fname=datapath+'s'+N+f+'.std'
openw,unit, fname, /get_lun
printf, unit, format='("F",I4,12I5,F8.2,F7.2)',a1,b1
printf, unit, format='(6I5,5F10.3)',a2,b2
printf, unit, format='(6F10.3,I5,F10.3,A5)',a3(0:5),b3,a3(6),c3
printf, unit,format='(4I5)',a3a1
printf,unit,format='(8F10.3)',a3a2
printf, unit, format='(5I10)',a4
printf, unit, format='(I5)',a5
free_lun,unit
end
```

INPUT.PRO

```
;************* LTJG PANAGIOTIS KARAVAS HELLENIC NAVY*****************
;********************* THESIS RESEARCH*****************************
;***VALIDATION EVALUATION OF THE POLARIZATION VERSION OF SEARAD******
;PROGRAM NAME :input.pro
;PURPOSE: Provide input to SEARAD Tape5 files
function  input,filename,ask2,fn
;read transmittance and path radiance
shipout='c:\Thesis\data\out\'+fn+'\ship\s'+fn+'2.std';where the out file for the ship is
    tr=0.0
    pathr=0.0
    openr,unit,shipout,/get_lun
          point_lun, unit, 1435         ;offset to get the zenith angle
          readf, unit,tr
          point_lun, unit, 1695         ;offset to get the zenith angle
          readf, unit,pathr
          free_lun,unit
print,'The path transmittance is :',tr
print,'The path radiance is :',pathr
A=leia_pte(filename,'imagem',2);get the unpolarized image
pi = 3.1416
;find hotspot
hot=hotspot(A)
;get the area of interest
box=[0,255,124,0]
;get the horizon
horizon=horizont(A)
seam=element(A(*,*,ask2),hot,box,horizon)
;convert digital level to thermal level and then to temperature
dat=leia_pte(filename,'resultado',2)
T1=dat(16,ask2+1)          ;the temperature of the stack in C
print,'hot tmp',T1
rad=radiance(T1,tr)
rad(0)=rad(0)+pathr
print,'The corected radiance is ',rad
Tref=invrad(rad)
print,'The corrected Temp is :',Tref-273
lrange=leia_pte(filename,'lrange',2)
range=lrange(1,ask2)
level=lrange(0,ask2)
B=isotherm(A(*,*,ask2),range,level)               ;convert image matrix from Digital level to isotherm
units
tvscl,B,order=1
h=isotherm(hot(0,ask2),range,level)               ;convert hotspot digital level to IU
print,'hot',h
print,'max arr',max(B)
os=offset(h,Tref,2)  ;Find the offset for the frame
print,'offset:',os
;reference point to aply geo data
xref=hot(1,ask2)
```

98

```
yref=hot(2,ask2)
xdim=box(2)-box(0)
ydim=box(1)-box(3)
b=fix(xdim/9)
c=fix(ydim/9)
val=fltarr(14,(b+1)*(c+1),3)
val(11,*,2)=os        ;gives the offset
val(12,*,2)=dat(15,ask2+1)*180/pi ;azimuth at the reference point
val(13,*,2)=dat(14,ask2+1)*180/pi ;zenith angle at the reference point
y=-9
l=-1
for i=0 ,c do begin
y=y+9                           ;steps of about 0.5 degrees for 7 deg lens
x=-6
        for j= 0 ,b do begin
   x=x+9                                ;steps of about 0.25 degrees for 7 deg lens
        ;get the diference in azimouth and elevation
        dx=x-xref
        dy=y-yref
        dazim=(-dx)*0.0009774
        delev=dy*0.0004772
        azim=dazim+dat(15,ask2+1)
        elev=delev+dat(14,ask2+1) ;zenith angle
        r=(27.439-7.3)/cos(180-(elev/pi)*180) ;compute the range from the zenith angle
   os=-0.0043*r + 12.162
        A(x,y)=temp(B(x,y),os, 2) ;matrix which contains temperatures
        l=l+1
        val(0,l,2)=A(x,y) * seam(x,y)    ;temperature value calibrated
        ;print,x,y
        val(1,l,2)=(elev/pi)*180     ;zenith angle at  that point in deg
        val(2,l,2)=(azim/pi)*180     ; true azimuth angle
        val(3,l,2)=dat(8,ask2+1)-val(2,l,2);wind direction relative to LOS
        val(4,l,2)=x
        val(5,l,2)=y
        endfor
endfor
val(6,*,2)=dat(7,ask2+1)                  ;wind speed
val(7,*,2)=dat(13,ask2+1)         ;range to reference point in meteres
val(8,*,2)=dat(9,ask2+1)                  ;sea surface temperatures
info = leia_pte(filename, 'info',2)
time = leia_pte(filename, 'tempo',2)
val(9,*,2)=info(0)+90
; transform time hhmmss.cc to ssssss.ss, make the corection + 8hours to make it GMT
;and then divide by 3600 to take decimal hours GMT
hour                                    =                    (time(0,ask2)*3600.00+
time(1,ask2)*60.0+time(2,ask2)+time(3,ask2)/100.0+(8*3600.0))/3600.0
val(10,*,2)=hour

for i=0,1 do begin
A=leia_pte(filename,'imagem',i);get the polarized images
dat=leia_pte(filename,'resultado',i)
lrange=leia_pte(filename,'lrange',i)
```

```
B=isotherm(A(*,*,ask2),range,level)              ;convert image matrix from Digital level to isotherm
units
for j=0,l do begin
 val(0,j,i)=B(val(4,j,2),val(5,j,2))*seam(val(4,j,2),val(5,j,2))   ;get the IU values of the polarized
frames
 val(1:6,j,i)=val(1:6,j,2)
 val(8:11,j,i)=val(8:11,j,2)
endfor
 val(7,*,i)=dat(13,ask2+1)         ;range to reference point in meteres
 val(12,*,i)=dat(15,ask2+1)*180/pi ;azimuth at the reference point
 val(13,*,i)=dat(14,ask2+1)*180/pi ;zenith angle at the reference point
endfor
return,val
end
```

ISOTHERM.PRO

```
;************** LTJG PANAGIOTIS KARAVAS HELLENIC NAVY******************
;********************* THESIS RESEARCH*************************************
;***VALIDATION EVALUATION OF THE POLARIZATION VERSION OF SEARAD******
;PROGRAM NAME :isotherm.pro
;PURPOSE: Convert Digital Level to Isotherm Units
function isotherm,DL,range,level
case range of
        5:begin
        a=0.001221
        b=level-2.5
        end
        10:begin
        a=0.002442
        b=level-5
        end
        20:begin
        a=0.004884
        b=level-10
        end
endcase
IU=DL*a+b
return,IU
end
```

INVRAD.PRO

```
;************** LTJG PANAGIOTIS KARAVAS HELLENIC NAVY******************
;********************* THESIS RESEARCH*************************************
;***VALIDATION EVALUATION OF THE POLARIZATION VERSION OF SEARAD******
;PROGRAM NAME :invrad.pro
;PURPOSE: Convert Radiance to Temperature, using Stefan Boltzmann's Law
;rad(0) radiance
;rad(1) fraction of radiance in the 8-12 band
function invrad,rad
pi=3.141592654
s=5.66961*10.0^(-8.0)
e=1
T=(pi*rad(0)/(rad(1)*e*s))^0.250
return,T
end
```

RADIANCE.PRO

```
;************* LTJG PANAGIOTIS KARAVAS HELLENIC NAVY*****************
;********************** THESIS RESEARCH***********************************
;***VALIDATION EVALUATION OF THE POLARIZATION VERSION OF SEARAD******
;PROGRAM NAME :radiance.pro
;PURPOSE: Calculate Radiance from Temperature, using Stefan Boltzmann Law.
function radiance,T,tr
pi=3.141592654
rad=fltarr(2,27)
rad(0,0)=0.140
for i=1,26 do begin
rad(0,i)=rad(0,i-1)+0.010
endfor
rad(1,*)=[0.0079053,0.013023,0.019962,0.028858,0.039754,0.052613,$
0.067331,0.083750,0.10168,0.12091,0.14122,0.16239,0.18423,0.20653,$
0.22911,0.25183,0.27454,0.29712,0.31947,0.34150,0.36314,0.38432,0.40502,0.42518,$
0.44479,0.46382,0.48227]
tl1=8.0*(T+273.0)/10000

tl2=12.0*(T+273.0)/10000
tl=[tl1,tl2]


res = INTERPOL(rad(1,*), rad(0,*), tl)  ;Interpolate.
plot,rad(0,*),rad(1,*),psym=2
oplot,tl,res,psym=6
fra=res(1)-res(0)
print,'fraction',fra

s=5.66961*10.0^(-8)

e=1
W=tr*fra*e*s*(T+273.0)^4/pi
;print,'radiance',W
result=fltarr(2)
result(0)=W
result(1)=fra
return,result
end
```

OFFSET.PRO

```
;************* LTJG PANAGIOTIS KARAVAS HELLENIC NAVY******************
;********************** THESIS RESEARCH**********************************
;
;***VALIDATION EVALUATION OF THE POLARIZATION VERSION OF SEARAD******
;PROGRAM NAME :Offset.pro
;PURPOSE: Calculate Offset from input IU and Temperature
function offset,TL, T, casep
case casep of
   0 : begin
                A = double(1675)
                B = double(1348)
                C = double(1)
        end

        1 : begin
                A = double(1675)
                B = double(1348)
                C = double(1)
        end
  2 : begin
                A = double(6808)
                B = double(1511)
                C = double(1)
        end
endcase
os=TL - (A/(C*exp(B/T)-1))
return, os
end
```

TEMP.PRO

```
;************* LTJG PANAGIOTIS KARAVAS HELLENIC NAVY*****************
;********************** THESIS RESEARCH********************************
;***VALIDATION EVALUATION OF THE POLARIZATION VERSION OF SEARAD******
;PROGRAM NAME :Temp.pro
;PURPOSE: Calculate Temperature from input Offset and Temperature

function temp, TL,os, casep
aux1 = size(TL)
case casep of
  0 : begin
                A = double(1675)
                B = double(1348)
                C = double(1)
                ;os=double(39)
        end
        1 : begin
                A = double(1675)
                B = double(1348)
                C = double(1)
                ;os=double(39)
        end
  2 : begin
                A = double(6808)
                B = double(1511)
                C = double(1)
                ;os=double(12)
        end
endcase
w=alog(((A/(TL-os))+1)/C)
T=B/w-273
return, T
end
```

TAPE5.PRO

```
;************** LTJG PANAGIOTIS KARAVAS HELLENIC NAVY******************
;********************** THESIS RESEARCH************************************
;***VALIDATION EVALUATION OF THE POLARIZATION VERSION OF SEARAD******
;PROGRAM NAME :Tape5.pro
;PURPOSE: This program writes formatted input files tape5 files for the
; specified geographical positions we choose, for use by the polarized SEARAD

; pro tape5
; define variables
a1=intarr(13)
b1=fltarr(2)
a2=intarr(6)
b2=fltarr(5)
a2a=fltarr(3)
b2a=intarr(1)
a2b=fltarr(3)
a2c=intarr(3)
b2c=strarr(18)
a2c1=fltarr(6)
b2c1=strarr(15)
a2c2=fltarr(8)
b2c2=fltarr(8)
a2c3=fltarr(3)
b2c3=intarr(5)
a2d=intarr(4)
a2d1=fltarr(1)
b2d1=strarr(18)
a2d2=fltarr(4)
b2d2=fltarr(4)
c2d2=fltarr(4)
d2d2=fltarr(4)
a3=fltarr(7)
a3a1=intarr(4)
a3a2=fltarr(8)
a3b1=intarr(1)
a3b2=fltarr(6)
b3=intarr(1)
c3=strarr(1)
a4=intarr(5)
a5=intarr(1)
;pick the file of interest
basepath ='c:\Thesis\data\basic\'     ; where is the BASEN.PTE
filename = pickfile(/read, path = basepath , filter = '*.pte', title='Select file to Analyse')
A=leia_pte(filename,'imagem',2)
; dimensions & initial val
aux1 = size(A)


; Assign dimensions
nima = 1
```

```
if (aux1(0) eq 3) then nima = aux1(3)
;choose desired frame to analyze
print,'THE NUMBER OF FRAMES FOR THE UNPOLARIZED CASE ARE:'
print,nima
read, ask2, prompt = 'CHOOSE NUMBER OF FRAME TO ANALYZE'
;choose desired frame to analyze
;get the name for the tape5 file
N = ''
read, N, prompt = '?PTE : Sequential number to store data  (t__.std) : '
datapath = 'c:\Thesis\data\tape5\'+N+'\' ;where the tape 5 files will be written
val=inputcal(filename,ask2,N)
j=0
s=size(val(*,*,2))
for i=0,s(2)-1 do begin
        if (val(0,i,2) GT 0.0) then begin
        j=j+1                    ;count the number of tape 5 files we will create

;card 1 inputs
a1(0)=2 ; Mid-Latitude summer
a1(1)=3 ;slant path between to space
a1(2)=2 ; Radiance mode with solar/lunar scattered radiance included
a1(3)=1 ; multiple scattering
a1(4)=0 ; default
a1(5)=0 ; default
a1(6)=0 ; default
a1(7)=0 ; default
a1(8)=0 ; default
a1(9)=0 ; default
a1(10)=0 ; default
a1(11)=0 ; normal operation(IM)
a1(12)=0 ; normal operation (NORT)
b1(0)=273.15+val(8,i,2);Tbound
b1(1)=0 ; SALB=0 assumes the surface is blackbody

; card2 input
a2(0)=3 ; Navy maritime extinction model
a2(1)=0 ; Defaults to seasons of selected model'
a2(2)=0 ; Default to stratospheric background'
a2(3)=3 ; Air mass parameter
a2(4)=0 ; No clouds or rain
a2(5)=0 ; IVSA not used
b2(0)=0  ; meteoroligical range
b2(1)=val(6,i,2)  ; current wind speed
b2(2)=4.481 ; 24 hour average wind speed from metoc 2 data'
b2(3)=0 ; rain rate
b2(4)=0 ; ground altitude

;card3 input
a3(0)=0.027 ; camera altitude 90 ft 27.4meters
a3(1)=0  ; point altitude
a3(2)=val(1,i,2)   ; zenith angle of point
a3(3)=0  ; range ,we do not need to specify it
```

```
a3(4)=0              ; no need to specify it
a3(5)=0 ; earth radius set to default
b3=0 ; normal operation
a3(6)=val(3,i,2); wind azimuth relative to  LOS
c3='T' ;seaswitch

;card3a1 input
a3a1(0)=1 ; IPARM defines card3a2
a3a1(1)= 2; MIE generated data base of aerosol phase functions for lowtran models
a3a1(2)=val(9,i,2);Julian day
a3a1(3)=0 ; sun as source of radiance

;card3a2 input
a3a2(0)=32.665 ; observer latitude (+ means North)
a3a2(1)=117.242 ;observer longitude (0 to 360)
a3a2(2)=0
a3a2(3)=0
a3a2(4)=val(10,i,2);Greenwich time in decimal hours
a3a2(5)=val(2,i,2)           ; path azimuth
if (val(10,i,2) gt 24.0) then begin
    a3a2(4)=a3a2(4)-24.0
    a3a1(2)=a3a1(2)+1
 endif
;card4 input
a4(0)=833 ; initial frequency (wavenumber cm-1 )
a4(1)=1250 ; final frequency(wavenumber cm-1 )
a4(2)=10 ; frequency increment (or step size) (cm-1)
a4(3)=5 ; IFWHM

;card5 input set to default mode i.e. end program
; write input cards
g=strtrim(string(fix(j)),1)  ; gives the number of the tape 5 file
fname=datapath+'t'+N+'_'+g+'.std'
openw,unit, fname, /get_lun
printf, unit, format='("F",I4,12I5,F8.2,F7.2)',a1,b1
printf, unit, format='(6I5,5F10.3)',a2,b2
printf, unit, format='(6F10.3,I5,F10.3,A5)',a3(0:5),b3,a3(6),c3
printf, unit,format='(4I5)',a3a1
printf,unit,format='(8F10.3)',a3a2
printf, unit, format='(5I10)',a4
printf, unit, format='(I5)',a5
free_lun,unit
          endif
endfor
;get the name for the data file
basename = 'DAT' + strtrim(string(N),1)+'.PTE'


; create the DATA file
val1=fltarr(6,3)
value=fltarr(6,j,3)
for k=0,2 do begin
```

```
val1(0:1,k)=val(6:7,0,k);get the wind speed and distance to the ship
val1(2,k)=val(12,0,k)          ;get the azimuth at the ship
val1(3,k)=val(13,0,k)          ;get the zenith at the ship
val1(4,k)=val(11,0,k)          ;get the offset for the temperature
val1(5,k)=j                    ;get the number of sea pixels that are analyzed
m=-1
for i=0,s(2)-1 do begin
        if (val(0,i,k) GT 0.0) then begin
                m=m+1
                value(0:5,m,k)=val(0:5,i,k)          ;choose useful elements of the val array to
write
        endif
endfor
endfor
openw, unit, datapath+basename, /get_lun
printf,unit,val1
printf, unit, value
close, unit
free_lun, unit
end
```

OUT.PRO

;PROGRAM NAME :Out.pro
;PURPOSE: This program reads formatted output files "out" from the polarized SEARAD, as well as experimental radiance, and provides an output file containing the polarization degrees and the radiance from the Experiment and SEARAD.

```
pro  out

pi = 3.1416
fn=' '
read, fn , prompt = 'CHOOSE FILE NUMBER : '
basepath='c:\Thesis\data\tape5\'+fn+'\'
basepath1='c:\Thesis\data\out\'+fn+'\'
pn=2
pns=strtrim(string(pn),1)   ;convert pn to string
val1=fltarr(6,3)
filename=basepath+'Dat'+fn+'.pte'
openr, unit, filename, /get_lun
readf, unit, val1         ; wind speed ,range ,#of tape 5 files, offset,azimuth ,zenith at the ship
nu=fix(val1(5,0))
val=fltarr(6,nu,3)
readf, unit, val         ; # polarization cases
u=fltarr(11,nu)
for i=0,nu-1 do begin
        is=strtrim(string(i+1),1)     ;convert i+1 to string
        file=basepath1+'T'+fn+'_'+is+'.std'
        openr,unit,file,/get_lun
        point_lun, unit, 980          ;offset to get the zenith angle
        readf, unit,s
        u(0,i)=s
        point_lun, unit, 1020         ;offset to get the  range
        readf, unit,s1
        u(1,i)=s1
        point_lun, unit, 1432         ;offset to get the path azimuth
        readf, unit,s2
        u(2,i)=s2
        point_lun, unit, 1810         ;offset to get subsolar lat
        readf, unit,s3
        u(9,i)=s3
        point_lun, unit, 1876         ;offset to get subsolar lon
        readf, unit,s4
        u(10,i)=s4
        point_lun, unit, 2900         ;offset to get the unpolarized full range radiance
        readf, unit,q
        u(3,i)=q
        point_lun, unit, 2958         ;offset to get the full range unpolarized temperature
```

```
              readf, unit,q1
              u(4,i)=q1
              point_lun, unit, 3872        ;offset to get the full range  horizontal p radiance
              readf,unit,r
              u(5,i)=r
              point_lun, unit, 3958        ;offset to get the full range horizontal p temperature
              readf,unit,r1
              u(6,i)=r1
              point_lun,unit,3894          ;offset to get the full range  vertical p radiance
              readf,unit,s
              u(7,i)=s
              point_lun,unit,3967          ;offset to get the full range vertical p temperature
              readf,unit,s1
              u(8,i)=s1
              free_lun,unit
     endfor
     uc=fltarr(6,nu)
        uc(0,*)=u(0,*)  ;zenith angle
        uc(1,*)=u(3,*)  ;radiance for the unpolarized case from searad
        uc(2,*)=searad(val(0,*,2));get the values of the experiment(unpolarized)
        camera = [1959.9,7034.52,27.439] ; lat, lon, alt. of the camera in minutes
        sun=fltarr(3,nu)
        auxzeros = make_array(1,nu,/float, value=0.0)
        sun=[u(9,*)*60,u(10,*)*60,auxzeros]  ; lat, lon, alt. of the sun in minutes
        auxones = make_array(1,nu,/float, value=1.0)
        gpscam = camera#auxones
        sunposition = Geography(sun,gpscam)
        sunazimuth=sunposition(2,*)*180/pi
        uc(3,*)=u(2,*)-sunazimuth
              uc(4,*)=(val(0,*,0)-val(0,*,1))/(val(0,*,0)+val(0,*,1))*100;Degree  of  polarization  from
     the experiment
              uc(5,*)=(u(5,*)-u(7,*))/(u(5,*)+u(7,*))*100;degree of polarization from searad
     ;make a plot of the results
     a=[min(uc(2,*)),min(uc(1,*))]
     b=[max(uc(2,*)),max(uc(1,*))]
     plot,uc(0,*),uc(1,*),/ynoz,psym=2,$
     title='experiment  and  searad  unpolarized  radiances',xtitle='Zenith  angle',ytitle='Radiance  in
     W*m2/sr',$
     yrange=[min(a)-0.5,max(b)+2.5]
     oplot,uc(0,*),uc(2,*),psym=3
     val1s=strtrim(string(val1),1)           ;convert pn to string
     stat=fltarr(5)
     stat = moment(abs(uc(1,*)-uc(2,*)),sdev=sd)              ;statistics ,mean,stdev of the temperature diff
     between searad and experiment
     stats=strtrim(string(stat),1)
     sds=strtrim(string(sd),1)
     xyouts,min(uc(0,*)),max(b)+3.4,'* searad temp.'
     xyouts,min(uc(0,*)),max(b)+2.6,'. experiment temp.'
     xyouts,(max(uc(0,*))+min(uc(0,*)))/2,max(b)+3.4,'offset: '+val1s(4)
     xyouts,(max(uc(0,*))+min(uc(0,*)))/2,max(b)+2.6,'range to ship: '+val1s(1)
     xyouts,(max(uc(0,*))+min(uc(0,*)))/2,max(b)+1.8,'aver.abs. error: '+stats(0)
     xyouts,(max(uc(0,*))+min(uc(0,*)))/2,max(b)+1,'stdv: '+sds
```

```
window,1
stat1 = moment(abs(uc(4,*)-uc(5,*)),sdev=sd1)          ;statistics ,mean,stdev of the temperature diff
between searad and experiment
stats1=strtrim(string(stat1),1)
sds1=strtrim(string(sd1),1)
stats1=strtrim(string(stat1),1)
sds1=strtrim(string(sd1),1)
a1=[min(uc(4,*)),min(uc(5,*))]
b1=[max(uc(4,*)),max(uc(5,*))]
plot,uc(0,*),uc(4,*),psym=3,$
title='experiment   and   searad   degree   of   polarization',xtitle='Zenith   angle',ytitle='Percent
Polarization',$
yrange=[min(a1)-0.5,max(b1)+0.5]
oplot,uc(0,*),uc(5,*),psym=2
xyouts,min(uc(0,*)),max(b1)+0.5,'* searad % pol.'
xyouts,min(uc(0,*)),max(b1)+0.3,'. experiment % pol.'
xyouts,(max(uc(0,*))+min(uc(0,*)))/2,max(b1)+0.1,'aver.abs. error: '+stats1(0) +'%'
xyouts,(max(uc(0,*))+min(uc(0,*)))/2,max(b1)-0.1,'stdv: '+sds1
statistics=fltarr(6)
statistics(0)=valls(4)    ;offset
statistics(1)=valls(1)    ;range
statistics(2)=stats(0)    ;average absolute error
statistics(3)=sds         ;standard deviation
statistics(4)=stats1(0)   ;average absolute error in polarization
statistics(5)=sds         ;standard deviation in polarization
;write  the results
basename = 'OUT' + fn+'.PTE'
openw, unit, basepath1+basename, /get_lun
printf,unit,statistics
printf, unit, uc
close, unit
free_lun, unit
end
```

APPENDIX F

SEARAD INPUT AND OUTPUT FILES

This Appendix contains three sample SEARAD files. The first one is a sample of a TAPE 5 file which is the input file for SEARAD, and provides all the necessary information for the calculation of the sea radiance. The second one is a sample of an OUT file generated by SEARAD which provides the values of unpolarized sea radiance, and its polarized components. Finally the third file is a sample OUT file for the case where we have a situation where we do not wish to calculate the sea radiation, and only wish to calculate the transmittance and the path radiance. This kind of OUT files was used in the calibration procedure.

SAMPLE TAPE5 (INPUT) FILE

```
F  2  3  2  1  0  0  0  0  0  0  0  0  0 290.19  0.00

   3  0  0  3  0  0   0.000   5.814   4.481   0.000   0.000

  0.027   0.000  92.000   0.000   0.000   0.000  0  78.809  T

  1  2  99  0

32.665  117.242   0.000   0.000  20.335 202.227   0.000   0.000

   833    1250    10     5     0

0
```

BRIEF EXPANATION OF THE TAPE 5 FILE

Card 1 (Line 1): 2 = Model Midlatitude Summer, 3= Slant path to space, 2 = program execution in thermal radiance mode with solar/lunar scattered radiance included, 1 = Program executed with multiple scattering, 290.12 = Boundary Temperature in K.

Card 2 (Line 2): 3 = Navy Maritime extinction, 3 = Air mass character 3, 5.814 = Current wind speed (m/sec), 4.481= 24 hour average wind speed.

Card 3 (Line 3): 0.0027 = Initial altitude in Km, 92 = Initial zenith angle (degrees) as measured from the initial altitude, 78.809 = Wind azimuth with respect to look angle, T = Sea Switch is True.

Card 3A1 (Line 4): 1 = Method of specifying the solar geometry in card 3A2, 2 = MIE generated internal database of aerosol phase functions for the MODTRAN models, 99 = Day of the year to specify the sun's location in the sky.

Card 3A2 (Line 5): 32.665 = Observer latitude, 117.242 = Observer longitude, 20.335 = Greenwich time in decimal hours, 202.227 = path azimuth.

Card 4 (Line 6): 833 = Initial frequency in cm^{-1}, 1250 = Final frequency in cm^{-1}, 10 = Frequency increment in cm^{-1}, 5= Triangular Slit function.

SAMPLE OUT FILE

***** SEARAD, A MODIFICATION OF LOWTRAN7 *****

DATE: 02/09/1999   TIME: 00:32:43.36

THERMAL PLUS SOLAR RADIANCE MODE

MULTIPLE SCATTERING USED

MARINE AEROSOL MODEL USED

     WIND SPEED   =   5.81 M/SEC

     WIND SPEED   =   4.48 M/SEC, 24 HR AVERAGE

     RELATIVE HUMIDITY =   76.11 PERCENT

     AIRMASS CHARACTER =   3.0

     VISIBILITY   =   .00 KM

SLANT PATH TO SPACE

     H1   =   .027 KM

     HMIN =   .000 KM

     ANGLE = 91.727 DEG

FREQUENCY RANGE

     IV1 =   830 CM-1 (12.05 MICROMETERS)

     IV2 =   1250 CM-1 (8.00 MICROMETERS)

     IDV =   10 CM-1

     IFWHM =   5 CM-1

     IFILTER =   0

SUMMARY OF THE GEOMETRY CALCULATION

     H1   =   .027 KM

     H2   =   .000 KM

     ANGLE = 91.727 DEG

     RANGE =   .897 KM

     BETA =   .008 DEG

     PHI = 88.280 DEG

     HMIN =   .000 KM

     BENDING =   .001 DEG

LEN   =   0

SEA AT 290.19 K REPLACES BLACK BODY BOUNDARY

UPWIND =   83.345 DEG EAST OF LINE OF SIGHT

SUMMARY OF OBSERVATION GEOMETRY

BETA   = .00807 DEG
PATH AZIMUTH   = 197.691 DEG EAST OF NORTH
WIND AZIMUTH   = 281.036 DEG EAST OF NORTH
RECEIVER LATITUDE   = 32.665 NORTH OF EQUATOR
RECEIVER LONGITUDE = 117.242 WEST OF GREENWICH
FOOTPRINT LATITUDE = 32.657 NORTH OF EQUATOR
FOOTPRINT LONGITUDE = 117.245 WEST OF GREENWICH
SUBSOLAR LATITUDE   = 7.057 DEG NORTH OF EQUATOR
SUBSOLAR LONGITUDE = 124.444 DEG WEST OF GREENWICH

VALUES SEEN FROM FOOTPRINT

RECEIVER ZENITH ANGLE = 88.280 DEG
RECEIVER AZIMUTH   = 263.347 DEG WEST OF UP WIND
SOLAR ZENITH ANGLE = 26.461 DEG
SOLAR AZIMUTH   = 84.829 DEG WEST OF UP WIND
SOLAR SPECULAR TILT = 30.922 DEG (5.02 SIGMA, PROB = 3.284E-05)

ZERO RANGE UNPOLARIZED VALUES

SEA EMISSION   = 19.85953 W M-2 SR-1 (AV. EMISS. .5997)
SKY REFLECTION . = 10.26155 W M-2 SR-1
SUN GLINT   = .00001 W M-2 SR-1

TOTAL RADIANCE   = 30.12108 W M-2 SR-1
BLACK BODY TEMP.   =   11.9 C
FULL RANGE UNPOLARIZED VALUES

117

SEA EMISSION   = 15.11176 W M-2 SR-1

SKY REFLECTION   = 7.73348 W M-2 SR-1

SUN GLINT   = .00000 W M-2 SR-1

PATH TO FOOTPRINT   = 8.44320 W M-2 SR-1 (AV. TRANS. .7515)

TOTAL RADIANCE   = 31.28845 W M-2 SR-1

BLACK BODY TEMP.   =   14.0 C

                HORIZONTAL   VERTICAL   (H-V)/(H+V)
                (W M-2 SR-1) (W M-2 SR-1)   (%)

ZERO RANGE POLARIZED VALUES

    SEA EMISSION   8.80812   11.05140   -11.3
    SKY REFLECTION   5.91030   4.35124   15.2
    SUN GLINT   .00001   .00000   93.2

    TOTAL RADIANCE   14.71843   15.40264   -2.3
    BLACK BODY TEMP. (C)   -23.3   -21.3

FULL RANGE POLARIZED VALUES

    SEA EMISSION   6.70654   8.40522   -11.2
    SKY REFLECTION   4.45081   3.28267   15.1
    SUN GLINT   .00000   .00000   93.1
    PATH TO FOOTPRINT   4.22160   4.22160   .0

    TOTAL RADIANCE   15.37895   15.90950   -1.7
    BLACK BODY TEMP. (C)   -21.3   -19.8

OUT FILE USED TO CALCULATE TRANSMITTANCE AND PATH RADIANCE

***** SEARAD, A MODIFICATION OF LOWTRAN7 *****

DATE: 02/05/1999   TIME: 01:37:25.11

THERMAL PLUS SOLAR RADIANCE MODE

MULTIPLE SCATTERING USED

MARINE AEROSOL MODEL USED

    WIND SPEED   =   5.81 M/SEC
    WIND SPEED   =   4.48 M/SEC, 24 HR AVERAGE
    RELATIVE HUMIDITY =   76.11 PERCENT
    AIRMASS CHARACTER =   3.0
    VISIBILITY   =   .00 KM

 SLANT PATH, H1 TO H2

    H1   =   .027 KM
    H2   =   .007 KM
    ANGLE =   90.825 DEG
    RANGE =   .000 KM
    BETA =   .000 DEG
    LEN =   0

FREQUENCY RANGE

    IV1 =   830 CM-1 (12.05 MICROMETERS)
    IV2 =   1250 CM-1 (8.00 MICROMETERS)
    IDV =   10 CM-1
    IFWHM =   5 CM-1
    IFILTER =   0

SUMMARY OF THE GEOMETRY CALCULATION

    H1   =   .027 KM
    H2   =   .007 KM
    ANGLE =   90.819 DEG
    RANGE =   1.400 KM
    BETA =   .013 DEG
    PHI =   89.188 DEG
    HMIN =   .007 KM
    BENDING =   .000 DEG
    LEN   =   0

TBOUND SET TO   .10 K FOR MARINE SKY

INTEGRATED ABSORPTION = 140.66 CM-1 FROM 830 TO 1250 CM-1
AVERAGE TRANSMITTANCE = .6651

MAXIMUM RADIANCE = 4.957E-02 W M-2 SR-1 (CM-1)-1 AT 830.0 CM-1
MINIMUM RADIANCE = 1.813E-02 W M-2 SR-1 (CM-1)-1 AT 1090.0 CM-1
BOUNDARY TEMPERATURE = .10 K
BOUNDARY EMISSIVITY = 1.000
FILTERED RADIANCE = 1.150E+01 W M-2 SR-1
BLACKBODY TEMPERATURE = -33.6 C

APPENDIX G

RESULTS

1.   UNPOLARIZED RADIANCE PLOTS

This Appendix contains a list of plots of sea radiance as a function of the camera zenith angle. Both the experimental, and the SEARAD calculated radiance, are plotted for various ship camera distances.
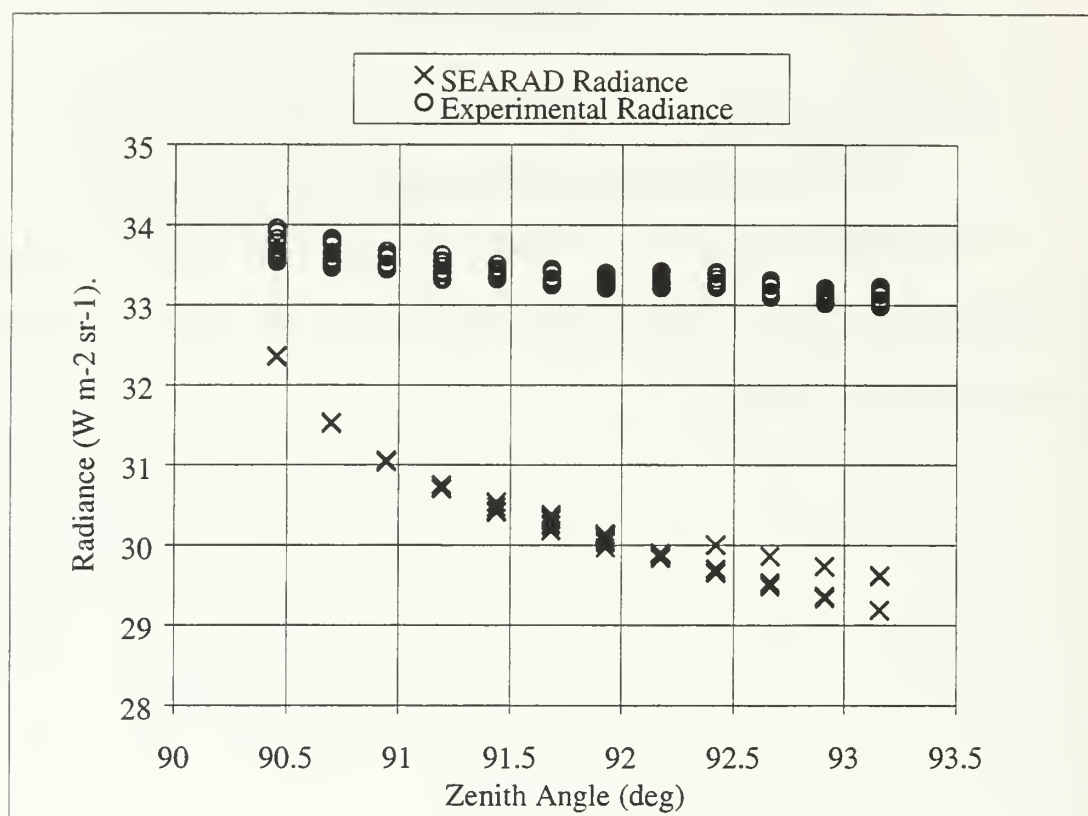
Figure G1.1 Experimental and SEARAD Sea Radiance as a Function of the Zenith Angle. Different Values of Radiance for the Same Zenith Angle Correspond to Different Azimuth Angles. The Ship Camera Slant Range is 1016 m. The Average Absolute Error is 2.96 $Wm^{-2}sr^{-1}$ and the Standard Deviation is 0.7 $Wm^{-2}sr^{-1}$
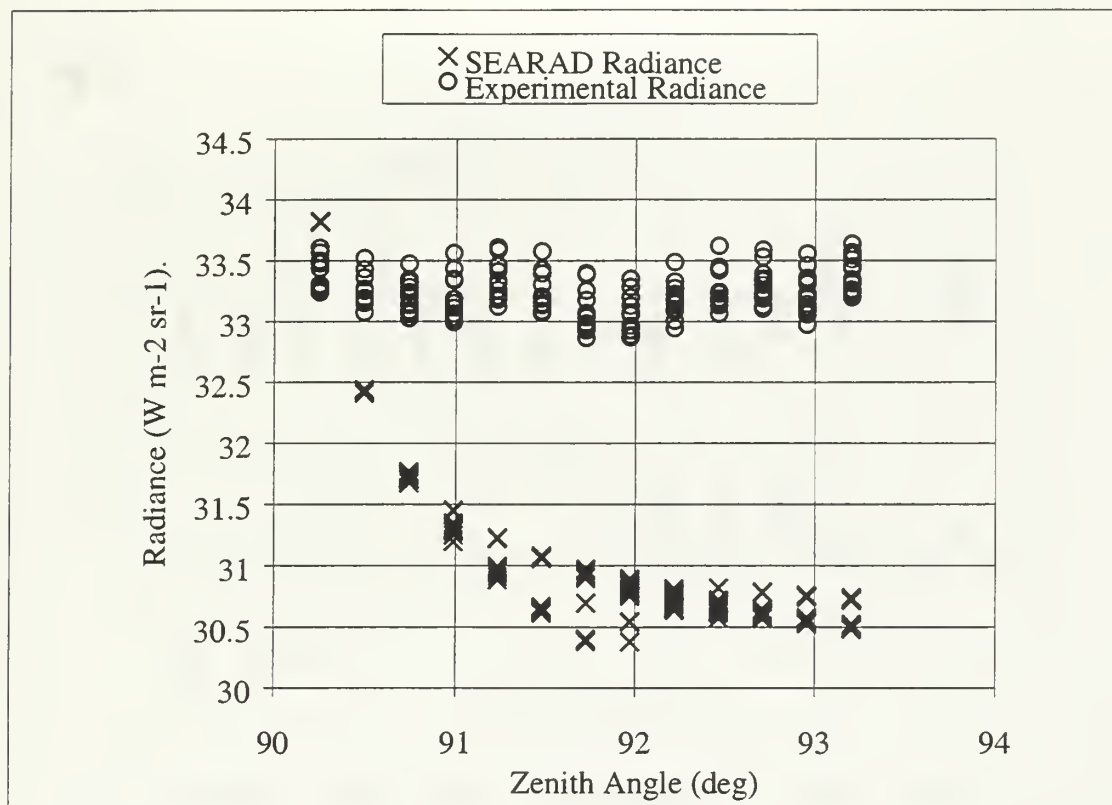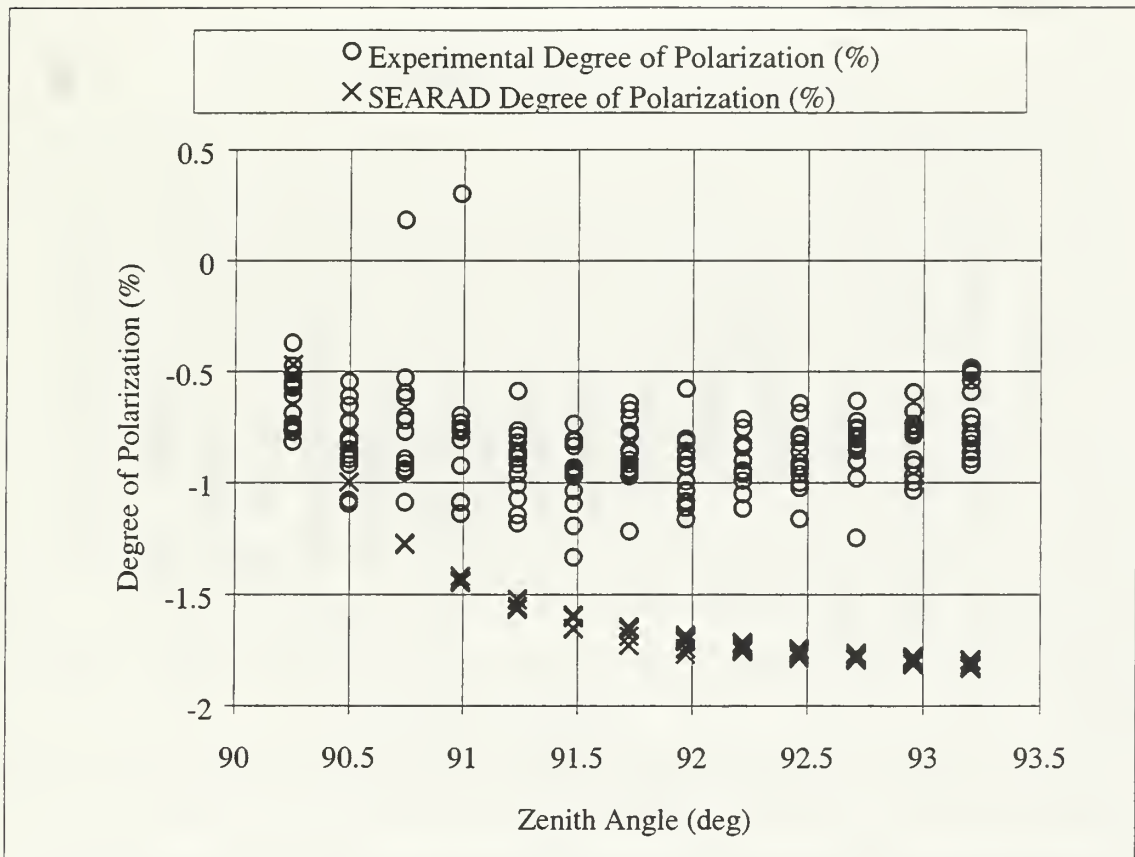
Figure G1.2 Experimental and SEARAD Sea Radiance as a Function of the Zenith Angle. Different Values of Radiance for the Same Zenith Angle Correspond to Different Azimuth Angles. The Ship Camera Slant Range is 1399 m. The Average Absolute Error is 2.07 $Wm^{-2}sr^{-1}$ and the Standard Deviation is 0.73 $Wm^{-2}sr^{-1}$
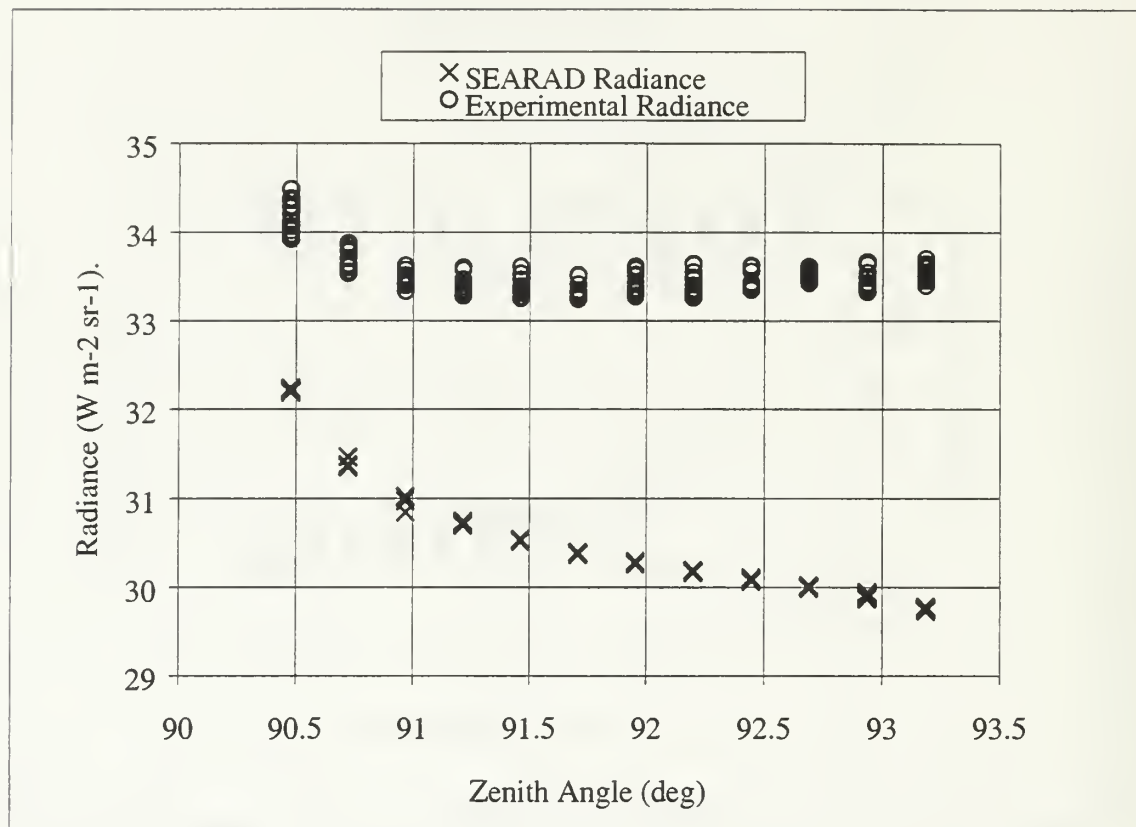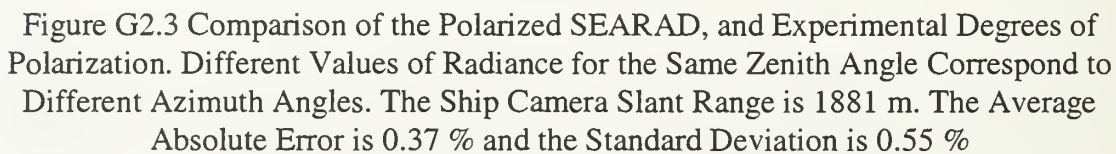
Figure G1.3 Experimental and SEARAD Sea Radiance as a Function of the Zenith Angle.
Different Values of Radiance for the Same Zenith Angle Correspond to Different
Azimuth Angles. The Ship Camera Slant Range is 1881 m. The Average Absolute Error
is 2.98 $Wm^{-2}sr^{-1}$ and the Standard Deviation is 0.55 $Wm^{-2}sr^{-1}$
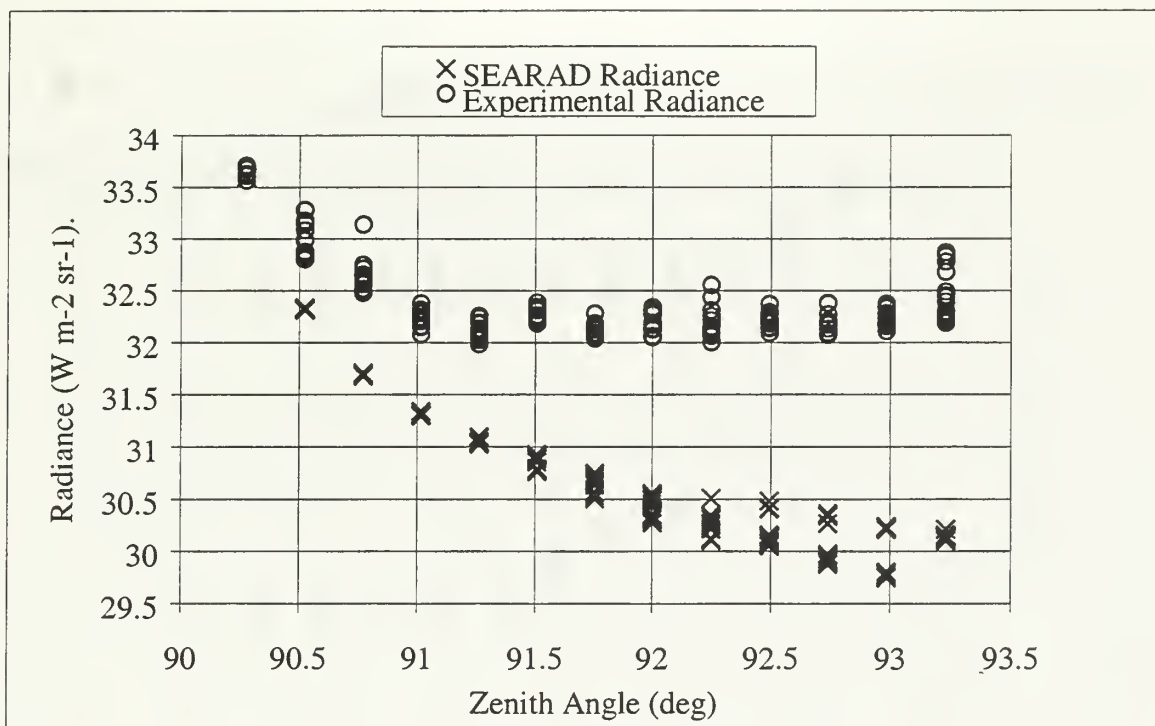
Figure G1.4 Experimental and SEARAD Sea Radiance as a Function of the Zenith Angle. Different Values of Radiance for the Same Zenith Angle Correspond to Different Azimuth Angles. The Ship Camera Slant Range is 2201 m. The Average Absolute Error is 1.5 $Wm^{-2}sr^{-1}$ and the Standard Deviation is 0.63 $Wm^{-2}sr^{-1}$
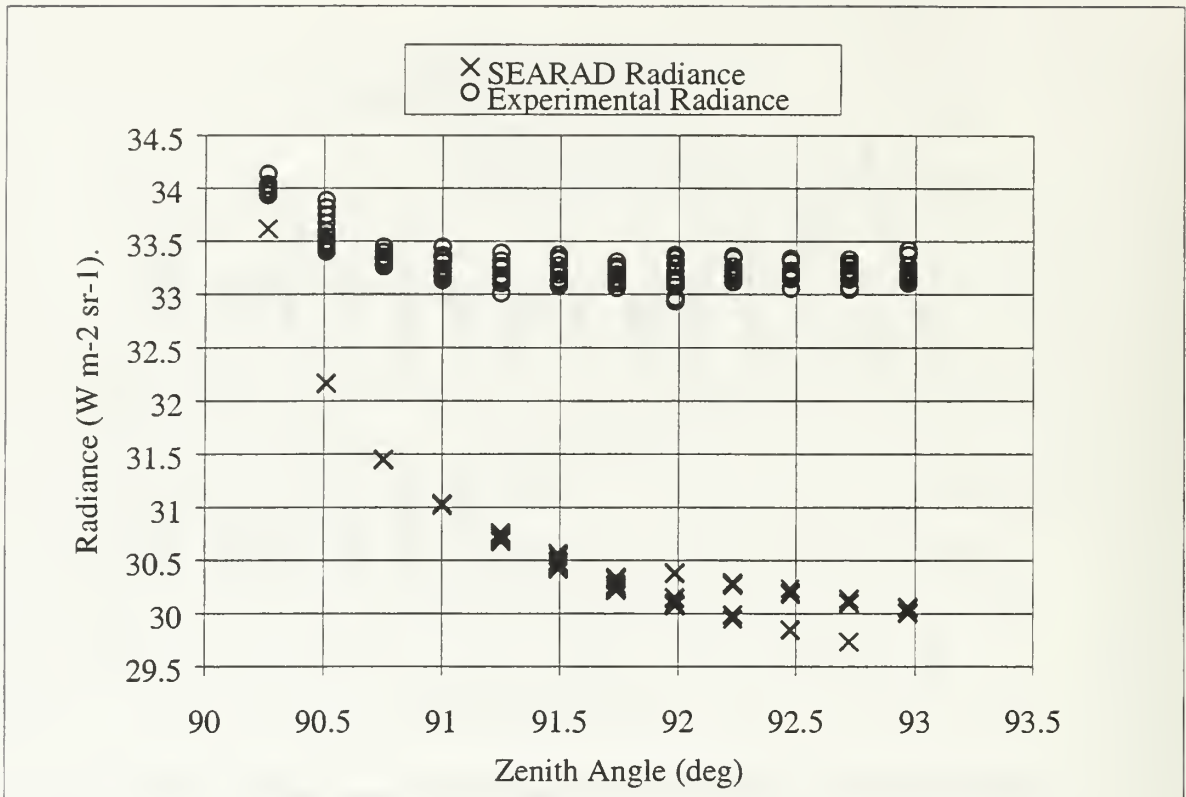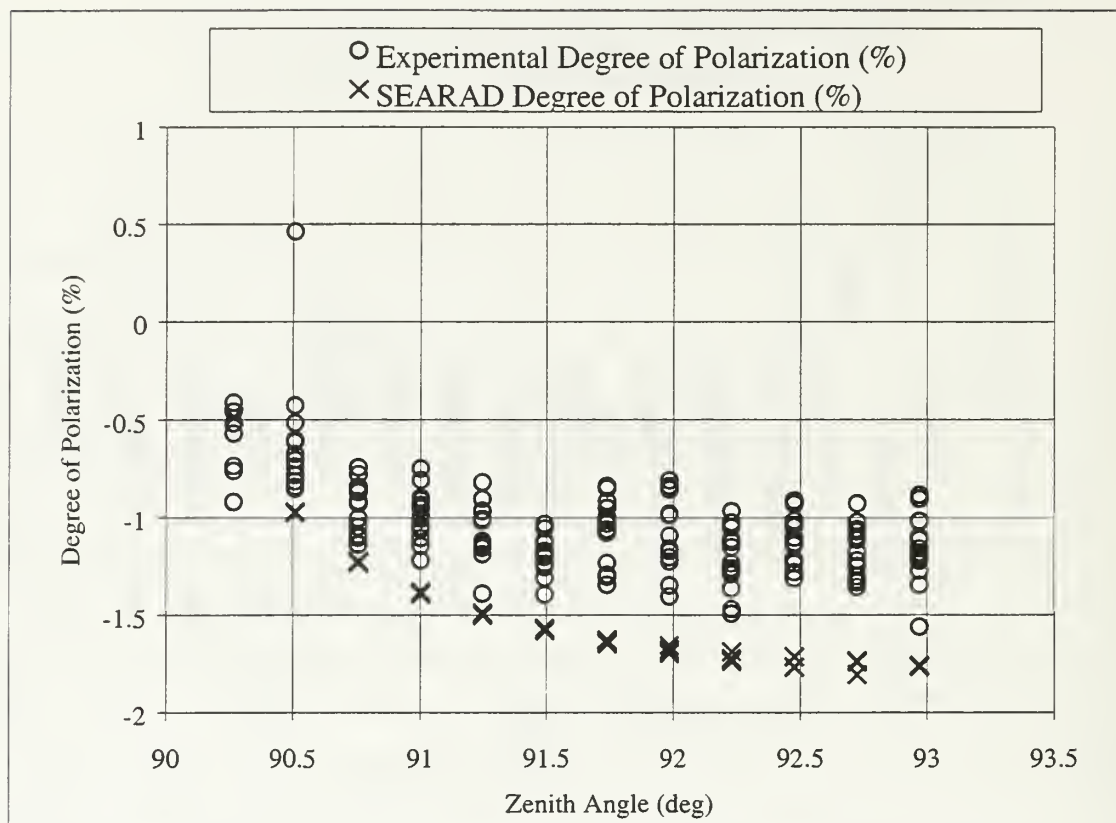
Figure G1.5 Experimental and SEARAD Sea Radiance as a Function of the Zenith Angle. Different Values of Radiance for the Same Zenith Angle Correspond to Different Azimuth Angles. The Ship Camera Slant Range is 2704 m. The Average Absolute Error is 2.56 $Wm^{-2}sr^{-1}$ and the Standard Deviation is 0.73 $Wm^{-2}sr^{-1}$

2. DEGREE OF POLARIZATION PLOTS

This Appendix presents plots that compare, the polarized SEARAD degree of polarization, and the experimental degree of polarization.
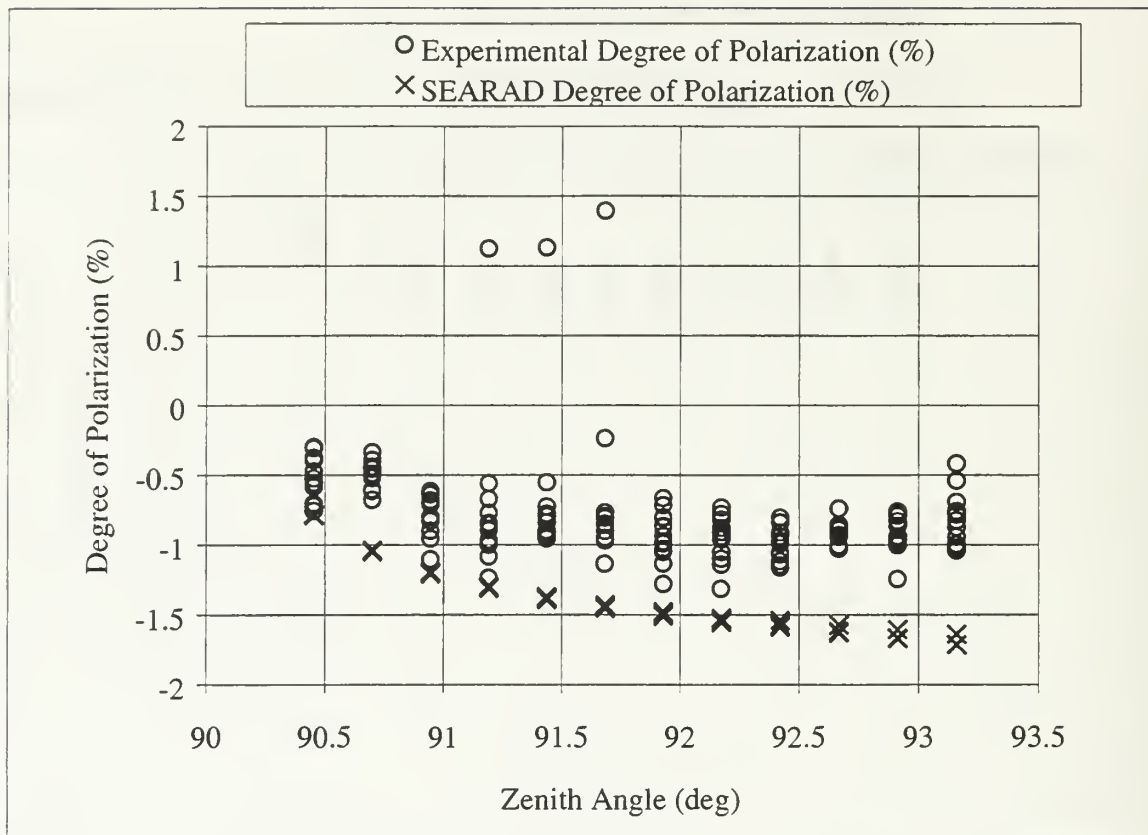
Figure G2.1 Comparison of the Polarized SEARAD, and Experimental Degrees of Polarization. Different Values of Radiance for the Same Zenith Angle Correspond to Different Azimuth Angles. The Ship Camera Slant Range is 1016 m. The Average Absolute Error is 0.6 % and the Standard Deviation is 0.7 %

Figure G2.2 Comparison of the Polarized SEARAD, and Experimental Degrees of Polarization. Different Values of Radiance for the Same Zenith Angle Correspond to Different Azimuth Angles. The Ship Camera Slant Range is 1399 m. The Average Absolute Error is 0.71 % and the Standard Deviation is 0.73 %

Figure G2.3 Comparison of the Polarized SEARAD, and Experimental Degrees of Polarization. Different Values of Radiance for the Same Zenith Angle Correspond to Different Azimuth Angles. The Ship Camera Slant Range is 1881 m. The Average Absolute Error is 0.37 % and the Standard Deviation is 0.55 %
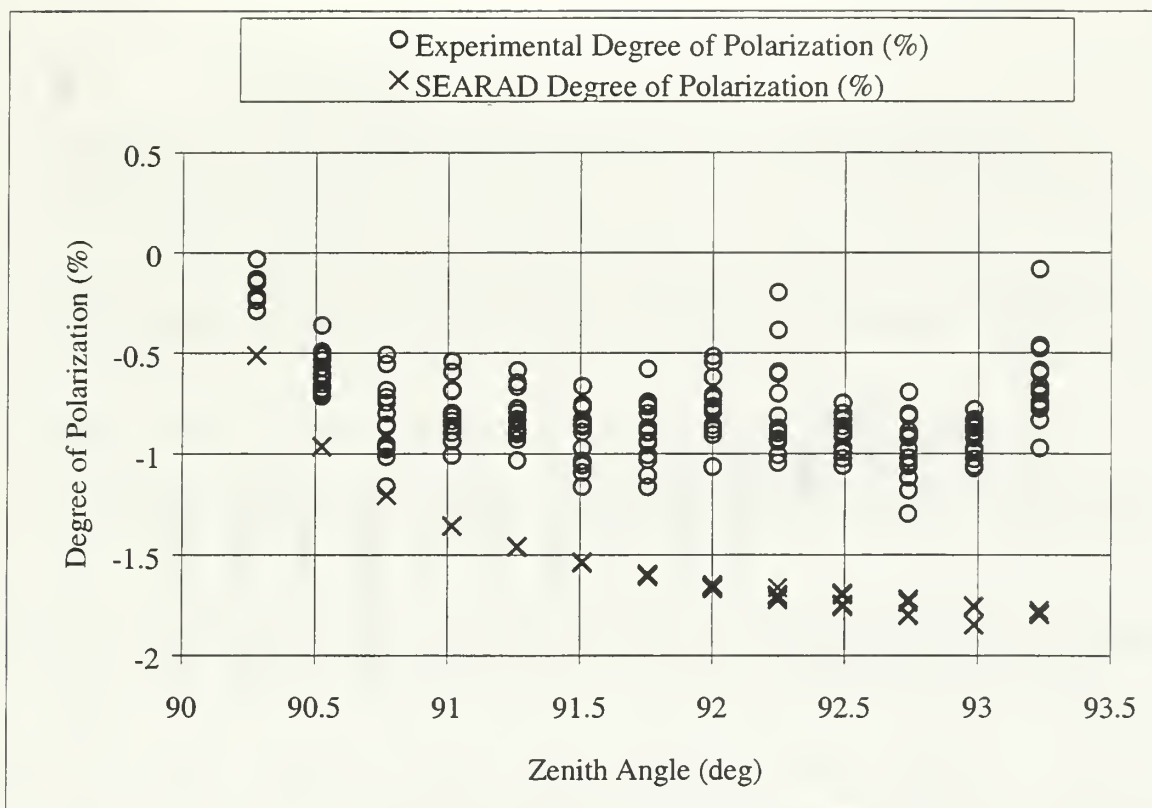
Figure G2.4 Comparison of the Polarized SEARAD, and Experimental Degrees of Polarization. Different Values of Radiance for the Same Zenith Angle Correspond to Different Azimuth Angles. The Ship Camera Slant Range is 2201 m. The Average Absolute Error is 0.72 % and the Standard Deviation is 0.63 %

Figure G2.5 Comparison of the Polarized SEARAD, and Experimental Degrees of Polarization. Different Values of Radiance for the Same Zenith Angle Correspond to Different Azimuth Angles. The Ship Camera Slant Range is 2704 m. The Average Absolute Error is 0.48 % and the Standard Deviation is 0.73 %

LIST OF REFERENCES

1. Gregoris, D.J., Yu, S., Cooper, A.W., and Milne, E. A., "Dual band infrared polarization measurements of sun glint from the sea surface," *SPIE Proceedings*, vol. 1687, pp. 381-393, 1992.

2. Cooper, A.W., Crittenden, E.C., Milne, E.A., Walker, P.L., Moss, E., and Gregoris, D.J., "Mid and Far Infrared Measurements of Sun Glint From the Sea Surface," *SPIE Proceedings*, vol. 1749, pp. 176-185, 1992.

3. Cooper, A.W., Lentz, W.J., Walker, P.L., and Chan, P.M., "Infrared Polarization Measurements of Ship Signatures and Background Contrast," *in* Characterization and Propagation of Sources and Backgrounds, *SPIE Proceedings*, vol. 2223, pp. 300-307, 1994.

4. Chan, P.M., Cooper, A.W., and Lentz, W.J., "Infrared Polarized Image Measurements in the NATO MAPTIP Exercise," *NPS Technical Report*, NPS-PH-94-011, June 1994.

5. Cooper, A.W., Lentz, W.J., Walker, P.L., and Chan, P.M., "Polarization Enhancement of Contrast in Infrared Ship/Background Imaging," *Paper 26, AGARD SPP Symposium on Propagation Assessment in Coastal Environments*, Bremerhaven, September 1994

6. Walker, P.L., Lentz, W.J., and Cooper, A.W., "Atmospheric and Sea State Dependence of Polarized Infrared Contrast," *SPIE Proceedings,* vol. 2469, pp. 393-403, 1995.

7. Cooper, A.W., Lentz, W.J., and Walker, P.L., "Infrared Polarization Ship Images and Contrast in the MAPTIP Experiment," *SPIE Proceedings*, vol. 2828, Paper 08, 1996.

8. Zeisse, C.R., "The Infrared Polarization of Sea Radiance," *Technical Report 1743*, NCCOSC, San Diego, July 1997.

9. Hudson, Jr, R.D., *Infrared Systems Engineering*, John Wiley & Sons, Inc., 1969.

10. *Electro-Optics Handbook*, Technical Series EOH-11, RCA Corporation, 8-1974.

11. Holst, G.C., *Electro-Optical Imaging System Performance,* JCD Publishing, and SPIE Optical Engineering Press, 1995.

12. Sandus, O., "A Review of Emission Polarization," *Applied Optics*, vol. 4, no 12, pp. 1634-1642, December 1965.

13. Sidran, M., "Broadband reflectance and emissivity of specular and rough water surfaces," *Applied optics*, vol. 20, no 18, pp. 3176-3183, 15 September 1981.

14. Cox, C. and Munk, W., "Measurement of the Roughness of the Sea Surface from Photographs of the Sun's Glitter," *Journal of the Optical Society of America*, vol. 44, pp. 838, 1954.

15. Cox, C. and Munk, W., "Slopes of the Sea Surface Deduced from Photographs of Sun Glitter," *Scripps Institution of Oceanography Bulletin*, vol. 6, pp. 401, 1956.

16. *AGA Thermovision 780 Operating Manual,* AGA Infrared Systems AB, Publication no 556 556 492, Ed II, 1980.

17. Pontes, M.C., "Polarization Effects on Infrared Target Contrast," Master's Thesis, Naval Postgraduate School, December 1993.

18. Kneizys, F. X., Shettle, E. P., Abreu, L. W., Chetwynd, J. H., Anderson, G. P., Gallery, W. O., Selby, J. E. A., and Clough, S. A., *Users Guide to LOWTRAN 7*, AFGL-TR-88-0177, Air Force Geophysics Laboratory, Hanscom, MA, 01731, 1988.

INITIAL DISTRIBUTION LIST